APPLIED RESEARCH AND EVALUATION OF PROCESS CONCEPTS FOR LIQUEFACTION AND GASIFICATION OF WESTERN COALS. QUARTERLY PROGRESS REPORT, JANUARY--MARCH 1977

UTAH UNIV., SALT LAKE CITY. DEPT. OF MINING, METALLURGICAL AND FUELS ENGINEERING

OCT 1977

One Source. One Search. One Solution.

NTIS

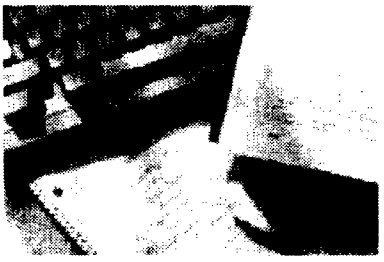

Providing Permanent, Easy Access to U.S. Government Information

National Technical Information Service is the nation's largest repository and disseminator of government-initiated scientific, technical, engineering, and related business information. The NTIS collection includes almost 3,000,000 information products in a variety of formats: electronic download, online access, CD-ROM, magnetic tape, diskette, multimedia, microfiche and paper.

Search the NTIS Database from 1990 forward

NTIS has upgraded its bibliographic database system and has made all entries since 1990 searchable on **www.ntis.gov.** You now have access to information on more than 600,000 government research information products from this web site.

Link to Full Text Documents at Government Web Sites

Because many Government agencies have their most recent reports available on their own web site, we have added links directly to these reports. When available, you will see a link on the right side of the bibliographic screen.

Download Publications (1997 - Present)

NTIS can now provides the full text of reports as downloadable PDF files. This means that when an agency stops maintaining a report on the web, NTIS will offer a downloadable version. There is a nominal fee for each download for most publications.

For more information visit our website:

www.ntis.gov

U.S. DEPARTMENT OF COMMERCE
Technology Administration
National Technical Information Service
Springfield, VA 22161

FE-2006-7
Distribution Categories UC-90c, UC-90d

Applied Research and Evaluation of Process Concepts for Liquefaction and Gasification of Western Coals

Quarterly Progress Report
for the Period Jan - Mar 1977

Dr. Wendell H. Wiser

Date Published - August 1977

Under Contract No E (49-18) - 2006

Prepared for
Energy Research and Development Administration

University of Utah - Department of Mining
Metallurgical and Fuels Engineering
Salt Lake City, Utah 84112

CONTENTS

II. OBJECTIVE AND SCOPE OF WORK

The research reported herein is all of fundamental importance in support of either a process for development of liquefaction of coal, catalysis or some related research. The information which will be gained by research on this contract should materially assist the application of coal in the solution of the energy problems now facing the United States and the world. In particular, the projects reported herein are intended to apply the expertise developed by the coal research team at the University of Utah to problems in four general areas:

a) Evaluation of process concepts in relation to liquefaction and gasification of coal,
b) Catalysis studies of fundamental importance in liquefaction and gasification of coal,
c) Studies of fundamental principles involved in processes for liquefaction and gasification of coal,
d) Properties of coal and coal conversion products of significance in liquefaction and gasification of coal.

A-1 Coal will be gasified by direct catalytic hydrogenation to produce a high-BTU gas. A liquid will be produced in a first stage reaction at 400-450°C. This product will be further hydrogenated to produce a high-BTU gas. Catalysts and reaction conditions for each stage will be studied.

A-2 Kinetics, yields and optimum reaction conditions for extraction of coal will be determined. Hydrogen donor solvents, ultrasonic energy, hydrogen pressures and catalysts will be employed. Extraction products will be analyzed and characterized.

A-4 Aromatic liquids derived from coal hydrogenation or extraction will be considered as feedstocks for steam reforming to make a high-BTU gas. Optimum conditions for the production of hydrogen or high-BTU gas, optimum catalysts, the effects of poisons and the degree of coke formation will be determined.

A-6 The gasification of coal char will be studied at 2000-3000 psi to produce hydrogen for coal hydrogenation. Steam and oxygen will be used for gasification. The thermal efficiency of producing hydrogen at the pressure at which it will be used will be studied.

A-7 Thermal hydrogenolysis of coal slurried with recycle solvent will be studied as such or in the presence of a vapor-phase catalyst to determine the extent of upgrading.

A-8 Fischer-Tropsch synthesis of C_2-C_4 hydrocarbons will be studied. New catalysts will be developed and a continuous test unit for long-term catalyst testing will be constructed.

A-9 The capacity and durability of a previously developed high-pressure gas recycle pump will be increased. A goal of 3000 psi operating pressure at 500°C is desirable.

B-1 Adsorption properties and penetration of aromatic molecules on typical cracking catalysts will be determined. These properties will be used to evaluate the ability of such catalysts to crack the large molecules present in coal-derived liquids.

B-2 (alternate) The mechanism of deactivation of molybdena hydrodesulfurization catalysts by coal-derived liquids will be studied. Kinetic studies involving the model compound benzothiophene will be employed.

B-3 Hydrogen transfer by metal halide catalysts during coal hydrogenation will be studied. Deuterium labled hydrocarbons will be used to elucidate reaction mechanisms.

B-4 The mechanism of catalytic hydrogenation of coal by metal halide catalysts will be investigated. The nature of active catalyst sight will be studied. Changes in properties of the reacting coal will be determined and the nature of reaction products will be determined. Catalyst regeneration will also be studied.

C-1 The mechanism of pyrolysis of coal will be studied by the use of isotopically labled model compounds. Products of pyrolysis will be examined to determine their precursors in coal.

C-2 Fluid mechanics and heat transfer studies involving gas-solid suspensions in vertical downward cocurrent flow systems will be conducted to obtain information on the effect of these variables in the University of Utah coal hydrogenation reactor.

D-1 The effect of coal and catalyst properties and pretreatment on the hydrogenation of western coals will be studied in the University of Utah short-residence-time, entrained-flow reactor.

D-2 The effect of coal structure on reactivity to hydrogenation, pyrolysis and dissolution will be studied. Pretreatment of the coal by specific reactions will be used to obtain samples with special structural features.

D-4 Liquid products from coal hydrogenation in the University of Utah reactor will be separated and characterized. Coal pyrolysis and hydrogenation mechanisms and model compound reactions will be studied.

III Summary of Progress to Date

Research Highlights

Donor solvent extraction of coal shows an initial regime of rapid conversion with little hydrogen transfer from the solvent followed by a regime of more rapid hydrogen transfer but slower conversion. During the second regime methyl indan and indan are formed from the tetralin solvent. These reactions are confirmed by GC-MS analysis.

Activities of $CoCu/Al_2O_3$ catalysts for the Fischer-Tropsch reaction correlate well with metal areas determined by O_2 chemisorption.

Adsorption rates of chrysene in two different aluminas were the same within experimental error and correlated well with a contracting-sphere model for diffusion as the rate-controlling process.

Multiring aromatic substances can be readily hydrogenated completely, while a mixture from a coal-liquid resists hydrogenation above about 65%. Experiments are continuing in an attempt to explain this result. Asphaltenes can be made soluble in cyclohexane by mild hydrogenation.

Special Activities

Papers were presented at the Rocky Mountain Fuel Symposium in Salt Lake City by S. Goyal, C. Yang, J. Lytle, Dr. S.W. Cowley, Dr. R. Beishline and Dr. W.H. Wiser. Dr. L.L. Anderson and C. Yang presented papers at the American Chemical Society Meeting in New Orleans.

Project A-1

Catalytic Gasification of Coal to High BTU Gas

Single Stage Coal Gasification

Faculty Advisor: Wendell H. Wiser
Graduate Student: Stevan L. Weber

Introduction

The objective of this project is to develope a composite catalyst in optimum conditions for the single stage gasification process of coal that will produce a high BTU gas, predominantly methane. The coal will be dissolved in a hydrogen-donor solvent such as tetralin.

Project Status

An extensive literature search of single stage gasification processes, their working conditions and catalysts has been completed. The equipment set-up has been designed and the parts ordered. A continuous flow reactor will be used in a temperature range of 500-700°C at 1500 psi. The initial catalysts to be tested are 6-12% Ni-S on SiO_2-Al_2O_3 and 0.5% Pd-S on SiO_2-Al_2O_3.

Future Work

After obtaining the necessary material, the catalyst will be made up in this laboratory. As the equipment arrives, it will be assembled and tested.

Project A-2

Dissolution of Coal in Hydrogen Donor Solvents with Application of Catalysts and Energized Conditions to Produce Clean Fuels

Solvent Extraction of Coal Utilizing Sonic Energy

Faculty Advisor: L.L. Anderson
Graduate Student: Doohee Kang

Introduction

This project involves the study of the dissolution of coal in a hydrogen donor solvent using a differential reaction system of the batch recycle type.

In previous reports the expanded time scale of conversions clearly shows two different reaction regimes during the dissolution process. In the first regime (the first several minutes) the reaction proceeds rapidly with a minimal transfer of hydrogen. The second regime is kinetically slower but hydrogen transfer is faster. The dissolution rate appears to be faster than had previously been reported by other investigators. At a particular temperature the data shows the ultimate conversion occurs within 10 minutes.

Project Status

Duplicate runs and runs of different temperature conditions have been conducted to supplement the previous data. Further characterization of product extracts also has begun by NMR analysis. GC-MS has been used to analyze the various solvent derived compounds.

Figures 1 and 2 show the data of conversion kinetics of coal and solvents at 400°C and 1500 psig hydrogen pressure. Data for residence times up to 35 min is included. In Figure 3, hydrogen consumption and benzene soluble plus gas conversions are correlated for runs of different reaction temperatures. Figure 4 is a typical mass chromatogram of total ion current for a liquid sample at a reaction period of 34 min at 400°C and 1500 psig H_2. To aid identification both electron impact and chemical ionization (Varian 1400) sources were used in the mass spectrometer.

As detailed in the previous reports, the initial 2 min of residence time show higher rates of reaction and lower H_2 consumption than later times. This initial reaction regime is shown in Figure 1 by the steep slopes at residence times less than 2 min. Figure 3 also shows the amount of H_2 transferred to be minimal during this period. This trend

indicates that a thermal reaction is dominating during the initial stages of coal dissolution. Over one-third of the total extract produced is cyclohexane soluble in the first two minutes. The short contact time (~4 sec per pass) and rapid quench aids in preserving primary fragmentation products. Without immediate quenching, these fragments would rearrange and recombine with other reactive free radicals present. Relatively large amounts of unsaturates in the gas produced is further evidence that the rapid quench effect preserves the highly reactive radicals.

Following the initial rapid thermal reaction (with little hydrogen consumption), there is a second regime characterized by a rapid increase in H_2 consumption. As shown in Figure 3, the hydrogen transfer then levels off at conversions (benzene soluble plus gas) of 35 and 50% for runs conducted at 375°C and 400°C, respectively. Thus at about ten minutes of reaction time the amount of H_2 transfer reaches a pseudo-plateau and is momentarily constant. In the second regime it is probable that the higher H_2 consumption is due to stabilization of the primary fragments produced by thermal reaction.

Figure 3 indicates the onset of a third reaction regime following the pseudo-plateau in H_2 transfer. Again the amount of H_2 consumption increases sharply but, as shown in Figure 1, there is little change in overall conversion. Also shown by Figure 1 is a net decrease in the solid and liquid extract produced. (The benzene soluble curve and the gas curve approach each other in this regime.) The large consumption of H_2 is most likely contributing to regressive reactions (hydrocracking) of those products formed in the two previous regimes and subsequent production of gases. Also material balance showed a net decrease in the solid extract. The solvent analysis by GC-MS, shown in Figure 4, indicates a substantial amount of methyl indan, indan and butyl-benzene. These species are indicative of ring opening as the result of hydrocracking reactions and the same phenomena could apply to the coal-derived products.

Figure 3 demonstrates the increase in H_2 utilization efficiency at higher temperature conditions. Less H_2 is required to give a specified conversion at higher temperatures, the balance apparently coming from the coal itself.

As part of the characterization of extract products, proton NMR spectra were run on the various fractions. This data is shown in Figures 5-8 as proton distribution versus conversion of the benzene soluble plus gas fraction. Although each fraction shows an overall decrease in paraffinicity, the α, β and γ protons, especially in the asphaltene fractions demonstrate the large changes in structural parameters between initial conversion and later regimes.

Future Work

Further characterization of product structural information will be carried out to support the existing NMR data. Elemental analysis and molecular weight determinations will be acquired to aid in the structural characterization. Kentucky #14 coal will be run in the dissolution system to provide a comparison with the work of other investigators using eastern coals.

Figure 1. Reactions of Hiawatha Coal with Tetralin at 400°C, 1500 psig H_2.

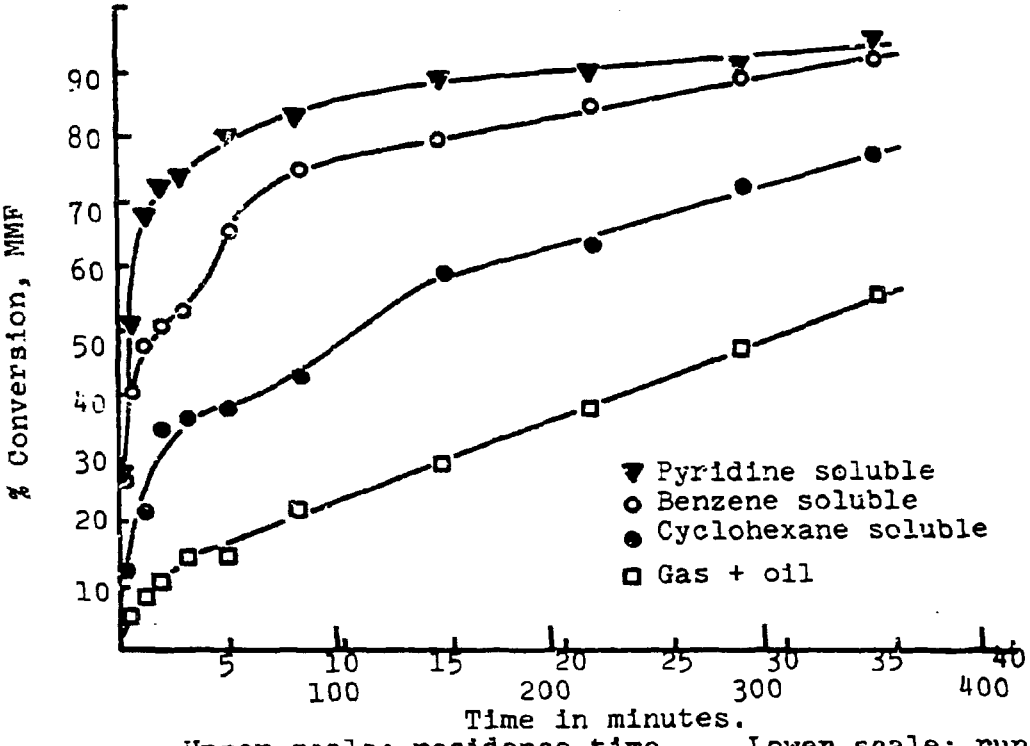

Figure 2. Tetralin Derived Compounds Vs. Conversion

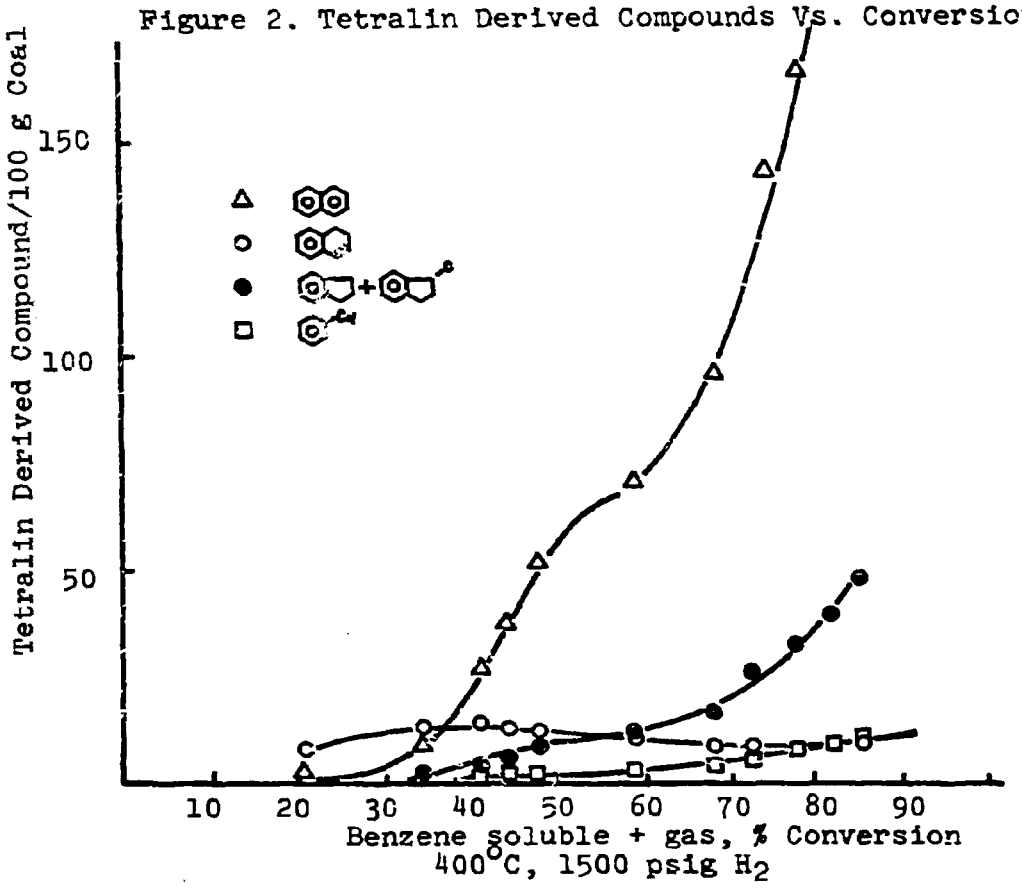

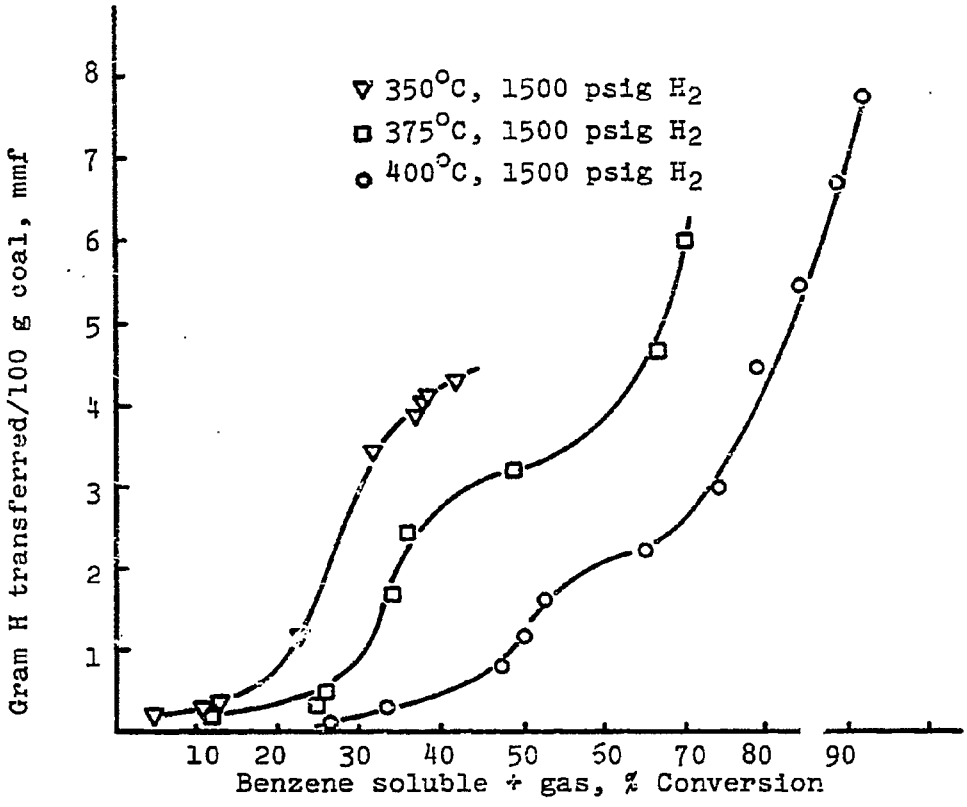

Figure 3. Hydrogen-Transfer vs. Conversion

Figure 4. Mass chromatogram for a liquid sample at 34 min residence time, 400°C and 1500 psi H_2.

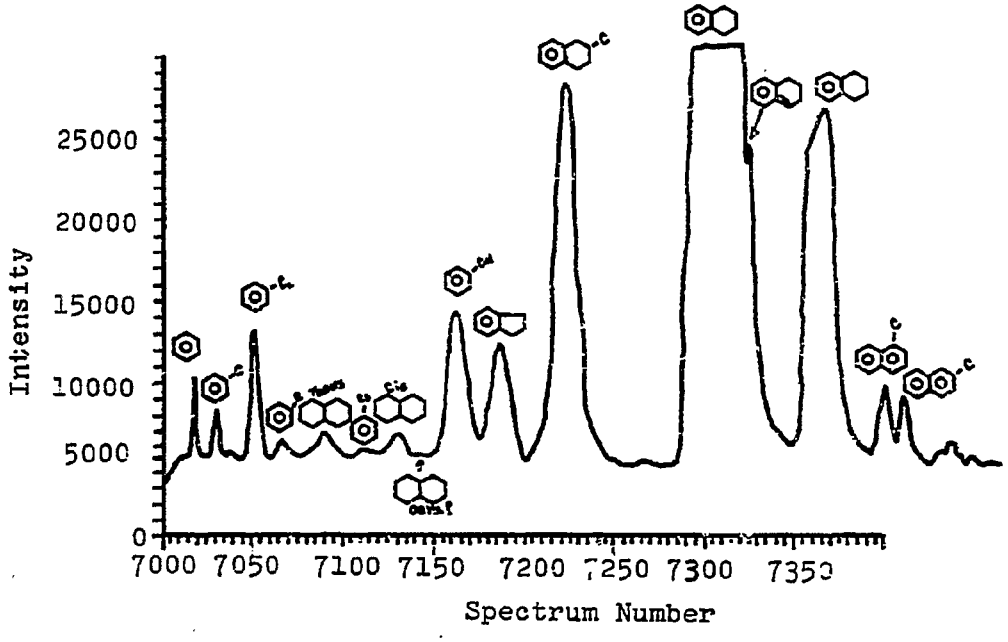

Figure 5. Distribution of Proton vs. Conversion
Total Dissolution Extracts

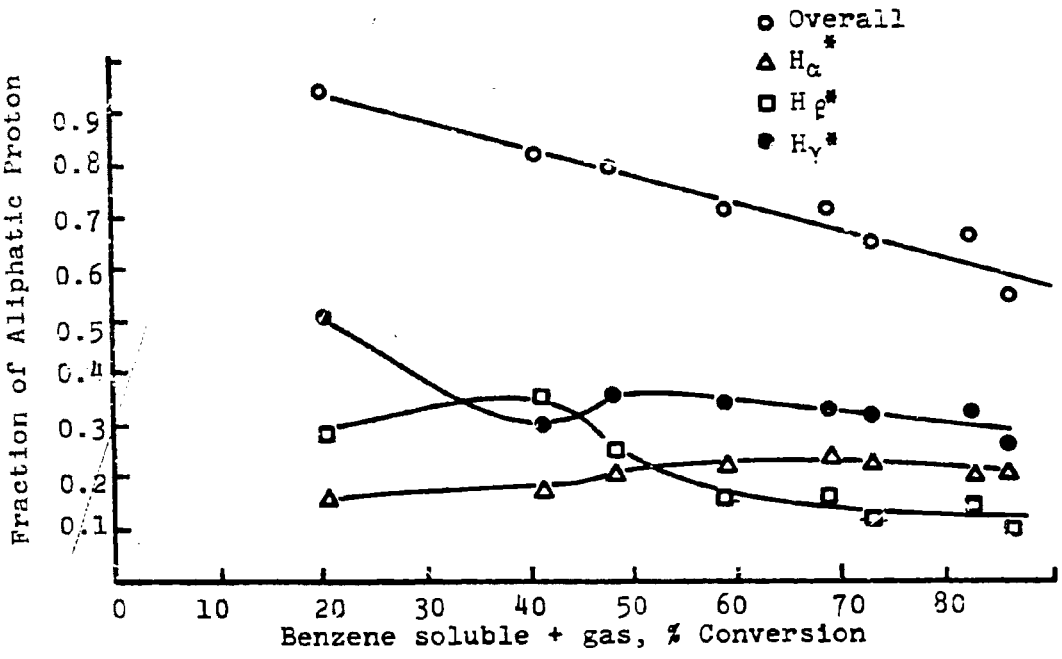

*normalized.

Figure 6. Proton Distribution vs. Conversion
Cyclohexane Soluble Fraction

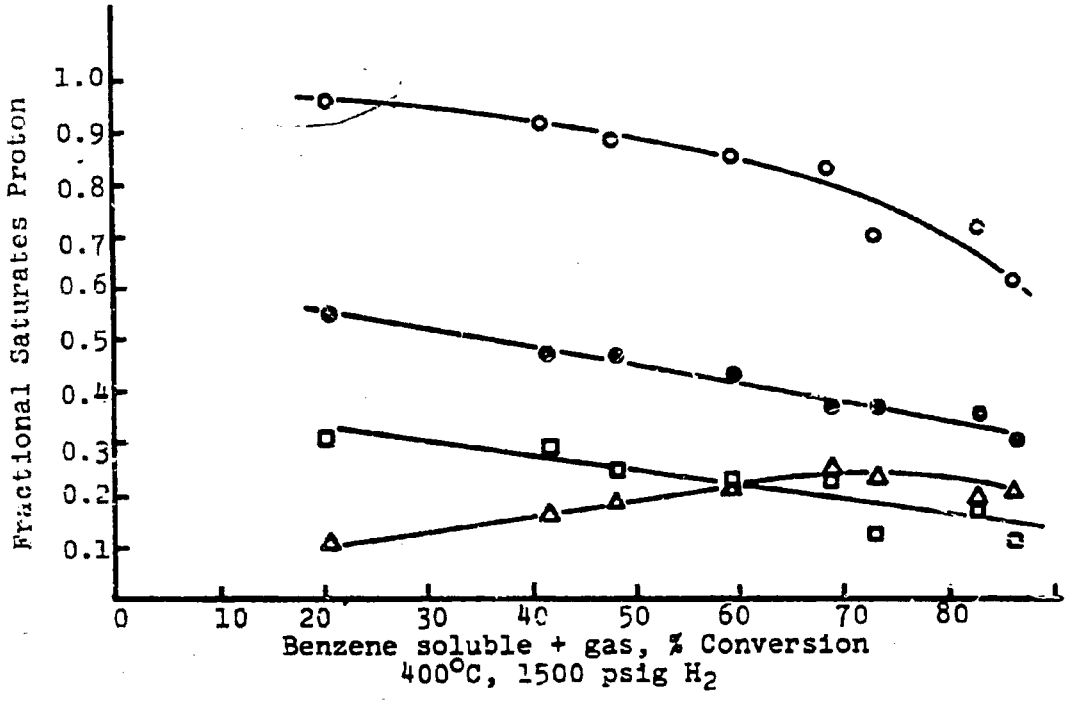

Figure 7. Proton Distribution vs. Conversion
Asphaltene Fraction

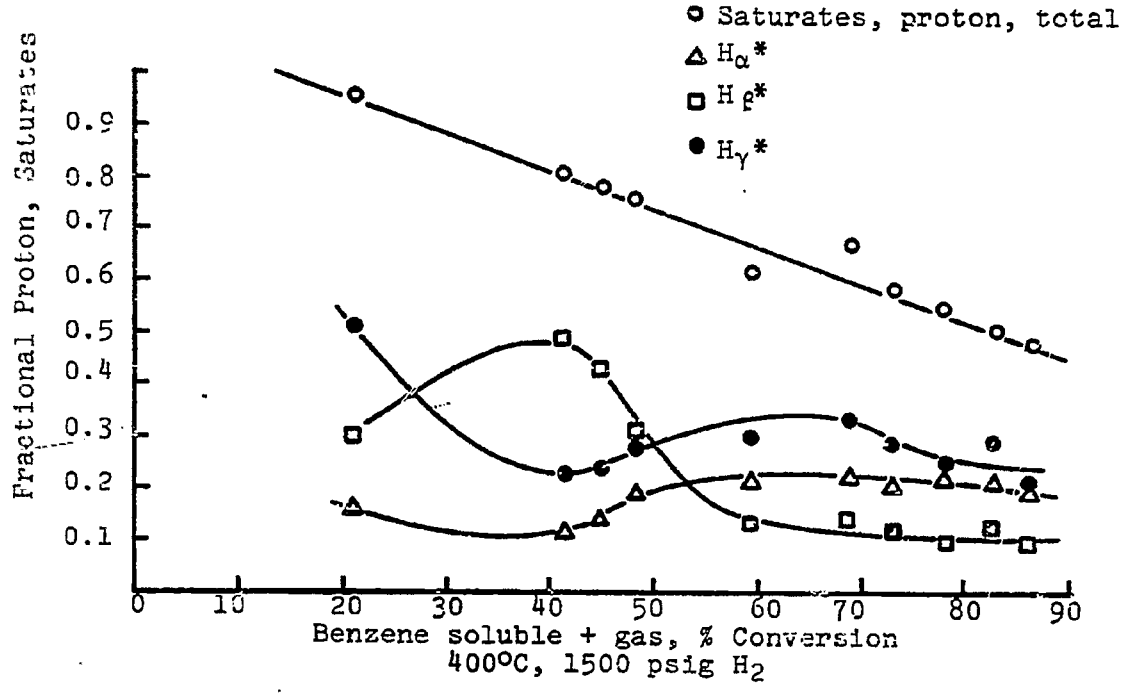

Figure 8. Proton Distribution vs. Conversion
Pyridine Soluble Fraction

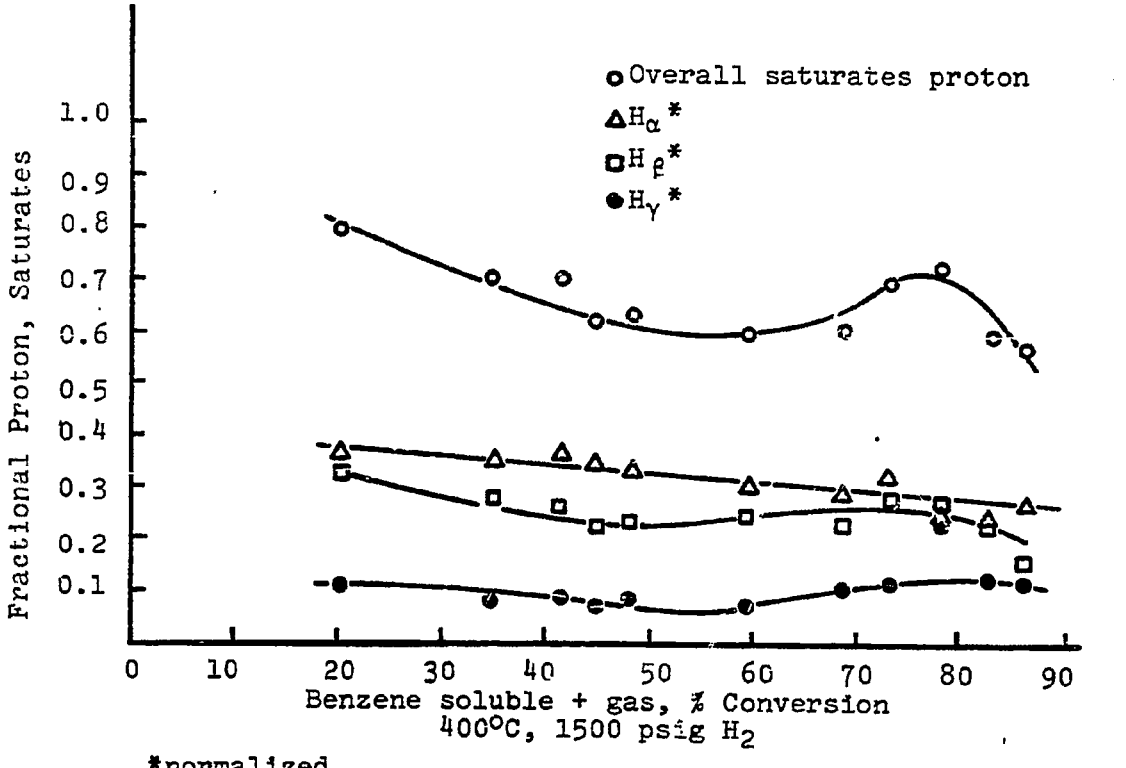

*normalized

Project A-2

Solvent Extraction of Coal for Separation and Identification of Chemical Species in Coal

Faculty Advisor: L.L. Anderson
Graduate Student: S. Jackson

Introduction

Research in solvent extraction of coal can be divided into several areas: (1) the successive use of various solvents which dissolve the greatest amount of coal, (2) the characterization of the coal extracts to better understand the structure of coal and its chemistry and (3) the use of extraction to lower the ash and/or sulfur content of the coal or to improve its solubility. Variables such as pressure, coal types and extraction times and temperatures will be kept constant during extraction studies so that the effect of the various solvents on coal can be determined.

The objective of this work is to (1) find similarities or differences in the extracts due to various solvents and/or coal types, (2) correlate these similarities or differences to some parameter of the solvent and (3) characterize an extract and its fractions with the possible identification of the compounds within the extract fractions.

Past work has included a literature search and preliminary extractions with anisole, benzyl alcohol, benzaldehyde and benzene. Experiments using different extraction methods determined the most useful method for obtaining data relevant to this project. Also several coal samples have been tried. GC, IR and NMR analyses were done to determine the usefulness and limitations of each of these analytical methods. Several solvents and their GC results have been reported.

Project Status

During this quarter several more extractions of Clear Creek coal were done using benzaldehyde, aniline, chlorobenzene and nitrobenzene as solvents. A gas chromatogram was obtained for each of the extracts and the results compared. The extract from the chlorobenzene extraction was sent for GC-MS analysis.

Table 1 shows the retention time of the various compounds removed by these solvents. Observation reveals that many of the same compounds are removed by the different solvents, but that these compounds are extracted in different relative amounts. Because there is no standard,

comparison between extracts from different solvents cannot be done. The results of these extractions also show that certain solvents are "selective" in the amount and type of material extracted. For instance in the nitrobenzene extraction the amount of material extracted is concentrated within fewer compounds. Thus it may be possible to obtain certain compounds in sufficient amounts from the coal for better analysis.

The extract of the chlorobenzene extraction was submitted for GC-MS analysis. Figure 1 shows a typical mass spectra obtained. In this spectra the peaks at m/e 56, 70 and 84 are evidence for a long chain alkyl group. The other peaks found within this spectra are not easily identifiable. There is the possibility of some extraneous peaks. However, further concentration of the sample before analysis will enable many of the spectra to be characterized.

Future Work

GC-MS work will be continued. More will be done to determine if there are any differences in the extracts of various coals.

Table 1

Solvent Extraction Products Derived from Coal at 25°C. (Area %)

R T (min)	Solvent Used			
	ϕ-Cl	ϕ-COH	ϕ-NO_2	ϕ-NH_2
0.82	--	--	--	0.48
0.97	--	0.01	--	0.34
1.09	--	0.89	--	--
1.17	--	--	--	0.46
1.28	--	6.00	0.47	0.31
1.41	--	--	--	0.29
1.61	--	2.98	--	--
1.71	--	--	--	4.09
1.80	--	--	1.52	--
1.89	--	7.09	--	--
1.97	--	--	0.37	--
2.04	--	--	--	0.33
2.21	--	1.79	--	--
2.37	--	--	3.14	--
2.44	--	11.80	--	--
4.95	4.67	--	--	--
6.77	0.10	9.32	--	--
7.39	--	9.85	--	--
7.87	0.21	--	--	--
8.10	--	7.64	--	--

R T	ϕ-Cl	ϕ-COH	ϕ-NO_2	ϕ-NH_2
8.50	0.24	3.16	--	--
8.73	0.54	5.57	--	--
9.11	--	0.97	--	--
9.20	--	3.08	--	--
9.49	--	--	--	0.27
9.95	--	5.25	--	0.40
10.43	0.85	0.40	--	--
10.77	--	--	11.82	0.64
10.81	1.65	--	--	--
10.99	--	1.82	--	--
11.11	--	--	--	1.75
11.28	0.89	5.61	--	--
11.40	--	--	--	0.29
11.64	--	--	--	1.54
12.01	--	--	1.55	2.27
12.45	2.28	--	3.83	5.75
12.79	--	--	--	1.39
12.97	0.93	0.67	1.62	--
13.01	--	--	3.49	4.80
13.28	5.55	--	10.46	2.02
13.45	--	0.43	--	--
13.71	--	0.33	7.13	33.53
13.85	6.64	--	--	--
13.95	--	0.24	--	2.81
14.20	3.01	0.52	--	--
14.33	--	--	6.32	9.81
14.42	8.86	--	--	--
14.70	6.77	--	--	--
14.80	--	0.80	--	--
15.03	9.38	0.44	1.23	6.27
15.25	--	0.27	2.49	--
15.38	5.66	--	--	--
15.46	--	0.35	--	--
15.53	--	--	--	2.85
15.69	--	0.39	16.43	--
15.79	7.32	--	--	--
15.96	--	0.91	--	0.54
16.23	--	--	15.85	--
16.38	--	0.56	--	--
16.57	--	0.48	--	--
16.71	--	--	--	1.58
16.81	2.02	--	--	--
16.95	--	0.12	--	0.75
17.13	--	0.15	--	--
17.22	--	--	0.26	--
17.34	0.16	--	--	--
17.49	0.51	0.35	--	--
17.77	--	0.52	--	--
18.00	2.12	0.28	3.20	0.36
18.22	--	--	0.71	--
18.33	1.26	--	--	--
18.49	--	0.33	--	--
18.76	--	0.24	--	--

R T	ϕ-Cl	ϕ-COH	ϕ-NO_2	ϕ-NH_2
18.85	--	--	--	0.59
18.99	--	0.16	--	--
19.17	0.39	0.95	0.24	0.40
19.69	--	--	--	0.35
19.93	1.07	0.17	--	--
20.13	--	1.41	1.05	--
20.23	1.66	--	--	--
20.37	--	--	--	0.58
20.57	--	--	--	0.54
20.74	--	1.10	--	--
21.07	--	--	1.81	0.84
21.20	1.04	--	--	--
21.75	--	--	--	0.43
22.16	--	1.41	1.49	--
22.27	0.66	--	--	--
22.63	--	--	--	0.67
23.15	--	--	--	3.28
23.31	--	0.43	--	--
23.55	2.85	--	--	--
24.03	--	--	--	2.64
24.97	--	0.18	1.34	--
25.19	2.75	--	--	--
25.67	5.31	--	2.18	--
27.11	--	0.01	--	--
27.21	1.18	--	--	--
27.78	--	0.02	--	--
29.81	3.27	0.01	--	3.21

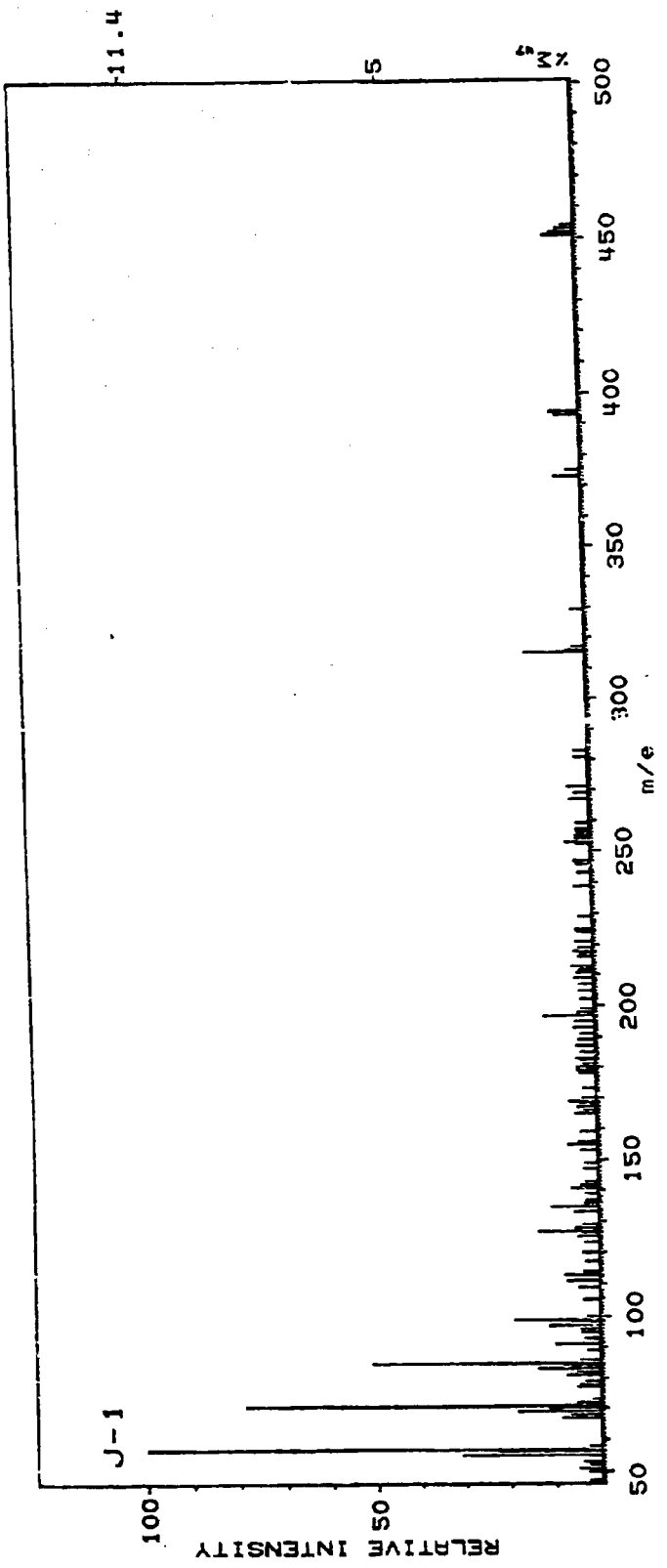
J-1
11.4
5
%
RELATIVE INTENSITY
100
50
50
100
150
200
250
300
350
400
450
500
m/e

Figure 1.

Project A-2

Solvent Treatment of Coal-Derived Liquids (CDL)

Faculty Advisor: L.L. Anderson
Graduate Student: Kwang Eun Chung

Introduction

The objective of this investigation is to separate CDL into chemically different fractions of potential industrial value. Major achievements have included (1) the isolation of paraffinic material, (2) the separation of CDL into highly H-bonded and less H-bonded fractions, (3) the observation of free OH-bonds in the infrared spectra of CDL fractions, and (4) a qualitative interaction study on the highly H-bonded fraction with some model compounds by infrared spectrophotometry.

A new expression for activity in liquid solution has been formulated by analyzing the experimental data of two binary solutions. It is a more general form of Wilson's equation and complies with existing laws and thermodynamic reasoning.

Project Status

Traditionally the activity for component i in solution is expressed as Eq (1), where γ_i is the activity coefficient and X_i the mole fraction.

$$a_i = \gamma_i X_i \qquad (1)$$

In a binary mixture with components A and B, the activities of both components are related to free energy as shown by Eq (2).

$$\Delta g_{mixing} = RT\,(X_A \ln a_A + X_B \ln a_B) \qquad (2)$$

In ideal cases activities are replaced by mole fractions. For convenience excess free energy, gE, has been defined as Eq (3) which becomes Eq (4) using Eq (2).

$$gE = \Delta g_{mixing} - \Delta g_{ideal} \qquad (3)$$

$$gE = RT\,(X_A \ln \frac{a_A}{X_A} + X_B \ln \frac{a_B}{X_B}) \qquad (4)$$

Activity is such an important property of a component in solution that many attempts have been made to construct methods for predicting the activity or activity coefficents from pure-component data alone using the expression for gE.[1]

However this report has outlined the use of an empirical equation for finding the activity.

In the previous report the experiments with a vapor pressure osmometer suggested a new kind of mole fraction, $\bar{X}_A$, for a binary mixture with components A and B as in Eq (5).

$$\bar{X}_A = \frac{\alpha n_A}{\alpha n_A + n_B} \stackrel{?}{=} a_A \qquad (5)^*$$

Since activity is conceptually an effective or corrected concentration, it is necessary to determine if the new form of mole fraction is the same as the activity. In Eq (5) α has been named the "interaction parameter."

Vapor-liquid equilibrium phenomena have been chosen for the testing of Eq (5). In general the partial pressure of a component in a binary solution is given in Eq (6) where P_A^o is the vapor pressure of pure A.

$$P_A = P_A^o \, a_A = P_A^o \, \gamma_A x_A \qquad (6)$$

$$P_A \stackrel{?}{=} P_A^o \, \bar{X}_A = P_A^o \, \frac{\alpha n_A}{\alpha n_A + n_B} \qquad (7)$$

Similar equations can be written for component B. If Eq (5) is correct, the partial pressure will follow Eq (7). Activity and α can be calculated by Eq (6) or (7), respectively, using the partial pressures at different mole fractions.

Initially α was calculated from the partial pressure and mole fraction for one component and then used as a constant to predict the partial pressures at different mole fractions. Figure 1 shows both the predicted values of dioxane-$CHCl_3$ and the experimental data taken from McGlashan and Rastogi's work.[2]

When using constant interaction parameters, the predictions are similar to the experimental data only in the region where α was determined. This was also observed with CS_2-acetone. Although these predicted values are only useful in a limited range of concentrations, the results suggest that Eq (7) will still apply.

Assuming that the concentration effects the parameters, the α's were calculated at different concentrations using Eq (7). Figure 2 shows a plot of α's vs. the mole ratio of the two components. The parameters are introduced into the activity expression so that they will decrease with an increase in the mole ratio. The two interaction parameters of dioxane-$CHCl_3$ behave in the same fashion. These trends

*$\bar{X}_A$ in Eq (5) is slightly different from that in the last report. The difference will be explained in the next report.

suggest an equation of reversible reaction rate which is similar to Eq (8),

$$-\frac{d\alpha}{dr} = k_1\alpha - k_2(\alpha_o - \alpha) \qquad (8)$$

where α_o is α at r=0.

Solving Eq (8) resulted in Eq (9) which gives α in terms of mole ratio, r, two constants, k_1 and k_2, and the initial value, α_o.

$$\alpha = \frac{k_1}{k_1+k_2}\alpha_o e^{-(k_1+k_2)r} + \frac{k_2}{k_1+k_2}\alpha_o \qquad (9)$$

The last term in Eq (9) is similar to an equilibrium value in the reversible reaction rate expression since α approaches this value as the mole ratio r becomes large; it will be called "final value" because of its association with mole ratio instead of time. The constants, k_1 and k_2, can be calculated from a few initial and final values of α. For a binary system, two equations are needed.

Eq (7) complemented with Eq (9) gave good predictions for dioxane-$CHCl_3$ (Figure 1). The predicted values are within $\pm 4\%$ of the experimental ones. The same solution was studied by McGlashan and Rastogi. Their results also showed good agreement with the experimental values but the deviation between the experimental and predicted values were not specified.

Table 1 gives two sets of predicted vapor compositions for nitromethane-CCl_4, one using Wilson's equation and the other using the new expression Eq (7) with (9). Both the predictions in Table 1 are very close to the experimental data at higher mole fractions. However at lower ends, Wilson's equation predicted much higher values while the new expression reproduced the experimental values exactly.

The good agreement with the experimental values is due to the simplicity of Eq (5) which gives the parameter α in terms of an exponential function. Eq (5) and Figure 2 describe the activity behavior exactly. The exponential functions have been introduced to approximate the exact relationship between α and mole ratio.

Although only two liquid solutions have been analyzed, they are good examples of non-ideal cases, one negatively and the other positively deviating from Raoult's Law. The satisfactory results with these solutions indicate the capability of Eq (5) and (9) as an activity expression.

Once the activity expression was formulated empirically, its validity was tested to see how the

expression complied in general with existing laws and related theories using binary liquid solutions with components A and B. Raoult's and Henry's Laws both describe the behavior of liquid solutions within limited concentration ranges.[5] As the mole fraction of component i, i being either A or B, approaches unity, Raoult's Law holds , that is $\gamma_i \simeq 1$ and $a_i \simeq x_i$ in Eq (1). The new expression for the activity agrees with Raoult's Law since as $X_A \to 1$, $n_A >> n_B$:

$$a_A = \lim_{\frac{n_A}{n_B} \to \infty} \frac{\alpha n_A}{\alpha n_B + n_B} \cong \frac{\alpha n_A}{\alpha n_A} = 1 \simeq X_A$$

As the mole fraction of component i approaches zero (Henry's Law) Eq (1) becomes

$$a_i = \gamma_i X_i = \lim_{x_i \to 0} H x_i$$

where H is the Henry's Law constant. Eq (5) will reduce to

$$a_A = \lim_{\frac{n_A}{n_B} \to 0} \frac{\alpha n_A}{\alpha n_A + n_B} \simeq \frac{\alpha n_A}{n_B} \simeq \alpha \frac{n_A}{n_A + n_B} = \alpha X_A$$

Therefore it also satisfies Henry's Law.

For wider concentration ranges Wilson's equation, Eq (10), has been used for numerous binary mixtures as well as multi-component solutions.[1] Table 1 only compares Wilson's equation with the new expression for a specific case. The application of the new expression to other systems will be discussed.

$$\frac{g^E}{RT} = X_A \ln \frac{\xi_A}{X_A} + X_B \ln \frac{\xi_B}{X_B} \qquad (10)$$

$$\xi_A = \text{local volume fraction} = \frac{b_A X_A}{b_A X_A + b_B X_B} \qquad (11)$$

In Eq (10) ξ_A is defined as Eq (11) where b_A and b_B are constants, changing only with temperature. (ξ_B is defined in the same manner.) Eq (11) and (5) are essentially the same by substituting mole fractions in Eq (11) with the numbers of moles and dividing the denominator and numerator by b_B. Wilson's equation Eq (10) is the same as Eq (4) except that ξ's replace a's. In the empirical derivation Eq (4) itself was not altered in anyway. Thus in both the expressions, the form of the thermodynamic formula Eq (4) has been conserved; only the activities have been replaced.

The good results reported with Wilson's equation may be due to the correct forms of Eq (10) and (11).[1] However the lack of the concentration dependency of b_A and b_B in Eq (11) resulted in only approximate agreements with the

experimental values (see Table). An improvement on Wilson's equation has recently appeared in the literature.[6-8] An expression for gE has been formulated based on Wilson's equation by adding more parameters. From that an activity coefficient relationship was derived. However a more direct approach seems possible by first measuring the activities and then deriving the activity expression, hence the new expression Eq (5) and (9).

Physically the activity can be considered as a "corrected" or "effective mole fraction" from Eq (1). Eq (5) indicates that the "effective mole fraction" is to be formulated from "effective number of moles." The effective number of moles could be different from a nominal number of moles due to the interactions in solution. Using coefficients a and b to obtain effective values from nominal values n_A and n_B, an activity expression is

$$a_A = \frac{an_A}{an_A+bn_B} = \frac{a/b\ n_A}{a/b\ n_A+n_B} = \frac{\alpha n_A}{\alpha n_A+n_B}$$

where $\alpha=a/b$. A better understanding of the physical phenomenon provides a means to explore other unknowns.

Future Work

Applications of the new activity expression will be sought for the characterization of the products as well as the solvents, the selection of the solvents for separation operations and the reactivity studies on the separated products.

References

1. J.M. Prausnitz, "Molecular Thermodynamics of Fluid-Phase Equilibria," Prentice-Hall, Inc., Englewood Cliffs, New Jersey, 1969, Chapters 6 and 7.

2. M.L. McGlashan and R.P. Rastogi, Trans. Faraday Soc., 54, 496 (1958).

3. I. Brown and F. Smith, Aust. J. Chem., 8, 501 (1955).

4. J. M. Prausnitz, "Molecular Thermodynamics of Fluid-Phase Equilibria," Prentice-Hall, Inc., Englewood Cliffs, New Jersey, 1969, p 231.

5. F. Daniel and R.A. Alberty, "Physical Chemistry," 4th ed, John Wiley and Sons, Inc. New York, N.Y., 1975, Chapter 4.

6. D.S. Abrams and J.M. Prausnitz, A.I.C.H.E. (Amer. Inst. Chem. Eng.) J., 21, 116 (1975).

7. T. Tsuboka and T. Katayama, J. Chem. Eng.(Japan), 8, 181(1975)

8. ibid, p 404.

Table 1

Comparison of Predicted Vapor Compositions of Nitromethane (A) - CCl_4 (B) Solution at 45°C.*

Experimental[3]			Predicted Y_A Wilson's Eq (4)[4]		Eq (7) with (9)	
X_A	P	Y_A	Y_A	Error %**	Y_A	Error %
0.0459	287.4	0.130	0.147	+13.1	0.130	0
0.0918	297.2	0.178	0.191	+ 7.3	0.178	0
0.1954	302.9	0.222	0.225	+ 1.4	0.222	0
0.2829	302.6	0.237	0.236	- 0.4	0.239	+0.8
0.3656	301.4	0.246	0.243	- 1.2	0.247	+0.4
0.4659	298.9	0.253	0.251	-0.8	0.254	+0.4
0.5366	296.9	0.260	0.258	-0.8	0.257	-1.2
0.6065	293.3	0.266	0.266	0	0.262	-1.5
0.6835	287.1	0.277	0.279	+0.7	0.272	-1.8
0.8043	264.7	0.314	0.318	+1.3	0.316	+0.6
0.9039	214.6	0.408	0.410	+0.5	0.415	+1.7
0.9488	171.0	0.528	0.524	-0.8	0.533	+0.9

*X_A = mole fraction of A in liquid phase.

Y_A = mole fraction of A in vapor phase.

P = total vapor pressure in mmHg.

**Calculated by the present author.

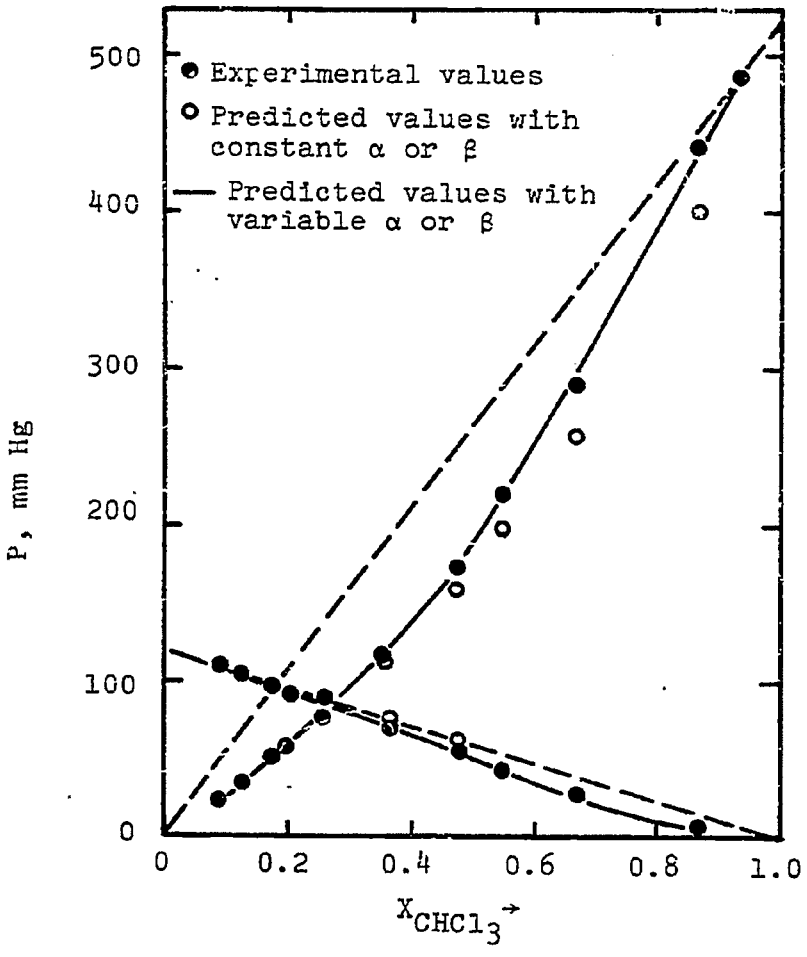

Figure 1. Partial Pressures of Dioxane (A) - $CHCl_3$ (B) Solution at 50°C.

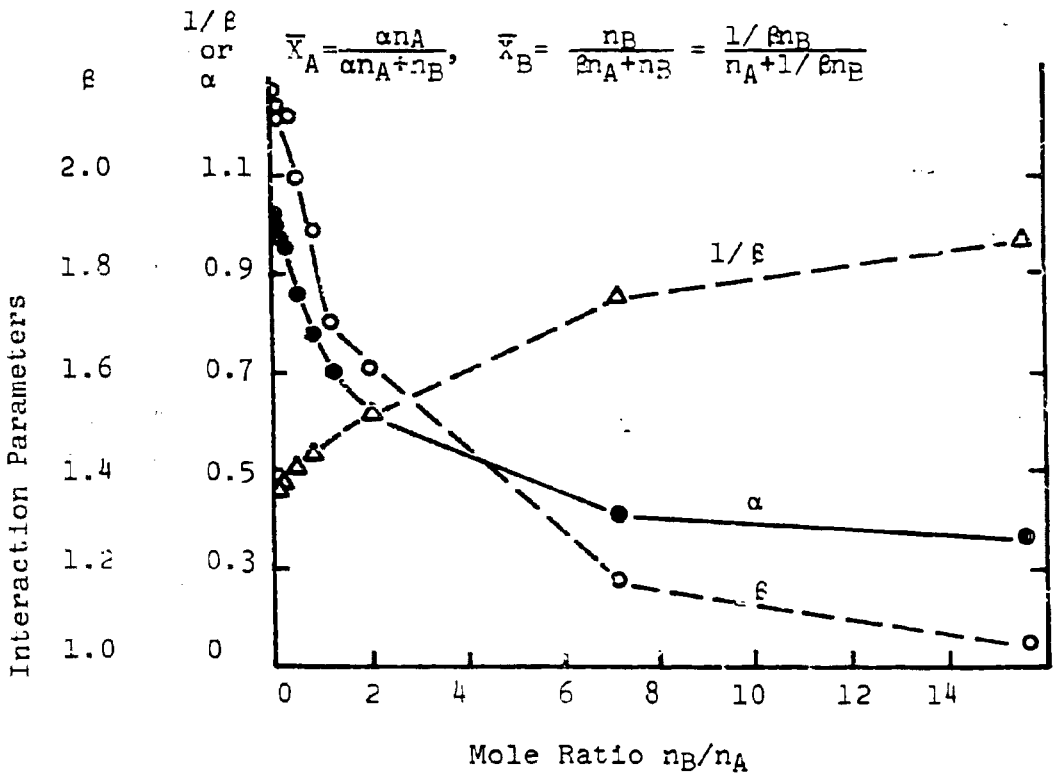

Figure 2. Changes of the Interaction Parameters, α and β, with Mole Ratio in Dioxane (A) - $CHCl_3$ (B) System at 50°C.

Project A-4

Steam Reforming of Aromatic Compounds

Faculty Advisor: A.G. Oblad
Graduate Student: Shri Goyal

Introduction

The objective of this research is (1) to study the thermodynamics and kinetics of steam reforming and (2) to develop an appropriate catalyst for the steam reforming of aromatic compounds. The general reforming process and details of the equipment have been previously reported.

Project Status

The results of the thermodynamic simulation studies for benzene-steam reforming were reported in the previous report. The calculations for naphthalene and anthracene have been done and the results may be obtained upon request. Also the effects of various parameters have been analyzed.

Effect of Steam Ratio

Figures 1 and 2 show the equilibrium concentrations of CH_4, CO, CO_2 and H_2 as a function of the steam ratio at 500°C and 400 psig and 800°C and 400 psig, respectively. An increase in the steam ratio decreases methane and carbon monoxide but increases the hydrogen. Also increased steam decreases CO_2 at lower temperatures but increases it at higher temperatures.

Effect of Pressure

The effect of pressure on the equilibrium concentration of the product gas is shown in Figures 3 and 4. An increase in pressure decreases CO and H_2 but increases CO_2 and CH_4. The abscissa on Figure 4 is logarithmic (base 10). The plots are straight lines showing that the pressure has approximately a logarithmic (base 10) effect on the equilibrium concentration and the heating values of the gases (also shown in Figures 1-6 in the previous report).

Effect of Temperature

The equilibrium constant values are shown in Figure 5 as a function of temperature for both the methane-steam and water-gas shift reactions. The methane-steam reaction is the most favorable. The equilibrium concentrations of CH_4 and CO_2 decrease with an increase in temperature but the concentrations of H_2 and CO increase sharply (Figure 6). Since methane

decreases with a rise in temperature the heating values should decrease.

Effect of H/C Ratio in Feed

The H/C ratio of the feed is the most important factor in operating a steam reformer to avoid coking the catalyst. The thermodynamic minimum steam ratio and operating steam ratio increase as the H/C ratio decreases in the feed at 800°C and 400 psig as shown in Table 1. The equilibrium concentrations of CH_4, CO, CO_2 and H_2 and the heating values as a function of the H/C ratio in the feed at 800°C, 400 psig with a steam ratio of 5 are shown in Figure 7. The decreases in the H/C ratio causes equilibrium concentrations of CH_4 and H_2 to decrease and those of CO_2 and CO to increase. A higher thermodynamic minimum steam ratio with a decrease in the H/C ratio of the feed indicates that the methane-steam reaction is less favored.

The results of steam reforming show the possibility of its practicality and will be used to define the activity and selectivity of the catalyst and their approach to equilibrium concentrations.

Future Work

Experimental work on the kinetic data and catalyst will begin. A set point of methane reforming will be obtained to check the activity of the catalyst while reforming other aromatic compounds. A gas chromatograph will be calibrated and the steam reforming of benzene will begin.

Table 1

Thermodynamic Minimum Steam Ratio

Feed	H/C Ratio	Thermodynamic Minimum Steam Ratio	Operating Steam Ratio
Methane (CH_4)	4.00	0.80	3
Naphtha ($CH_{2\cdot2}$)	2.20	1.20	6
Toluene (C_7H_8)	1.14	1.39	?
Benzene (C_6H_5)	1.00	1.41	?
Naphthalene ($C_{10}H_8$)	0.80	1.44	?
Anthracene ($C_{14}H_{10}$)	0.71	1.45	?

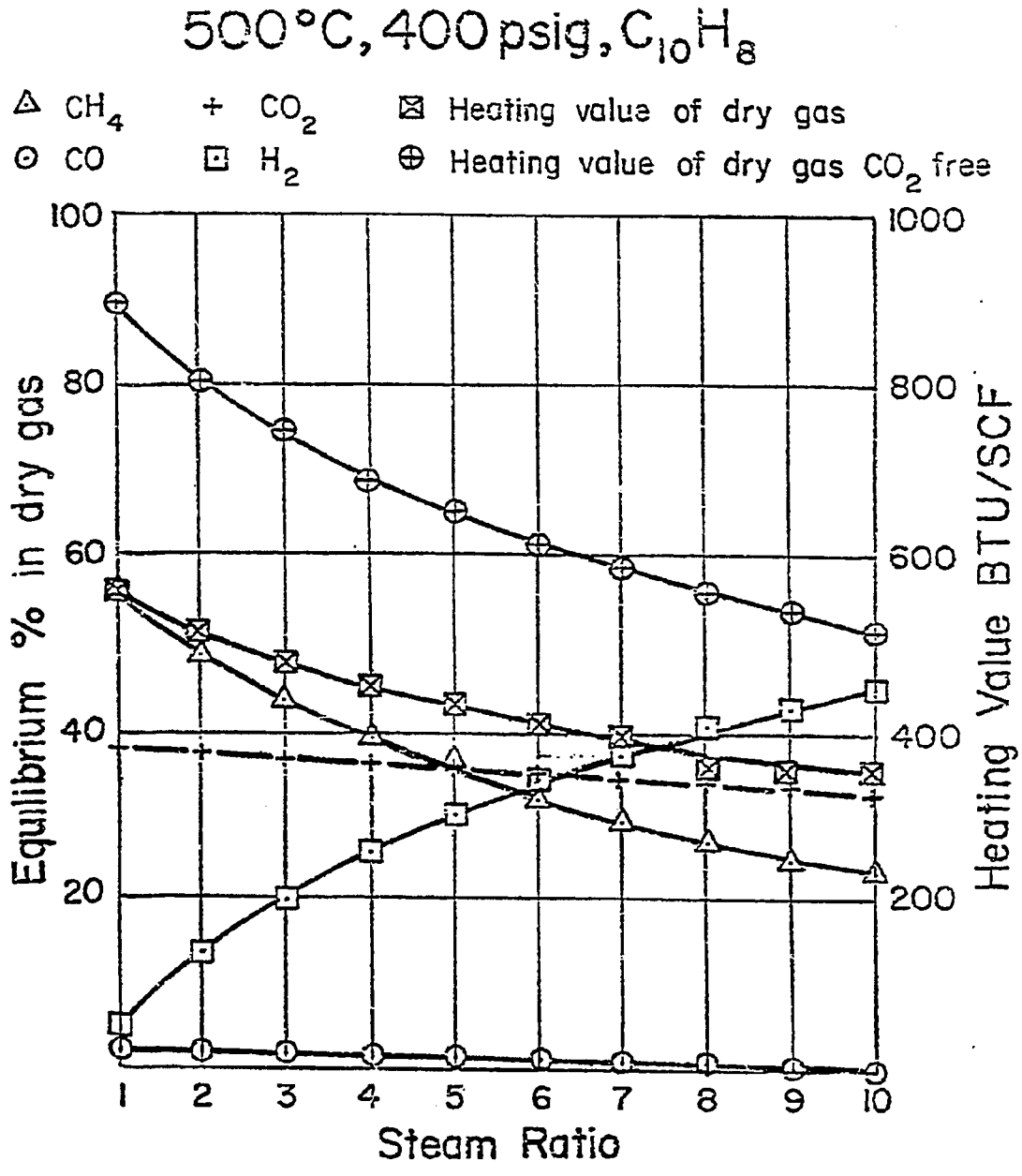

Figure 1. Equilibrium concentrations of product gas as a function of steam ratio at 500°C, 400 psig and for naphthalene.

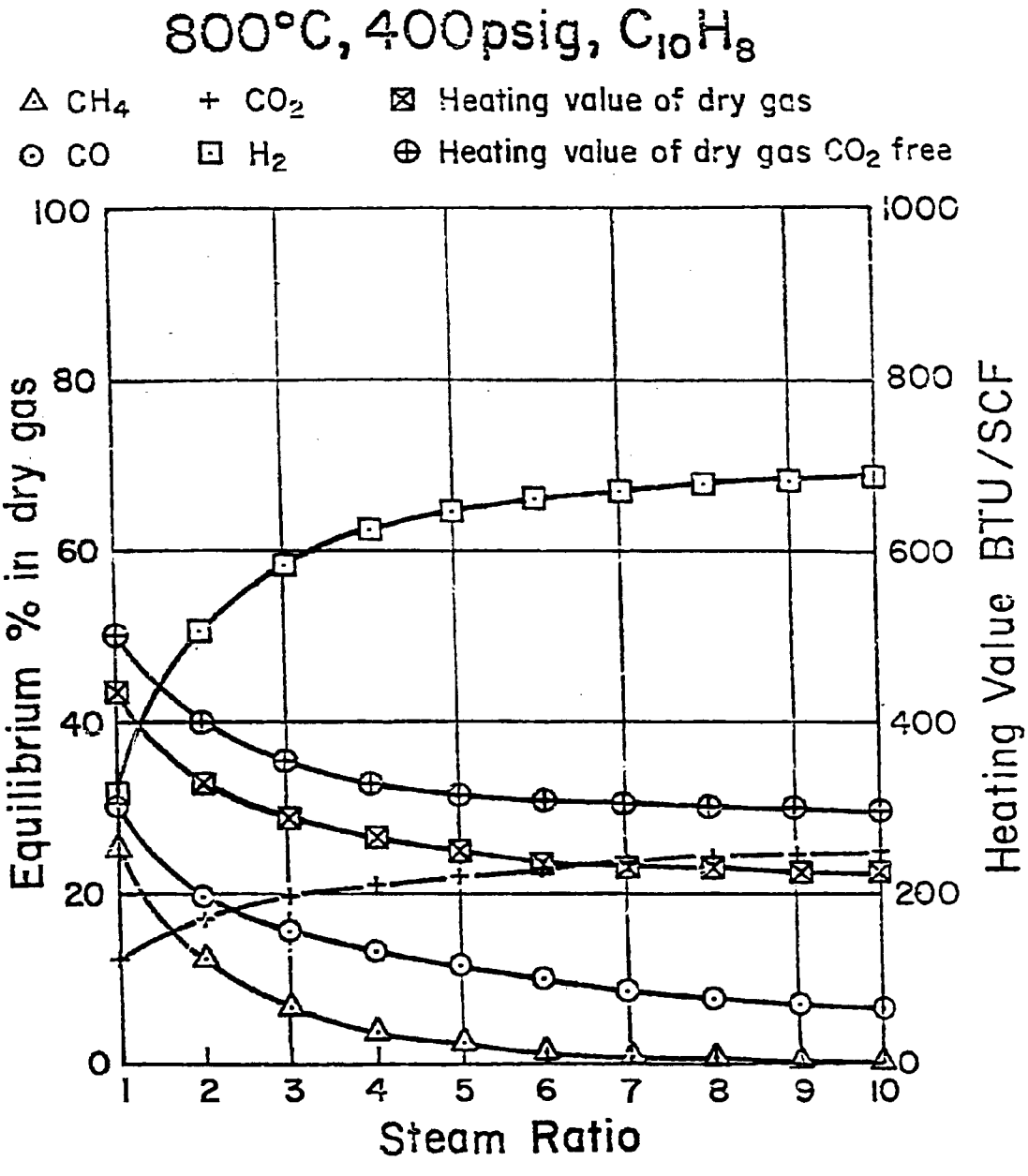

Figure 2. Equilibrium concentrations of product gas as a function of steam ratio at 800°C, 400 psig and for naphthalene.

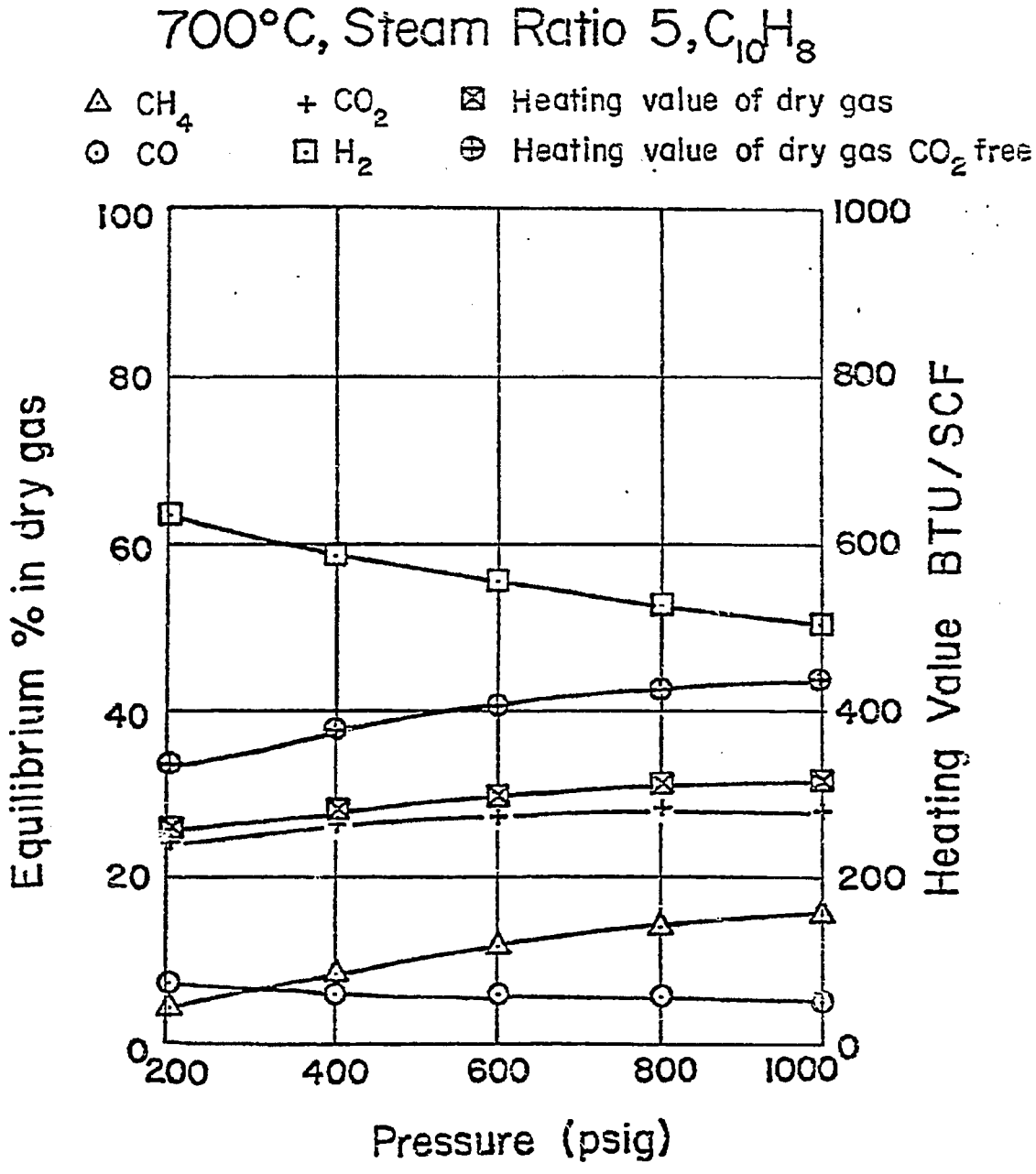

Figure 3. Equilibrium concentrations of product gas as a function of pressure at 700°C, steam ratio 5 and for naphthalene.

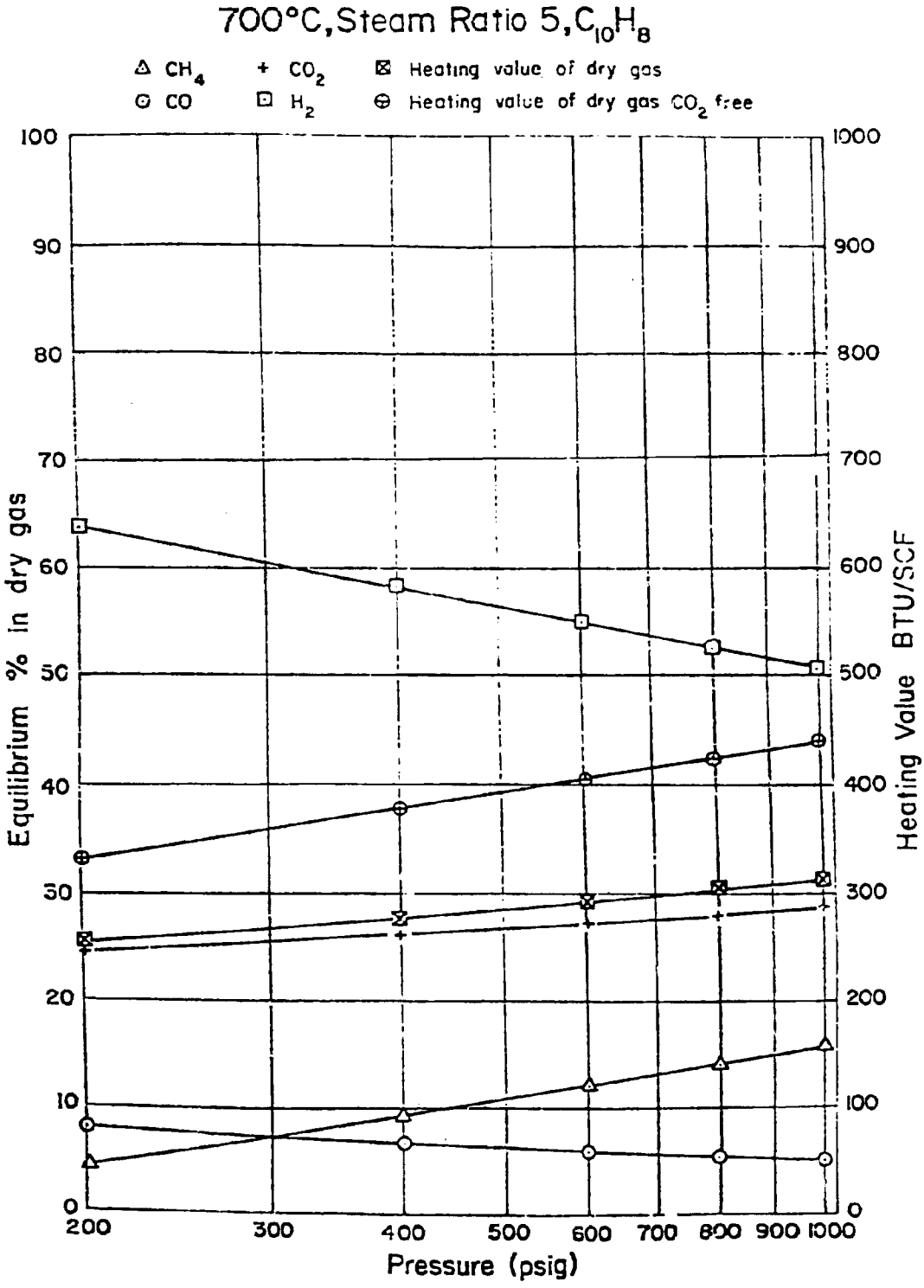

Figure 4. Equilibrium concentrations of product gas as a function of pressure at 700°C, steam ratio 5, and for naphthalene on semi-log chart.

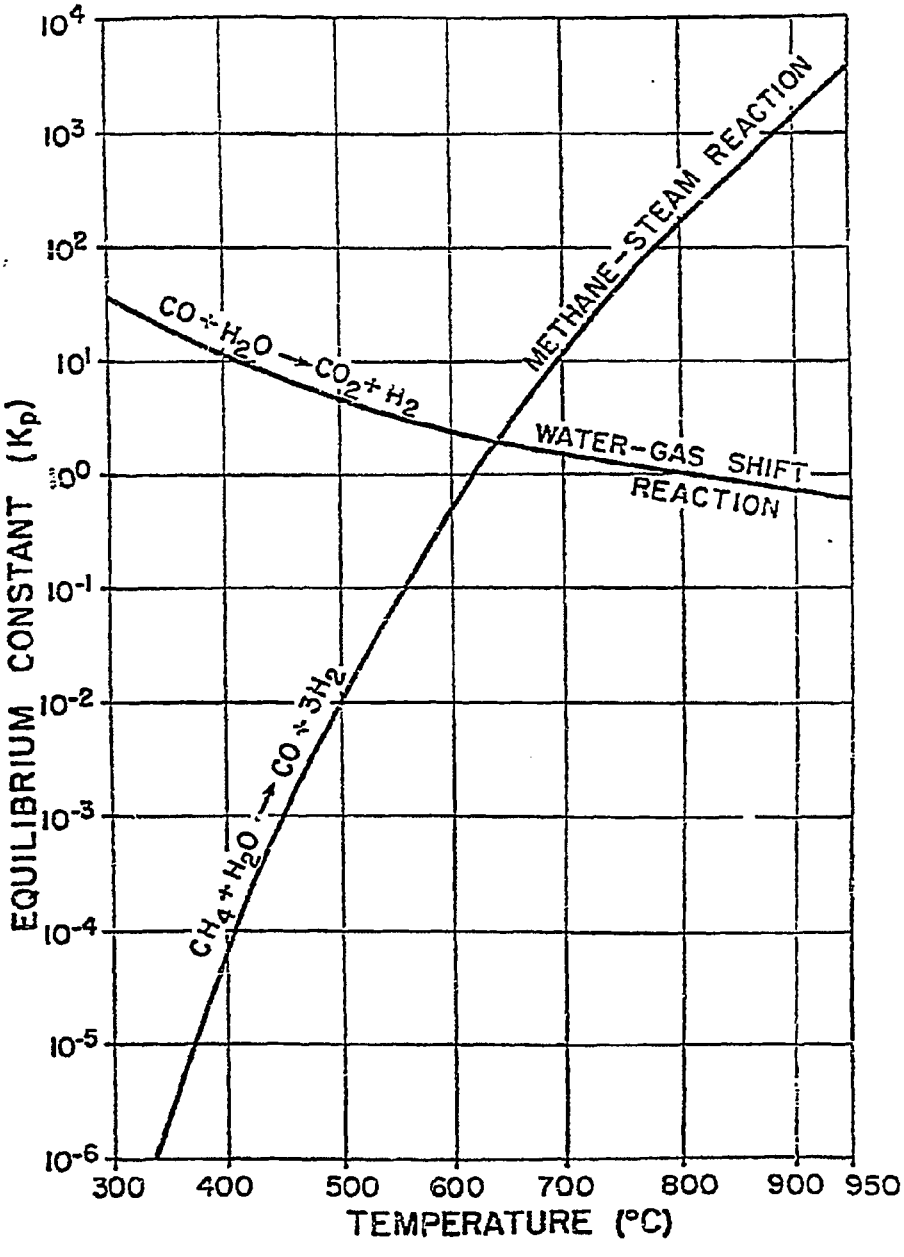

Figure 5. Equilibrium constants for methane steam reaction and water gas shift reaction as a function of temperature.

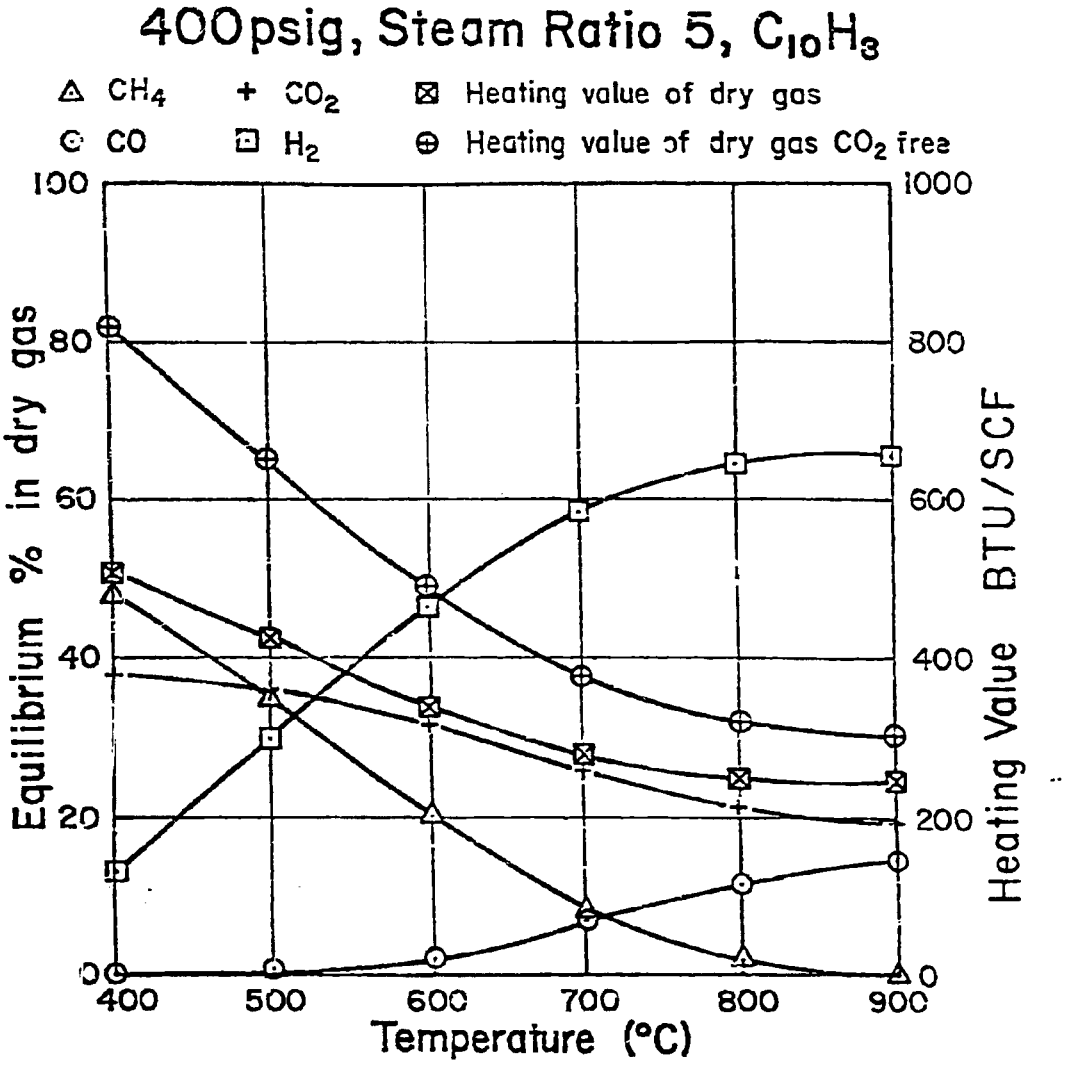

Figure 6. Equilibrium concentrations of product gas as a function of temperature at 400 psig, steam ratio 5 and for naphthalene.

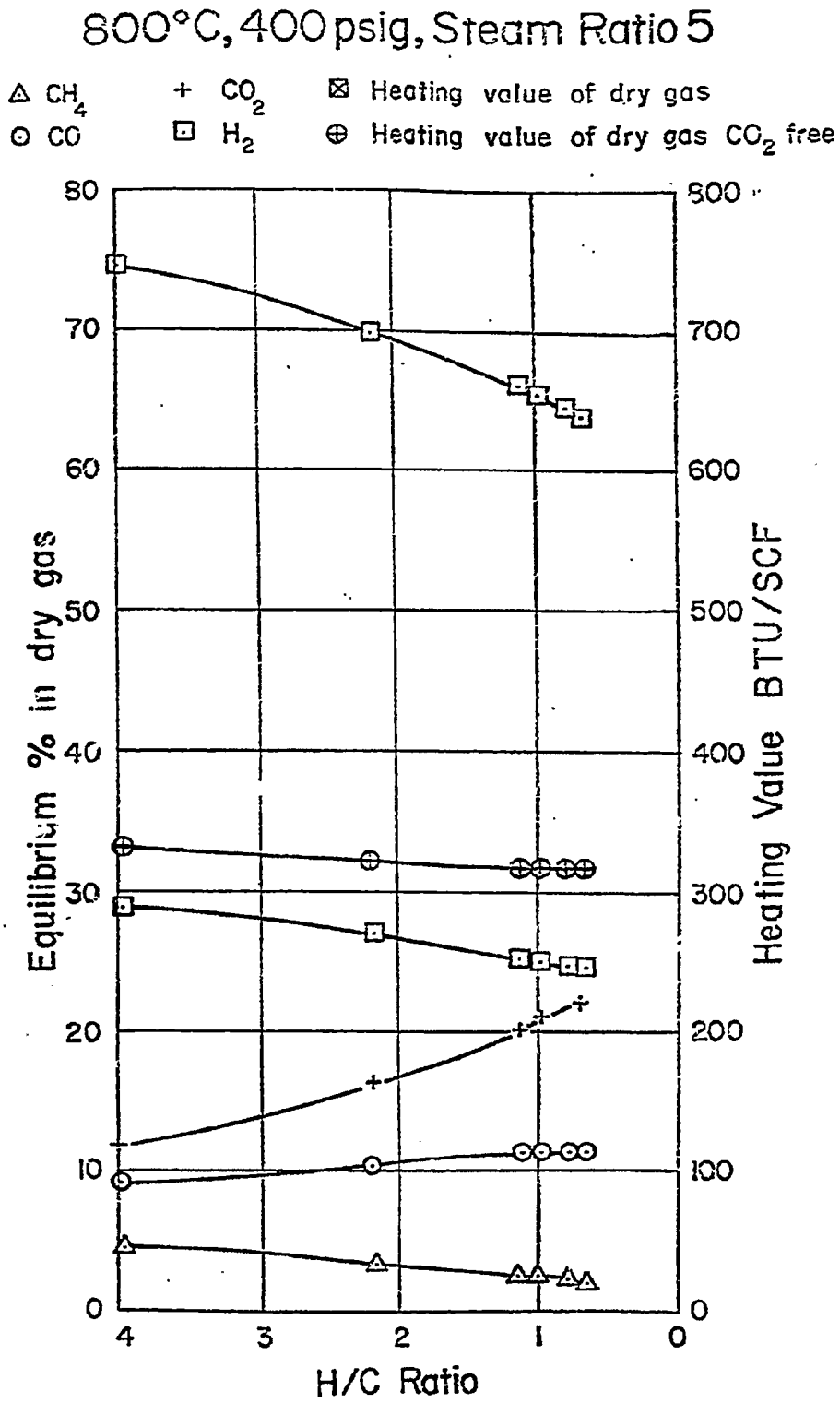

Figure 7. Equilibrium concentrations of product gas and heating values as a function of H/C ratio in feed at 800°C, 400 psig and steam ratio 5.

Project A-7

Study of Thermal and Vapor Phase Catalytic Upgrading to Coal Liquids

Faculty Advisor: A.G. Oblad
Graduate Student: R. Ramakrishnan

Introduction

This project is concerned with high temperature free radical and catalytic hydrogenolysis of coal-derived liquids. Preferential rupture of condensed ring aromatics by these means could lead to improved yields of liquid hydrocarbons and decrease consumption of hydrogen as compared with conventional processes for upgrading these liquids. Accordingly experimental apparatus and procedures have been developed to carry out this program.

The specific objective of this project is to study the reaction kinetics and product distribution of the hydrogenolysis of relevant pure compounds in a temperature range of 500-700°C and a hydrogen pressure up to 2000 psi.

Project Status

The reactor surface was sulfided to obtain better results of thermal hydrogenolysis of coal-derived liquids. The fabrication of a 500 l gas holder was also necessary to obtain a good material balance. Hexadecane was the first compound to be studied.

The effect of pressure on the conversion of hexadecane to gases and the composition of the gas products is shown in Figure 1. As reported earlier the concentration of olefins decreased with an increase in pressure. A plot of C_1, C_2, C_3 and C_4 as a function of pressure is given in Figure 2. The compositions are fairly constant indicating that the cracking mechanism does not change with pressure. Increased conversion of the feed to gas at higher pressures suggests that the hydrogen pressure aids in initiating the cracking of hexadecane.

Major components in the liquid product other than hexadecane were C_5, C_6, C_7 and C_8 paraffins (the higher the paraffin number the lower the concentration).

To minimize plugging and coking of the reactor, air was passed through the reactor between every few experiments to remove any coke deposits. The gas was analyzed for CO and CO_2 with no appreciable concentration of either in the combustion product. The reactor was sulfided before each batch of

experiments.

Future Work

More experiments are planned to study the effects of the temperature, reaction time and hydrogen/hexadecane ratio on hexadecane.

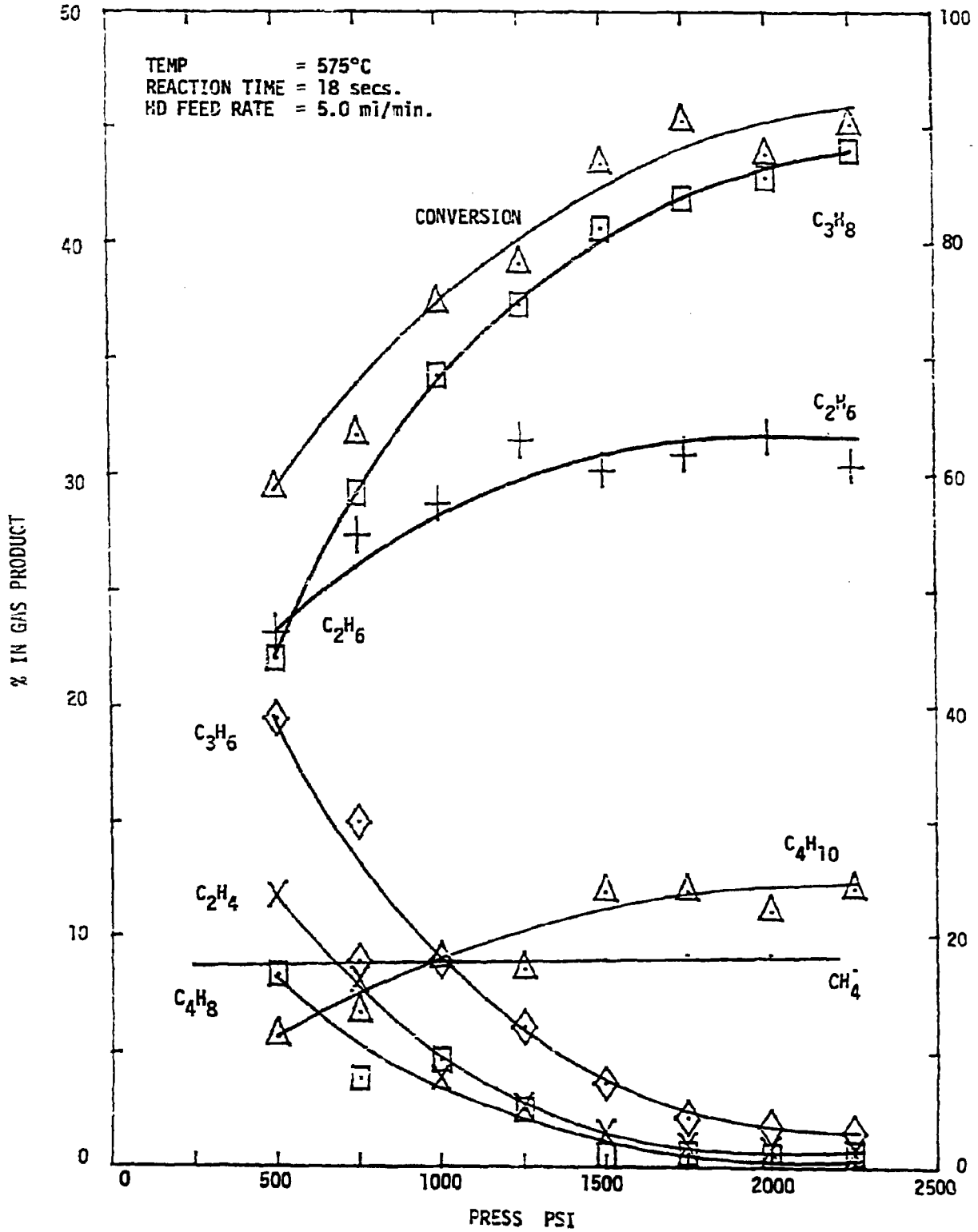

EFFECT OF PRESSURE

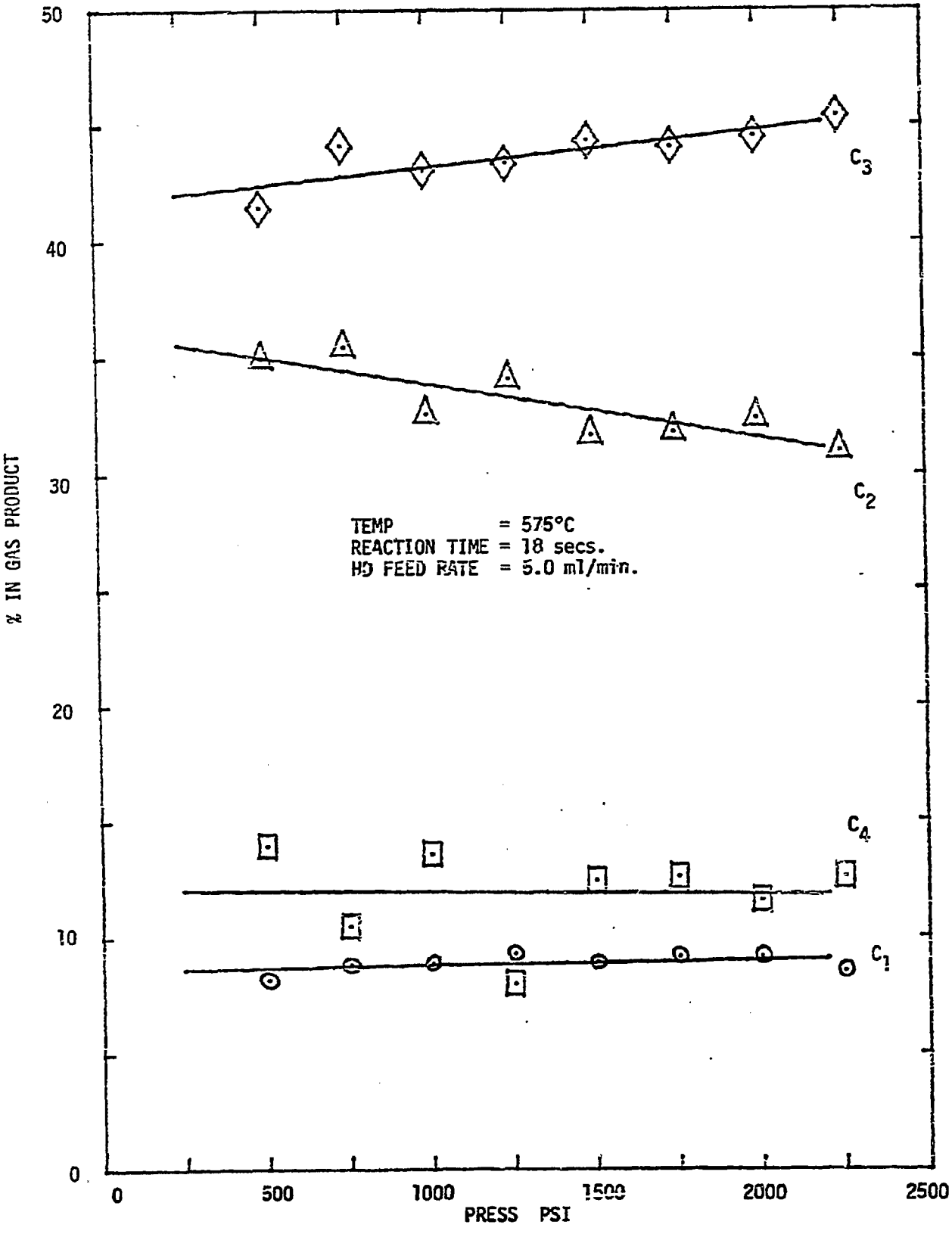

EFFECT OF PRESSURE

Project A-8

Synthesis of Light Hydrocarbons from CO and H_2

Faculty Advisor: A.G. Oblad
Graduate Student: C.H. Yang

Introduction

The objective of this research is to develop suitable catalysts for hydrogenation of carbon monoxide to C_2-C_4 gaseous lower molecular weight compounds particularly olefinic. Characterizations have been carried out intensively to different potential formulations. Catalytic stability, kinetics and mechanisms will be studied.

Conversion of CO has been found to correlate best with total metal loadings for the Co/Cu Al_2O_3 catalyst system. Hydrocarbon selectivities remained insensitive to the Co/Cu ratio and the C_2-C_4 fraction was at its maximum. Iron catalysts are more promising in the production of C_2-C_4 olefinic hydrocarbons.

Project Status

The following cobalt/copper catalysts have been prepared by coprecipitation methods:

CC #1 Co : Cu : Al_2O_3
4.8 : 5.2 : 90

CC #2 Co : Cu : Al_2O_3
4.8 : 5.2 : 90

The above catalysts used NH_4OH as the precipitation agent.

CC #3 Co : Cu : Al_2O_3
4.8 : 5.2 : 90

CC #4 Co : Cu : Al_2O_3
4.8 : 5.2 : 90

The above catalysts used NH_4CO_3 as the precipitation agent. CC #1 and CC #3 were prepared by adding the respective bases to the boiling metal nitrate solution. CC #2 and CC #4 were prepared by slowly pouring the metal nitrate solution into the precipitation agent solution. All results are shown in Figure 1.

The different preparation methods gave different activity. CC #1 and CC #2 were lower in activity compared with CC #3 and CC #4. The adding of the metal nitrate solution to the

precipitation agent solution gave a higher activity than the catalysts that were prepared by adding the precipitation agent to the boiling metal nitrate solution even with the same final pH values. However, the data of these catalytic activities did not match with the previous catalytic activity when $NaCO_3$ was used as the agent under similar conditions. Small amounts of sodium are probably very critical to the activity of Co/Cu catalysts.

The following iron catalysts have been prepared from metal nitrate solutions coprecipitated with NH_4CO_3. The resulted precipitate had a pH of 9.

Hematite iron ore
Magnetite iron ore

Fe #1	Fe	Cu	K
	100	20	2
Fe #2	Fe	Cr	K
	100	20	2
Fe #3	Fe	Zn	K
	100	20	2
Fe #4	Fe		
	100		
Fe #5	Fe	K	
	100	0.2	

Iron ore has been used in the Sasol Fischer-Tropsch process for the last 25 years in South Africa. Two iron ore samples were tested for their activity. They showed lower activity at 250°C, 500 psig, H_2/CO of 6/4, and SP vel of 1.06 cc/g sec when compared with other iron catalysts previously tested and reported. Although product selectivity yielded 50% of the C_2-C_4 fraction, the olefin/paraffin ratio was very low.

The activity of Fe #4 was low even at 250°C. However product selectivity yielded around 50% of C_2-C_4 and an O/P of 0.7. Fe #5 was a potassium promoted iron catalyst. Addition of K increased the activity of the catalyst to a high level of CO conversion (57% at 240°C, 500 psig, H_2/CO = 6/4, SP vel = 1.06 cc/g sec). The O/P ratio in the C_2-C_4 fraction was increased to 1.2. However, the selectivity to the C_2-C_4 fraction dropped to 35% and the CO_2 fraction increased to 32%.

Addition of Zn, Cr and Cu to the iron catalyst already promoted by K showed a high selectivity toward CO_2 production. However each metal had its own characteristic effect on the iron catalysts.

Fe #1 showed the same results as the previously tested catalyst ZK #22. It had only a fair degree of CO conversion but was highly selective to CO_2 with a low O/P in the C_2-C_4 fraction.

Chromium had a profound effect on both iron and cobalt catalysts. Fe #2 showed almost no activity even at 260°C, 500 psig and a H_2/CO of 6/4.

Zinc promoted the iron catalyst to a very high O/P ratio in the C_2-C_4 fraction. Catalyst Fe #3 showed a high activity for CO conversion, a high product selectivity to CO_2 but only about 15% to C_2-C_4. However this catalyst did get the highest O/P ratio in the C_2-C_4 fraction.

Future Work

The Co-Cu /Al_2O_3 catalyst system will be continued for optimal metal loadings with the appropriate promoter. Kinetic studies will be applied to the optimum catalysts. Extensive screening of iron catalysts with different promoters and supports will be continued.

Figure 1. Activity of CC#1, #2, #3, #4 at Different Temperatures.

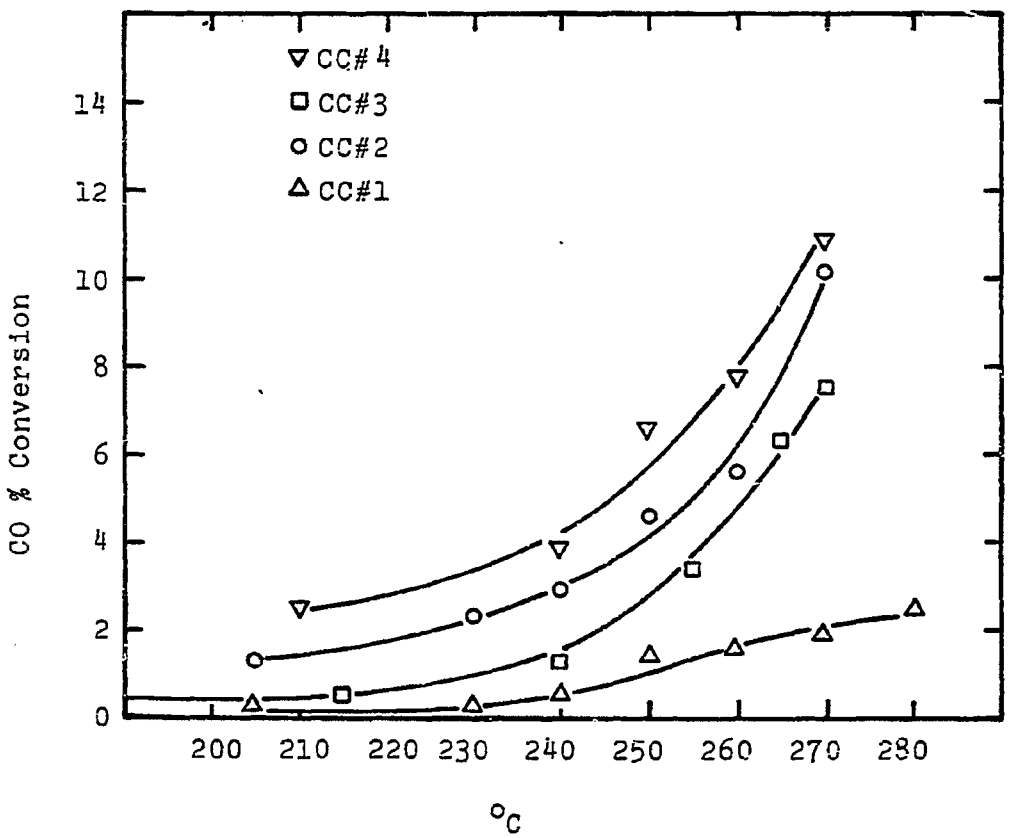

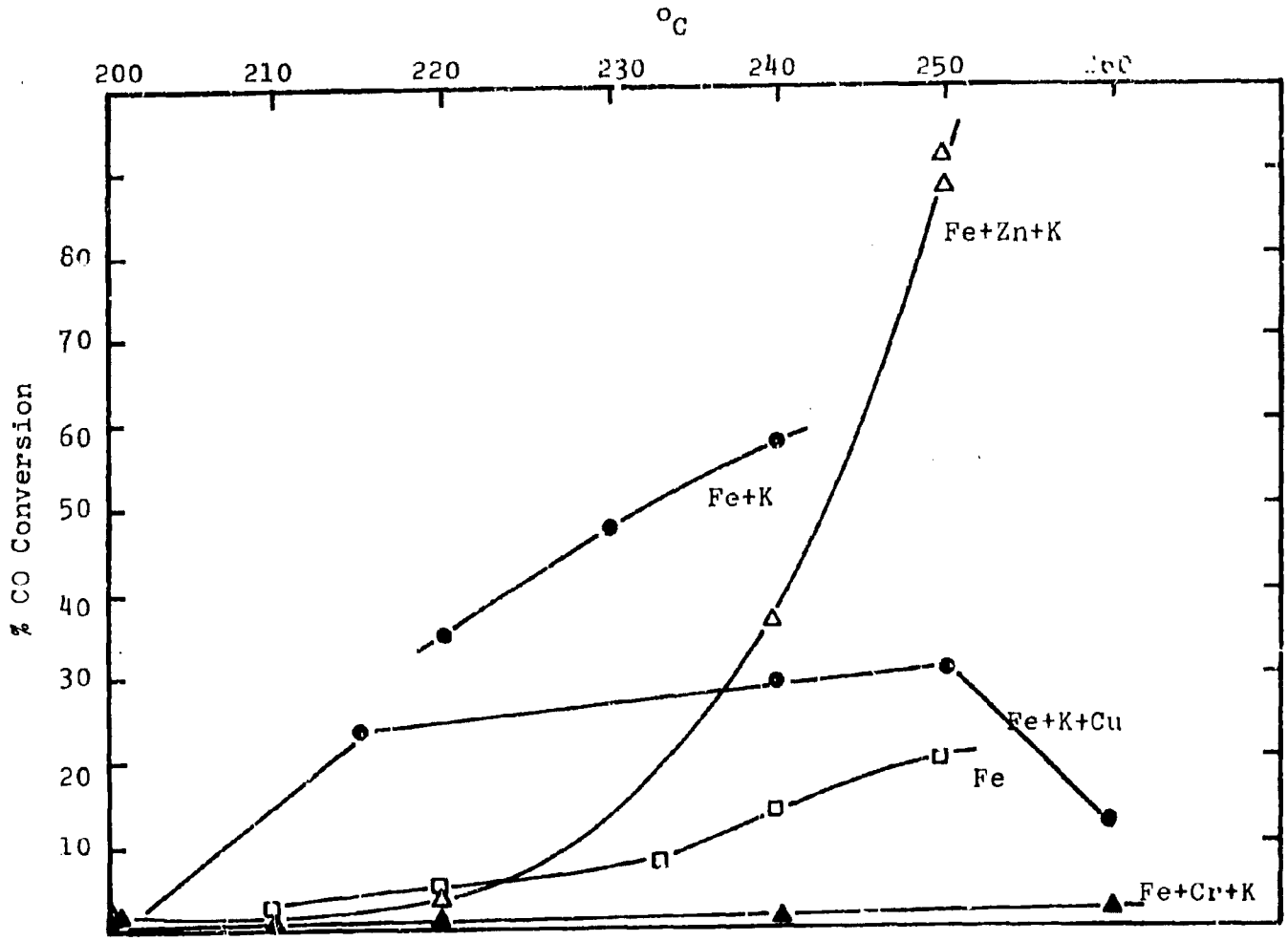

Figure 2. Activity of Iron Catalysts at Different Temperatures, 500 psig, H_2/CO = 6/4, Sp Vel = 1.06.

Project A-8

Synthesis of Light Hydrocarbons from CO and H_2 (Continued)

Catalyst Characterization Studies

Faculty Advisor: F.E. Massoth
Graduate Student: Brent Bailey

Introduction

This phase of the project is to supplement the high pressure reactor studies by detailed examination of the catalyst properties which enhance catalyst activity and selectivity. This is accomplished by characterization studies performed on the same catalysts which have been run in the reactor. Of particular interest are metal areas, evidence for alloy formation, phase structures and catalyst stability. Also, variables in catalyst preparation and pretreatment are examined to establish effects on catalyst properties. Finally, in-situ adsorption and activity are being studied under modified reaction conditions with a number of well-characterized catalysts to obtain correlating relationships.

Work has thus far concentrated on the $CoCu/Al_2O_3$ catalyst, which has shown some potential for producing low molecular weight hydrocarbons from the CO + H_2 Fischer-Tropsch reaction. Hydrogen pretreatment of the oven-dried catalyst was necessary to achieve large metal areas. Furthermore, a low temperature hold in H_2 during pretreatment gave even better metal dispersions. Cobalt helped to disperse the copper. The catalyst should not be calcined in air or N_2 prior to reduction. SEM studies indicated a possible alloy in the reduced state.

Project Status

A new TGA system has been set-up. A reactor has been built to fit an existing microbalance and furnace. A new gas flow system was also designed and built. The TGA system was tested and the results were essentially identical to those of the previous system.

Adsorption measurements were made on five additional catalysts which had been run in the high-pressure reactor. These were pretreated in H_2 at 520°C to similate the treatment given in the reactor prior to running the CO + H_2 reaction. To relate the adsorption values to catalytic activity for the various catalysts, a reaction rate order must be known. This has not been determined yet, but the

analogous methanation reaction over cobalt has been shown to obey a rate approximately of the form:[1]

$$r = kp_H p_{CO}^{-1/2} \qquad (1)$$

where r is the rate of formation of methane, k is the rate constant, p_H and p_{CO} are the partial pressures of H_2 and CO. Assuming this rate form also applies to our reaction, and since H_2 is in excess, the integrated equation becomes

$$\frac{kp_H}{SV} = 1 - (1-\frac{c}{100})^{3/2} \qquad (2)$$

where SV is the space velocity and c the conversion. Since p_H/SV is constant in all runs, changes in c reflect changes in k for various catalysts.

The results, together with previous values, are presented in Figure 1 in which the function of equation (2) is plotted against the weight of O_2 adsorbed (proportional to the metal surface area of the reduced catalyst). A fairly good correlation is obtained showing that reactivity is proportional to metal area for this catalyst. The adsorption values above about 9 mg/g are ineffective in that no additional conversion can be obtained. This may not hold at lower reaction temperatures where conversions will be lower.

The initially prepared catalysts using copper chloride in the preparation were less active than later catalysts using copper nitrate. This may be due to a lower metal area obtained in the presence of chloride. The data given in Table 1 demonstrate this effect for catalysts having approximately the same metal compositions. It is not known why the anion in the preparation affects the final metal dispersion at present.

Scanning electron microscope studies were done on AH-5, ZK-38 and ZK-42. Results at 12,000X on the ZK-42 catalyst showed a close relationship in the dispersion patterns of copper and cobalt on the surface. This is consistent with but not proof of alloy formation in the reduced catalyst.

Future Work

The present area of study will be continued. The characterization data will then be compared to catalyst

conversions obtained in the high pressure reaction to develop correlations between catalyst properties and activities.

Future areas of study are ESCA examination of reduced catalyst and IR studies of metallic surface components. In the IR study, peaks for CO adsorption on copper alone and cobalt alone on the support will be compared against copper-cobalt peaks in an attempt to confirm alloy formation.

References

1. M.A. Vannice, J. Catal., 37, 462 (1975).

Table 1.

Effect of Copper Salt on Catalyst Properties and Activities

Catalyst	6	7	38
Cu salt used	Cl	Cl	NO_3
O_2 adsorption, mg/g	6.3	5.6	7.6
CO conversion, %	66	58	89

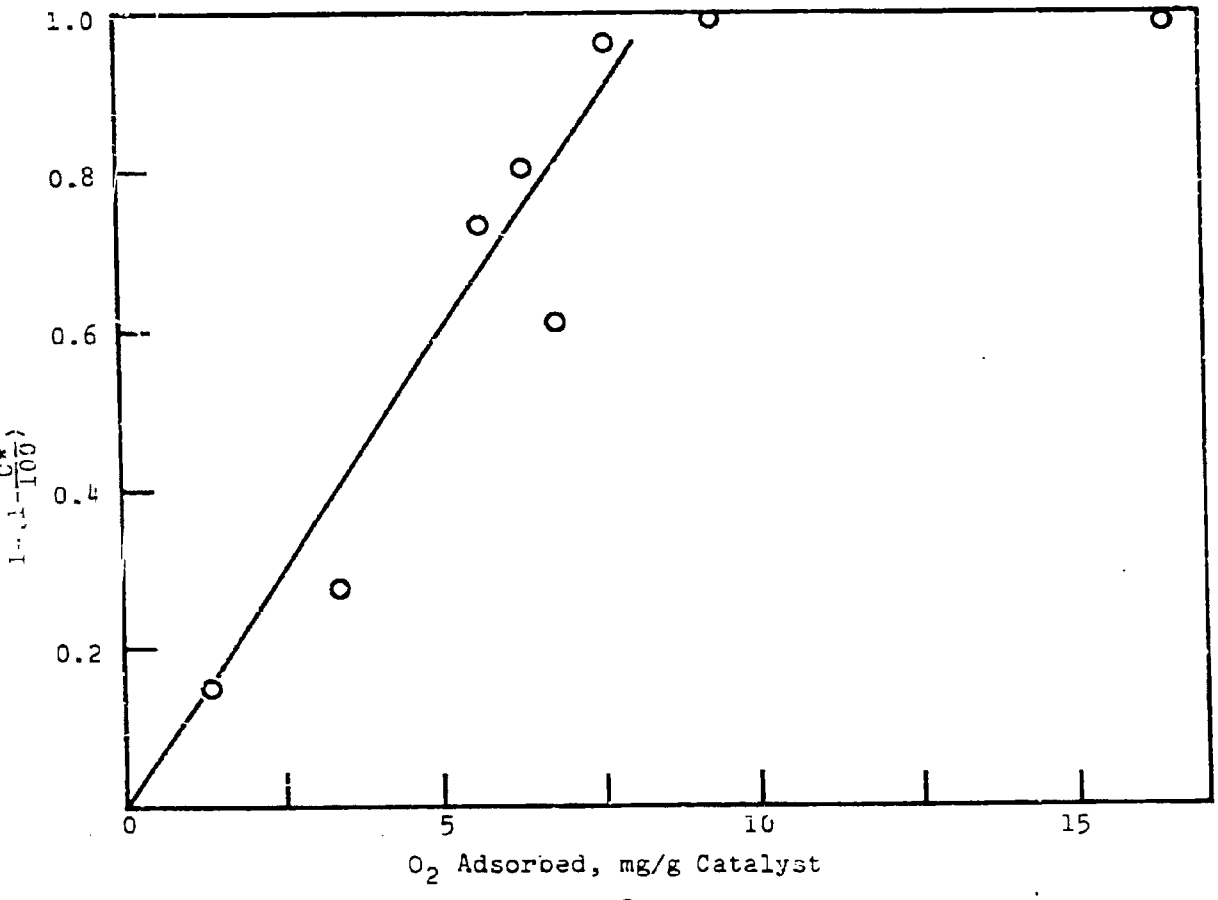

Reaction Conditions: 275°C, 750 psi,
$2H_2/CO$, 0.77 cc/g sec

Figure 1. Variation in Catalyst Activity with Amount of Oxygen Adsorbed.

*C=conversion.

Project B-1

Development of Optimum Catalysts and Supports

I. Development of Technique

Faculty Advisor: F.E. Massoth
Graduate Student: M. Moora

Introduction

This project involves assessing diffusional resistances within amorphous-type catalysts. Of primary concern is the question of whether the larger multiringed aromatics found in coal-derived liquids will have adequate accessibility to the active sites of typical hydrocracking catalysts. When molecular dimensions approach pore size diameters, the effectiveness of a particular support is reduced owing to significant mass transfer resistance. A window effect, also known as configurational resistance, may even result when adsorbate molecules are of the same order of magnitude as the micropore dimensions.

The project objective can be achieved through a systematic study of the effect of molecular size on sorptive diffusion kinetics relative to pore geometry. Conceptually, the diffusion of model aromatic compounds is carried out using a stirred batch reactor. The preferential uptake of the aromatics from the aliphatic solvent is measured using a UV spectrometer. Although the adsorbate molecules utilized thus far do not approach catalyst pore diameters, a substantial amount of ground work is needed before more advanced studies involving larger molecules can be attempted.

Previous work has involved design, fabrication and performance testing of a stirred batch recycle reactor to study diffusional kinetics. Early tests showed bulk transfer resistance to be negligible at stirring speeds exceeding 300 rpm. Inital runs using chrysene as the adsorbate on an alumina catalyst showed an unexpected slow desorption following a rapid adsorption. The majority of this desorption was caused by moisture present in the solvent (or air above the solvent) displacing chrysene from the catalyst surface. However, recent tests using greater spectrometer sensitivity indicated that some desorption was still actually occurring, which was undetected using the previous analytical sensitivity. This subject will be discussed in more detail.

Adsorption rates showed a particle size effect, suggesting diffusion-controlled adsorption. Further work with mathematical

modeling of the data showed that a shrinking-core or shell-progressive phenomenon could adequately describe the diffusional process. The solution to Fick's Law in spherical coordinates correlated with the experimental data poorly.

The effect of solvent upon rate was also observed. Chrysene adsorbed from cyclohexane solvent showed somewhat slower kinetics and reduced fractional uptake compared to identical tests using n-heptane. The lower diffusivity of chrysene in cyclohexane could be related to the decrease in sorption kinetics.

Project Status

The major investigative effort during this quarter was directed towards low depletion adsorption. Previous tests used to study the kinetics of chrysene adsorption on alumina utilized relatively large reductions in bulk concentration, on the order of 50 to 70%. The tests reported here were carried out using the same initial concentration (25 mg/l) of chrysene, but fractional depletion was held below 10%. The concept of using minimum depletion in studying the kinetics is based upon equilibrium considerations. For example, where high solution depletion occurs and adsorption is irreversible (strong), it may be possible to achieve nonequilibrium adsorption. A concentration profile could exist in the catalyst pellet cross-section, with the greatest concentration being at the outside edge. With time, this maldistribution of adsorbate would tend to adjust towards an equilibrium if slow desorption occurred. A low depletion of adsorbate from the bulk solution would minimize non-equilibrium adsorption and would be better suited to the study of kinetics.

Figure 1 is a plot of bulk chrysene concentration vs. time for a low depletion run. Note the slow desorption which immediately follows the uptake. Despite treatment of the solvent to remove moisture and flushing of the reactor with dry N_2, the desorption was noted on every low depletion test conducted. Although the rate of desorption is small compared to adsorption, in total magnitude it is as much as 65-70% of the adsorbed amount. Previously, no desorption was thought to occur following a high depletion uptake run. Therefore, a high depletion run was repeated and the desorption process was indeed observed using the more sensitive instrument setting. Further work is underway to determine if impurities present in the chrysene might be causing the desorption.

In spite of the effect of the competing desorption process, the adsorption kinetic data were still treated in the previous manner using the contracting sphere model. Figure 2 represents

the fractional uptake vs. time for the data presented in Figure 1, when desorption was ignored. As detailed in earlier reports, data may be handled to generate a parameter f_d. A linear relationship of f_d and time will result if the diffusion-controlled contracting sphere model applies. The data presented in Figure 2 is plotted as f_d vs. t in Figure 3. A good linear fit is observed.

Table 1 is a compilation of several low depletion runs carried out on two different catalysts and using three different particle sizes. The Harshaw alumina used previously had a mean pore diameter of about 70Å. The Kaiser type C alumina had a substantially higher mean pore diameter of approximately 150Å.

Four runs are given for each catalyst in Table 1; three low depletion tests and one high depletion. The high depletion test was carried out using particles of 18 x 24 mesh size while the three low depletion runs were conducted on 18 x 24, 24 x 35 and 35 x 50 mesh. Reported also are: values of f, fractional uptake; the catalyst weight in grams; the slope of the f_d vs. t plot; the final uptake in mg chrysene per g catalyst and the final bulk concentration in mg/l. All tests were conducted using an initial chrysene concentration of 25 mg/l.

In run C-17 the high depletion run on the Harshaw alumina had a slope of 5.94×10^{-5}, while run CC-1 the high depletion run on Kaiser C type alumina showed a slope of 5.40×10^{-5}. Similar agreement is noted for the other three low depletion runs. All of these show that the effective diffusivity of chrysene is virtually identical in the two catalysts. Since the critical molecular diameter of chrysene is between 9 and 10Å, a negligible amount of drag from the pore walls may be encountered by the molecules as they diffuse towards the particle interior. Therefore the diffusivities in both catalysts would be identical since the mean pore diameter is many times greater than molecular dimensions.

As demonstrated in earlier reports, the contracting sphere model should show an inverse relationship of rate to the square of the particle radius for pore-diffusion control. The particles of catalyst used in each of three mesh sizes were measured using a 60-power magnifier equipped with a measuring scale. Twenty measurements were made for each cut size and an average value calculated. Figures 4 and 5 show the six low depletion runs reported in Table 1 plotted as slope of the f_d vs. t plot against the inverse of r^2. A reasonable linear fit can be made for both sets of tests, thus providing good evidence for the shrinking core model.

Mention was made in the previous report of attempts to measure the concentration profile of adsorbate on the catalyst pellet cross-section. Such quantitative data would be extremely valuable evidence in support of the maldistribution theory presented above. Unfortunately, the low adsorbate concentrations were beyond the detectable limit of the scanning electron microscope or the electron microprobe.

Future Work

Further testing of chrysene impurities as the cause of the unexpected desorption will be done. Several runs using a smaller adsorbate, naphthalene, will also be made. Following the completion of experimental work, the data will be analyzed and correlated for publication as a technical report.

Table 1

Summary of Low Depletion Tests

Run No.	Catalyst	Mesh Size	f	Wt (g)	Slope of f_d vs. t ($\times 10^4$)	Uptake (mg/g)	C_f (mg/l)
LD-9	Harshaw-Al_2O_3	18x24	0.098	0.1782	1.10	3.44	22.55
LD-14	"	24x35	0.100	0.1501	1.87	4.16	22.50
LD-16	"	35x50	0.048	0.0999	6.32	3.00	23.80
C-17	"	18x24	0.859	0.9925	0.59	5.41	3.53
LDC-1	Kaiser C-Al_2O_3	18x24	0.078	0.1812	1.09	2.66	23.06
LDC-5	"	29x35	0.062	0.1490	2.54	2.61	23.45
LDC-7	"	35x50	0.107	0.1460	5.97	4.59	22.32
CC-1	"	18x24	0.641	0.9939	0.54	4.03	8.98

Figure 1 Bulk Chrysene Concentration vs. Time; LD-9; 18 x 24 Harshaw Al_2O_3.

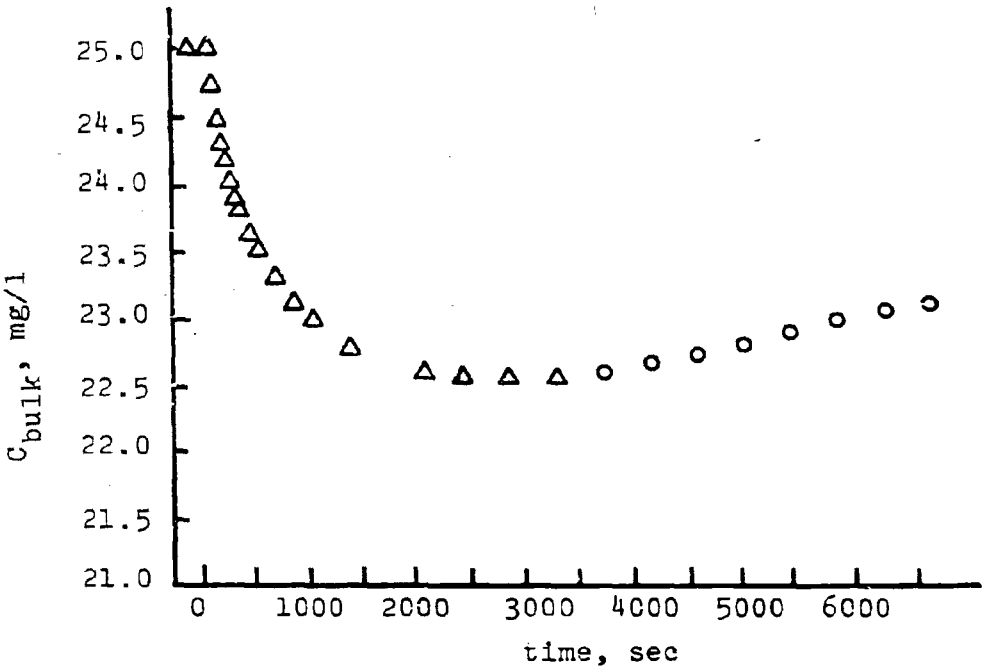

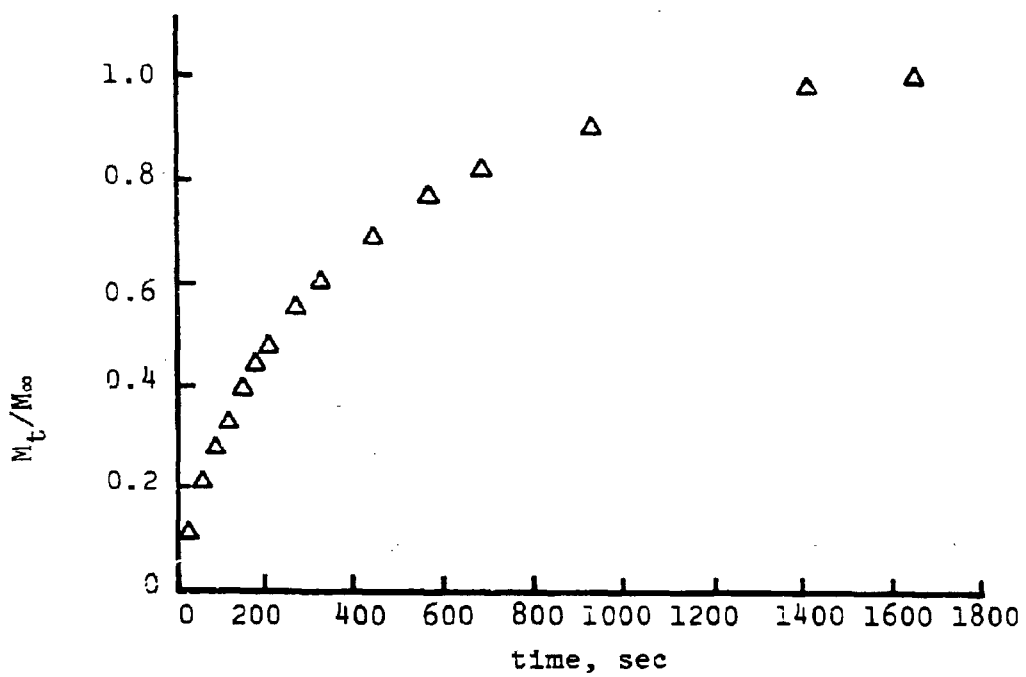

Figure 2. Fractional Approach to Maximum Uptake vs. Time; LD-9; 18 x 24 Harshaw Al_2O_3.

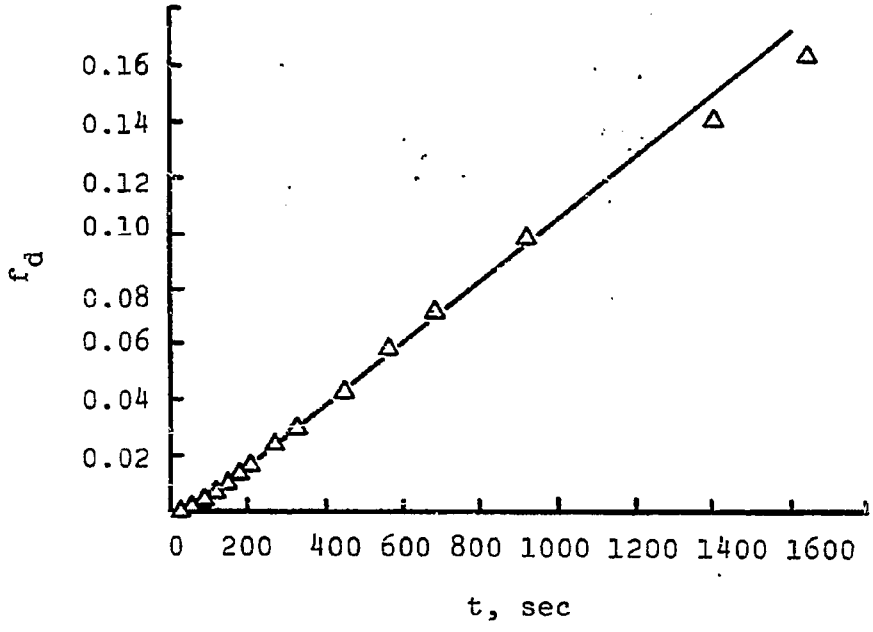

Figure 3. Shrinking Core Parameter f_d vs. t, LD-9 Harshaw Alumina, 18 x 24

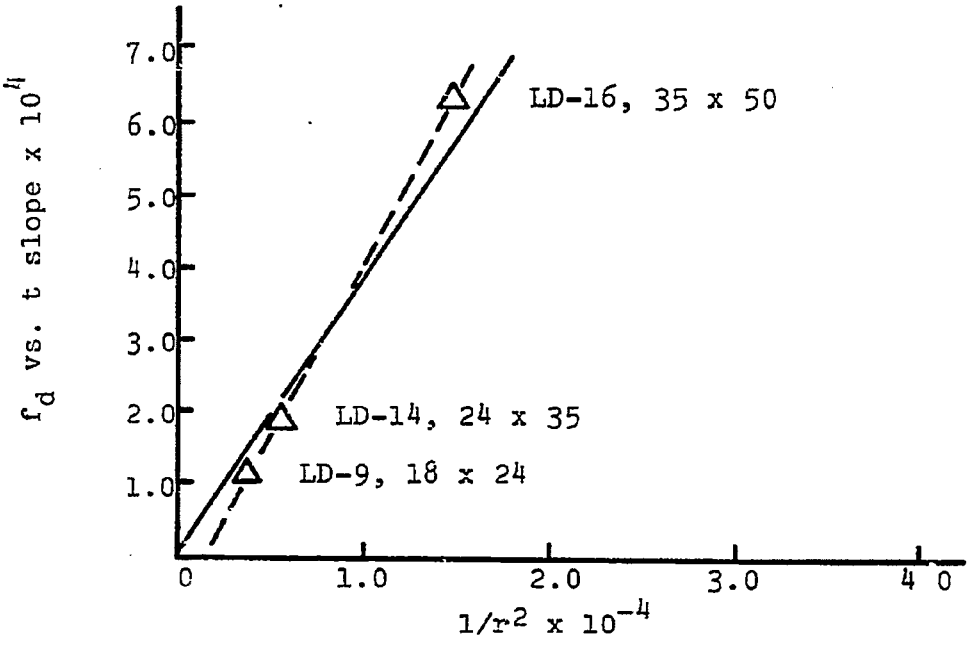

Figure 4. Relationship of Rate to Particle Radius Harshaw Alumina.

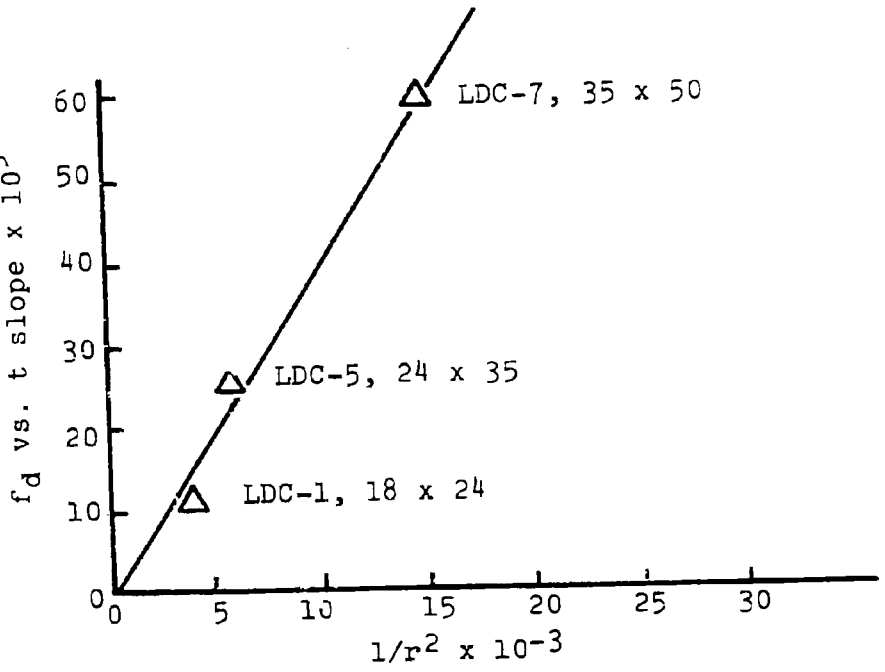

Figure 5. Relationship of Rate to Particle Radius Kaiser-C Alumina.

Project B-1

Development of Optimum Catalysts and Supports

II. Application to Large Molecules

Faculty Advisor: F.E. Massoth
Graduate Student: C.S. Kim

Introduction

Since coal liquids may contain rather large molecules, this phase of project B-1 extents the research to large molecules. The primary emphasis in this study is to assess the diffusional characteristics of macromolecules in realistic catalyst supports. Findings from previous work will be compared to the present results to determine if simple extension of principles derived therefrom will apply to the large molecules. Similar experimental techniques developed in the first phase are employed here, although experiments may have to be run at higher temperatures to achieve adequate solubility and diffusion rates.

Previous work involved the determination of adsorption isotherms at room temperature for polyaromatic compounds such as rubrene, meso-tetraporphine and chrysene with several aluminas. Isotherm data for rubrene and porphine correlated reasonably well with Langmuir isotherms. However, adsorption isotherm measurements on chrysene showed serious data scattering. Desorption tests showed that these aromatic compounds desorbed very little which suggests that adsorption is quite strong and irreversible. Mathematical formulation of the amount of adsorbed aromatics has been tried taking into account the effect of possible nonuniform adsorption along the radius of the catalyst particle based on irreversible adsorption. Adsorption data for chrysene and alumina C showed good correlation by using the formula. Different adsorption isotherms may be obtained at different levels of concentration depletion.

Project Status

Adsorption measurements were made at low solution depletions (5-10%) to check whether nonuniform adsorption was occurring within the catalyst particles during high depletion runs. At low solution depletion, such effects should be minimized. Tests with chrysene on catalyst C alumina still gave considerable scatter even at low

depletions. The results of two test series are shown in Figure 1 with estimated error limits. Scatter was more pronounced at the higher concentrations. A flat region of adsorption is suggested in the range of 10-40 ppm chrysene, but even here large scatter was obtained. Possible sources of error are (1) moisture pickup during handling and storage of samples, (2) impurities in the chrysene and (3) random errors in measuring the UV absorbance, especially in the smaller solution depletion runs. Obviously, the adsorption problem remains unresolved and better experimental procedures are needed.

To assess the acidic properties of the aluminas being used for the adsorption and later diffusion studies, acidity measurements were undertaken using the Benesi method.[1,2] This involves observing color changes of various Hammett indicators after titrating the sample with n-butylamine. Indicators were reagent grade and used without further purification. The n-butylamine was purified by simple distillation. Catalysts were ground into fine particles to remove any diffusional effects on the acidity value. Particle sizes ranged from 150 to 200 mesh. Ground catalysts were calcined at 500° overnight in a muffle furnace, and then about 1 gram of catalyst was put into several screw-capped vials, weighed, sealed and stored in a dry dessicator until use. About 10 ml of dry cyclohexane was added to the catalyst and titrated with an appropriate amount of 0.05 N of n-butylamine in cyclohexane. The catalyst suspension was divided into five fractions and each was subjected to the color test with five different Hammett indicators. Final results are summarized in Table 1.

The results of Table 1 show that most of the acidity resides in strong acid sites of $pK_a < -5.6$. This is contrary to the results of Ratnasamy et al. who found no acidity in this range but appreciable acidity in the range $-5.6 < pK_a < 3$ for their alumina catalyst.[3] Also, their adsorption amounts are less than ours. They may have had some adsorbed water on their catalyst, since exposure of our catalyst to laboratory air resulted in a loss in strong acidity. A similar effect was observed by Hirschler et al.[4] Catalyst C has a higher intrinsic acidity (surface area basis) compared with the others. When comparing the number of active sites used for aromatic adsorption, which was calculated from the adsorption isotherm data for rubrene and porphine, only less than 10% of the strong acid sites may be utilized for aromatic adsorption.

Future Work

Future work will involve adsorption isotherm tests for chrysene with a constant-stirred reactor, by injecting

a concentrated solution of the aromatic into the reactor containing catalyst and solvent. Solute will be injected step-wise to get a range of concentration and adsorption isotherms will be determined. Techniques obtained from the first phase of this project will be utilized for this purpose. Also kinetic studies on diffusion of these large aromatic compounds into catalyst pores will be started.

References

1. H.A. Benesi, J. Amer. Chem. Soc., 78, 5490 (1956).

2. ibid., 61, 970 (1957).

3. P. Ratnasamy, D.K. Sharma and L.D. Sharma, J. Phys. Chem., 78, 2069 (1974).

4. A.E. Hischler and A. Schneider, J. Chem. Eng. Data, 6, 313 (1961).

Table 1

Acidity of Alumina Catalysts

Al_2O_3	Surface Area, m^2/g	n-butylamine titre, mmol/g pK_a range[a]				Strong Acidity $mmol/m^2 x 10^3$
		-8.2 to -5.6	-5.6 to -3.0	-3.0 to 1.5	1.5 to 3.3	
C	200	0.48	0	0	0	2.4
D	245	0.27	0.06	0	0	1.1
L	350	0.22	0	0	0	0.6
CK-300[b]	183	0.17	-	-	-	0.9

[a] Indicators used: Chalcone (pK_a = -5.6), Dicinnamalacetone (-3.0), Benzeneazodiphenylamine (+1.5) and Butter Yellow (+3.3).

[b] A pure γ-Al_2O_3 from Ketjen.

Figure 1. Adsorption Isotherm of Chrysene

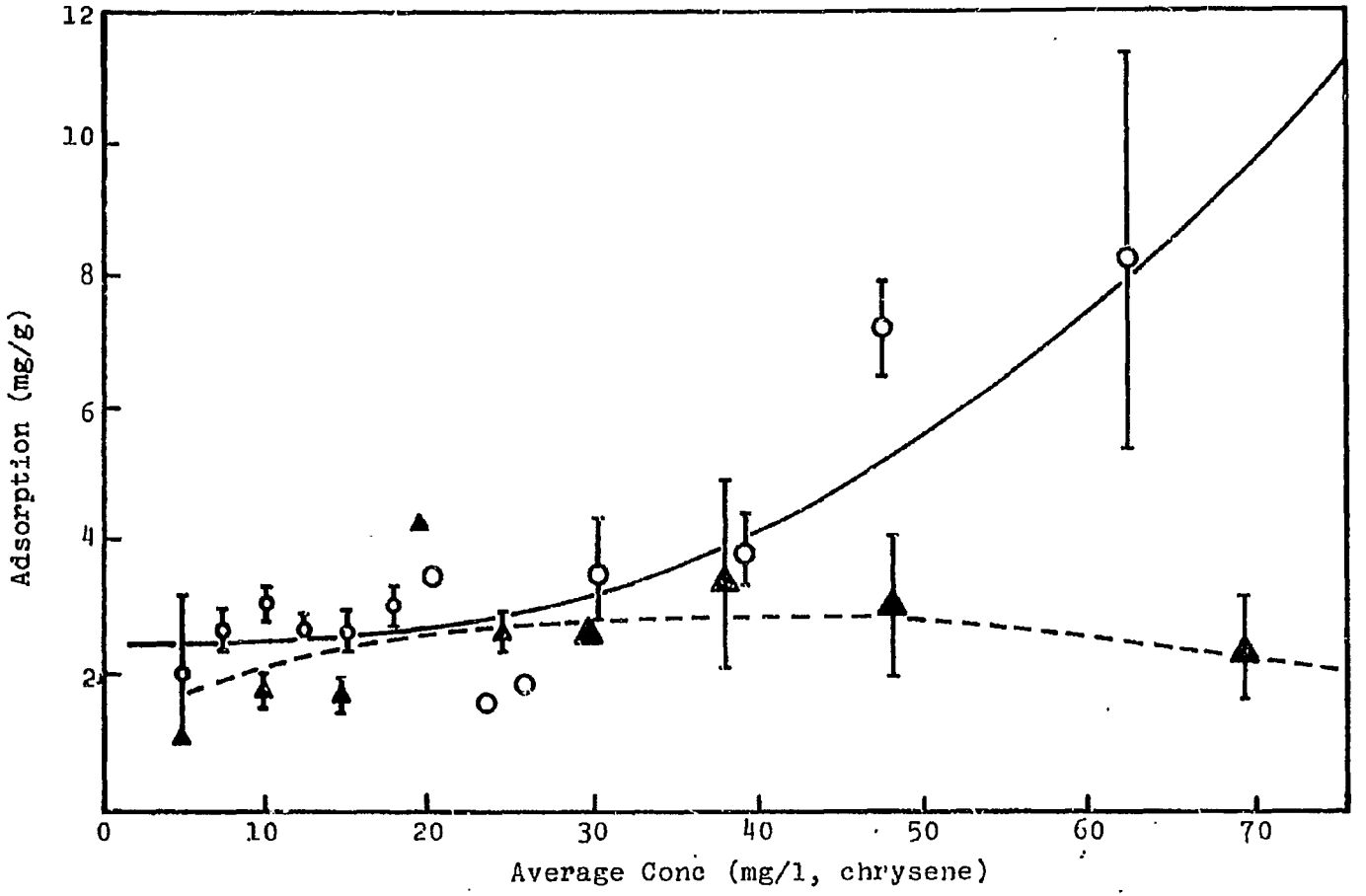

Project B-2 (alternate)

The Effects of Poisoning on the Desulfurization Activity of Cobalt-Molybdate Catalysts

Faculty Advisor: F.E. Massoth
Graduate Student: R. Ramachandran

Introduction

The importance of cobalt molybdena catalysts for hydrotreating and hydrodesulfurization of petroleum feed stocks is well known. These catalysts are also being studied in the hydrodesulfurization and liquefaction of coal slurries and coal-derived liquids. However, these complex feed stocks result in rapid deactivation of the catalysts. To gain an insight into the deactivation mechanism, detailed kinetic studies on the model compound, benzothiophene, is planned to assess the effect of poisons and coke precursors. The studies are planned using a constant stirred microbalance reactor enabling simultaneous measurement of catalyst weight change and activity.

Initial runs on benzothiophene hydrodesulfurization revealed the following:

1) An increase in temperature increased conversion only to a small extent.

2) An increase in benzothiophene partial pressure decreased conversion.

3) An increase in hydrogen sulfide partial pressure decreased conversion.

4) An increase in hydrogen partial pressure increased conversion.

5) Changes in ethylbenzene partial pressure had no effect on conversion.

6) The presence of water had a negligible effect.

7) The presence of pyridine decreased conversion to a large extent. Also benzothiophene and ethylbenzene formed coke in the absence of hydrogen.

The kinetic data obtained on benzothiophene hydrodesulfurization showed considerable scatter. To check the reactor performance, benzene hydrogenation studies were carried out.

Project Status

Previous tests with benzene hydrogenation showed that the microbalance reactor performed as a constant stirred tank reactor (CSTR).[1] However, these tests had been made using a gaseous benzene-hydrogen feed to the reactor, which was accomplished by passing the H_2 stream through benzene in a bubbler. To introduce the high-boiling benzothiophene, a side arm capillary was attached to the bottom of the reactor (see Fig 1 of reference 2) and a mixture of benzothiophene in heptane was introduced into this side arm by means of a Sage pump.[2] Since the initial kinetic data showed considerable scatter, it was decided to check the effectiveness of this new reactor arrangement with the benzene-hydrogen reaction, but now introducing the benzene into the side arm as liquid.

The same catalyst (Ni on Al_2O_3) was used as before.[1] The hydrogen flow was split into two parts, one entering the main shaft and the other the side arm; benzene was pumped into the side arm with the Sage pump. The benzene flow rate affected the degree of conversion indicating that imperfect mixing was occurring. Changes in stirrer speed also had an effect on conversion. At lower benzene concentrations, the variations in benzene flow rate had little effect on conversion compared with variations at higher benzene concentrations. At higher benzene concentrations, the effectiveness of mixing in the reactor is poor. Since the range of concentrations where the reactor performance approached the ideal CSTR was low for kinetic studies with benzothiophene, it was decided to modify the reactor design to improve the mixing characteristics. This entailed changes in the reactor configuration to allow better liquid vaporization and mixing prior to entering the reactor. The new reactor is currently undergoing fabrication in the glass shop.

Meanwhile, experiments are under way to study the reversible hydrogen sulfide adsorption characteristics on Co-Mo and Mo catalysts. The evalution of equilibrium constants from these experiments will be useful in the kinetic studies on benzothiophene later. The adsorption experiments are carried out in the microbalance on the presulfided catalyst. The extent and reversibility are determined from weight changes at various H_2S/H_2 ratios under flow conditions. Buoyancy corrections for gas density of the various mixtures have been

made using an inert charge. Preliminary results showed the expected increase in adsorption with increase in H_2S partial pressure; however, a hysteresis in the isotherm was observed.

Future Work

Sulfiding studies on the Co-Mo catalyst will be followed by that on a Mo catalyst. The effect of thiophene, water, ammonia and pyridine on the hydrogen sulfide adsorption will be studied. This is expected to give an idea of the nature of poisoning on the adsorption equilibrium of hydrogen sulfide on the catalysts.

The modified reactor will be fabricated and initial trial runs will be made with the benzene-hydrogen prior to running benzothiophene.

References

1. F.E. Massoth and S.W. Cowley, Ind.Eng. Chem. Fundamentals, 15, 218 (1976).

2. F.E. Massoth, S.W. Cowley and W.H. Wiser, ERDA Contract No. E(49-18)-2006, Quarterly Progress Report, Salt Lake City, Utah, Jan-Mar 1976, p 45.

Project B-3

Fundamental Studies on Hydrogen Transfer

Faculty Advisor: S.W. Cowley
Graduate Student: D.S. Moulton

Introduction

Coal liquids can be produced by the high temperature hydrogenation of coal impregnated with zinc chloride or similar substances. Zinc chloride catalyzes the reaction, but its role is not fully understood. The kinds of hydrogen transfer which take place on zinc chloride may be important factors in its catalytic activity. Comparing the types of hydrogen transfer promoted by zinc chloride with the types promoted by other catalysts will help determine the hydrogen transfer mechanism.

Hydrogen-deuterium exchange reactions are used to determine the types of hydrogen transfer. Model reactions, characteristic of particular catalytic functions, can be studied on well-known catalysts. The same reactions can then be used to establish the catalytic functions which are active on zinc chloride. The reactions take place in the gas phase. Reactant gases are circulated around a closed loop, glass vacuum system and through the catalyst bed. Continuous analysis of the gas phase with a mass spectrometer gives the extent of exchange.

The glass vacuum system has been constructed with a closed loop and an inert pump to circulate the reactant gases. A quadrupole mass spectrometer (Varian VGA 100) has been assembled on a heavy duty cart. A capillary tube connecting the glass vacuum system to the mass spectrometer inlet allows continuous analysis of the gas stream. Tests have been made on several catalysts of known acid function.

Project Status

The materials and catalysts were from the same stock as previously reported.[1,2] The gamma alumina was given the catalyst pretreatment previously described.[1] It was also evacuated (10^{-3} torr) at 540°C overnight.

A sample of the solid phosphoric acid catalyst was deuterated at 300°C by exposure to D_2O vapor and then evacuated for one hour. A mixture of 2-methylbutane (60 torr) and inert gas was circulated over the catalyst at 300°C for 24 hours without exchange. However surface exchange did occur when 2-methylpropene (6 torr) was added to the circulating mixture.

Figures 1 and 2 show the mass spectra before and after exchange. The parent peak of the 2-methylpropene is at m/e 56 and the peaks at m/e 57 through 64 are partly due to exchanged olefin. Breakdown fragments from the 2-methylbutane also contribute. The parent peak of 2-methylbutane is at m/e 72, and the peaks at m/e 73 to 83 are entirely due to the exchanged paraffin except for the natural isotope abundance at m/e 73. Exchange occurred in both the olefin and the paraffin; the m/e 59-64 peaks would have been smaller if olefin exchange had not occurred.

Deuterium is incorporated into the olefin by combining with a surface deuteron which produces an adsorbed carbonium ion. Loss of a proton returns the ion to an olefin with the deuterium incorporated in the molecule. This process may repeat several times resulting in multiple exchange of hydrogen for deuterium.

$$C-\overset{C}{\underset{|}{C}}=C \xrightarrow[cat]{D^+} C-\overset{C}{\underset{|}{\overset{|}{C}^+}}-C(D) \xrightarrow[cat]{-H^+} C-\overset{C}{\underset{|}{C}}=C(D)$$

(adsorbed)

The first peaks to appear after olefin addition were in the m/e 60-63 range indicating that the most rapid reaction was exchange with the olefin. Exchange peaks in the m/e 73-83 range appeared later indicating that the reaction producing carbonium ions from the 2-methylbutane occurred more slowly.

The C_4 carbonium ion formed in the above reaction may abstract a hydride ion from the tertiary position of 2-methylbutane resulting in a C_5 carbonium ion. Loss of a proton to the surface would result in C_5 olefin formation and would exchange in the same fashion as the C_4 olefin. However, a separate test indicated that a hydride ion was not abstracted, but that a small amount of C_5 olefin was produced at the expense of the C_4 olefin by some other route. The C_5 olefin may have exchanged with the surface in the same way as did the C_4 olefin. The C_5 olefin formation may be induced thermally, and an experiment is planned to test this possibility.

A separate sample of the solid phosphoric acid catalyst was hydrated at 300°C by exposure to H_2O vapor and then evacuated for one hour. A mixture containing 2-methylpropane-2d (120 torr), 2-methylbutane (40 torr) and an inert gas was circulated through the reactor at 300°C. No exchange was observed. Then a small amount of 2-methylpropene (15 torr) was added to the circulating mixture.

Changes in the m/e 70 and 73 peaks are shown in Figure 3. The m/e 73 peak is due to the 2-methylbutane containing a single deuterium. The m/e 70 peak is the parent peak of C_5

olefins. There was no significant increase in the m/e 73 peak other than from the natural isotope abundance indicating that no hydride transfer occurred before or after olefin addition. The increase in the m/e 70 peak following addition of the C_4 olefin indicates that some C_5 olefin was produced. The initial slight decrease in the m/e 70 peak was probably due to polymerization of some impurities on the fresh catalyst.

A sample of the gamma-alumina from the same stock used in earlier tests was pretreated and evacuated as already described. A mixture of 2-methylpropane-2d (120 torr), 2-methylbutane (40 torr) and an inert gas was circulated over the catalyst at 295°C. After 21 hours the temperature was increased to 320°C and remained there for 160 hours.

A number of changes occurred in the mass spectrum. The m/e 72 peak is the parent peak of 2-methylbutane. The peaks at m/e 73 and 74 result from the d_1 and d_2 exchanged molecules. Changes in these peaks are shown in Figure 4.

Exchange occurred only when the temperature was sufficient to induce cracking. This was evidenced by the formation of significant amounts of methane and hydrogen, accompanied by a decrease in the total amount of C_5 hydrocarbon. It is possible that deuteride (hydride) transfer did occur under these conditions along with some deuterium scrambling.

Some products may have been produced thermally in the gamma-alumina test. However, when the products of the solid phosphoric acid test were compared with the gamma-alumina test under similar conditions, no cracking occurred in the former test. Therefore the gamma alumina reaction must be catalytic.

Various types of acidity can now be characterized in terms of the hydrogen transfer reactions which have been observed. The reactions are (1) transfer of hydrogen between the catalyst surface and primary positions on the hydrocarbon, (2) transfer of hydrogen between a tertiary position and a tertiary position in another molecule, and (3) transfer of hydrogen between tertiary positions and other positions in other molecules. Table 1 summarizes the reactions observed.

Future Work

These reactions will be tried on zinc chloride and zinc chloride/coal combinations. A suitable inert and water-free support for zinc chloride must be selected. Following the tests on anhydrous $ZnCl_2$, different amounts of water will be added to the $ZnCl_2$ and the tests repeated. Tests on metallic zinc and zinc chloride/coal combinations will follow.

References

1. F.E. Massoth and D.S. Moulton, ERDA Contract No. E(49-18)-2006, Quarterly Progress Report, Salt Lake City, Utah, July-Sept 1976, pp 65, 69.

2. S.W. Cowley and D.S. Moulton, ibid., Oct-Dec 1976.

Table 1

Reactions Occurring over Catalysts of Known Acid Type

Reaction	1	1[a]	2	2[a]	3
Acid Type					
Bronstead only	no	yes	no	no	no
Lewis + Bronstead	yes		yes		no
Lewis + base	yes		no		yes

[a] 2-methylpropene (10%) added to reactants.

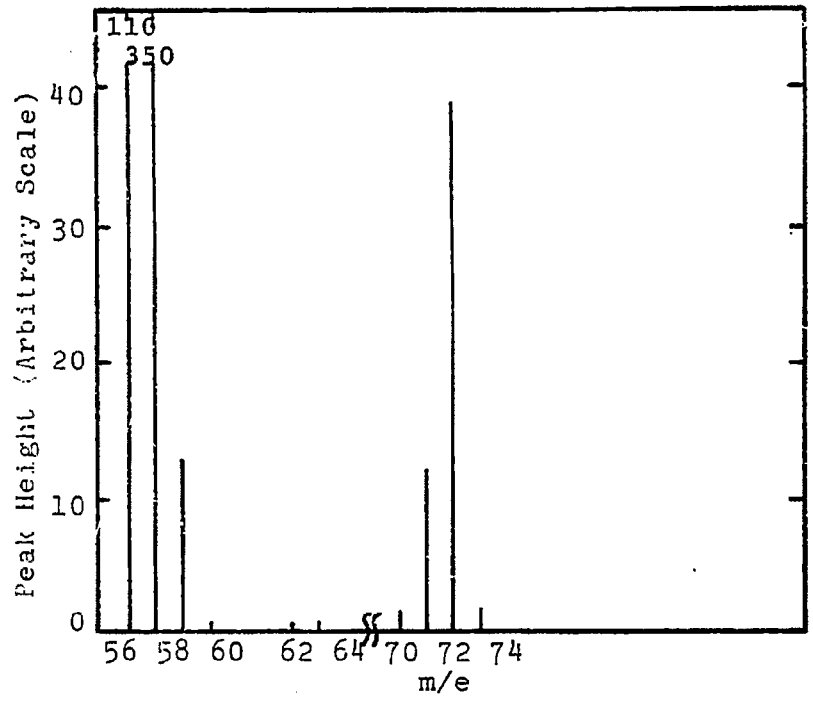

Figure 1. Mass Spectrum of 2-methylbutane Before Exposure to a Deuterated Phosphoric Acid Catalyst.

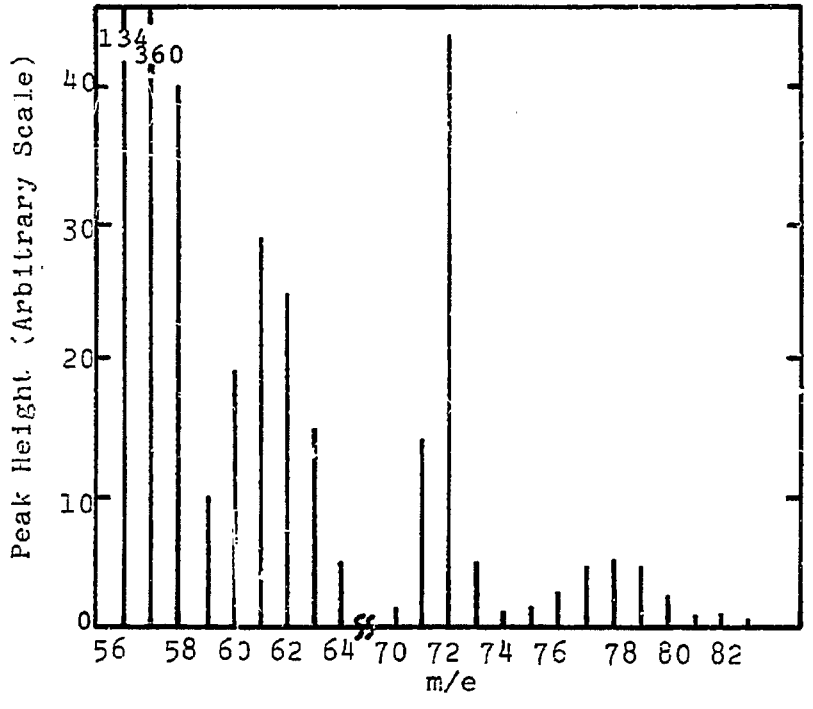

Figure 2. Mass Spectrum of 2-methylbutane and 2-methylpropene After 360 Min Exchange With a Deuterated Phosphoric Acid Catalyst.

Figure 3. M/E Peaks of 2-methylbutane d_1, (73) and Pentene(70) During Reaction Over Phosphoric Acid Catalyst.

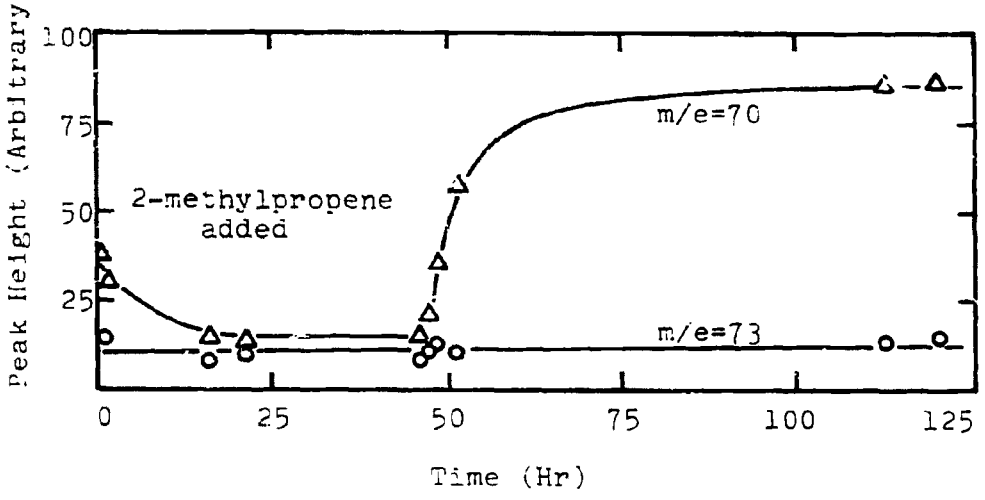

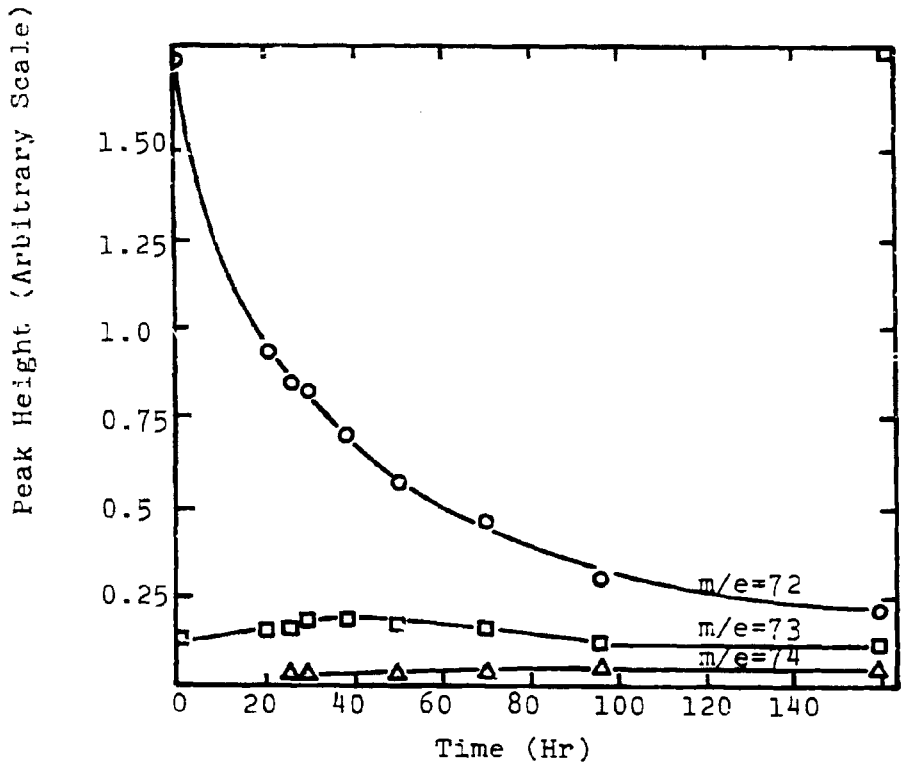

Figure 4. Mass Peaks of 2-methylbutane During Reaction with 2-methylpropane 2d Over Alumina.

Project B-4

Mechanism of Catalytic Hydrogenation by Metal Halide Catalysts

Chemical Structure of Heavy Oils Derived by Coal Hydrogenation

Faculty Advisor: D.M. Bodily
Postdoctoral Fellow: H. Itoh

Introduction

The chemical structure of the heavy oil fraction of coal is analyzed by structural analysis techniques to determine the properties of the oil and to follow the reactions. The oil is first separated on the basis of solubility and then on the basis of size. The heavy oils are produced by hydrogenating a high-volatile bituminous coal in an entrained-flow reactor using $ZnCl_2$ as a catalyst. No vehicle oil is used. The heavy oil is defined as the oil collected in the first condensor of the system. The amount of $ZnCl_2$ catalyst used during hydrogenation has a strong effect on the yield of products in the heavy oil, even when the total conversion is held constant. As the percentage of catalyst is increased from 1.5 to 6 percent by weight of zinc to coal, the yield of asphaltenes decreases significantly and the molecular weight of the asphaltene and hexane-soluble oil fractions decreases. Structural analysis of the products confirms that the type of products are the same, even though the yields change.

Average molecular structures of fractions derived from coal hydrogenation heavy oils have been reported in previous reports. The asphaltene, saturate, one-ring aromatic, two-ring aromatic, three to four-ring aromatic and polar-poly ring aromatic fractions have been studied.

Project Status

The structural parameters obtained by Brown and Ladner's technique have been reported for the asphaltene and aromatic oil sub-fractions. These results were based on the elemental analysis and the hydrogen types as determined by nuclear magnetic resonance, NMR. The hydrogens were divided into those that are α to aromatic rings and those that are β or further from aromatic rings. These results have been improved by introducing a third type of proton, the protons attached to methyl groups. The ratio of carbon to hydrogen is assumed to be 2 except in the methyl groups where it is three. The significant structural parameters are compared in Figures 1 and 2 for the asphaltenes

and Figures 3 and 4 for the aromatic oils. Structural parameters are plotted versus the gel permeation elution volume for the different sub-fractions.

A computer was used to determine optimum values for the average structural parameters. In addition to elemental analysis and proton distributions, molecular weight and density are also used. The optimum values for the parameters are also shown in Figures 1-4. The fraction of aromatic carbons, f_a, and the length of aliphatic side chains, $H_\sigma/H_\alpha+1$, show reasonable agreement. The degree of substitution, σ, and the hydrogen to carbon ratio of the hypothetical unsubstituted aromatic ring unit, H_{au}/C_a, show wide fluctuations. The computer results suggest a more condensed system.

The computer program was modified and the parameters were recomputed. The modification involved the method in which the aromatic rings were calculated. Results from the two methods of calculation are shown in Figures 5 and 6, their greatest difference being in the degree of polymerization of structural units. The second method gives more reasonable results. The computer results are quite sensitive to the assumptions involved in the calculations and the methods of calculation.

Future Work

The structural analysis of two solvent refined coals and the oil from coal hydrogenation will be compared with the results previously reported.

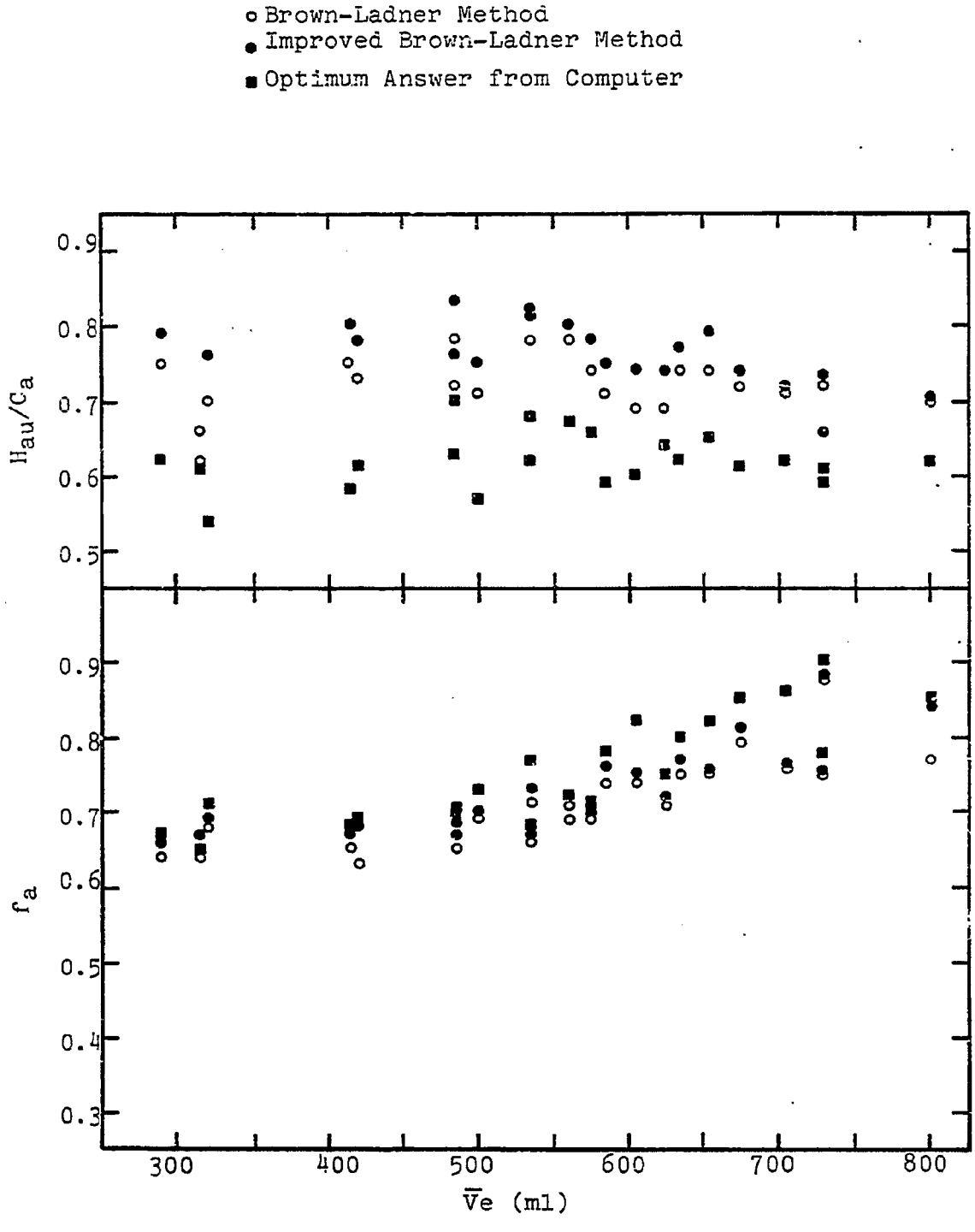

Figure 1. Carbon Aromaticity (f_a) and the Atomic Hydrogen to Carbon Ratio of the Hypothethical Unsubstituted Aromatic Material (H_{au}/C_a) vs. Elution Volume (Ve) for Asphaltenes.

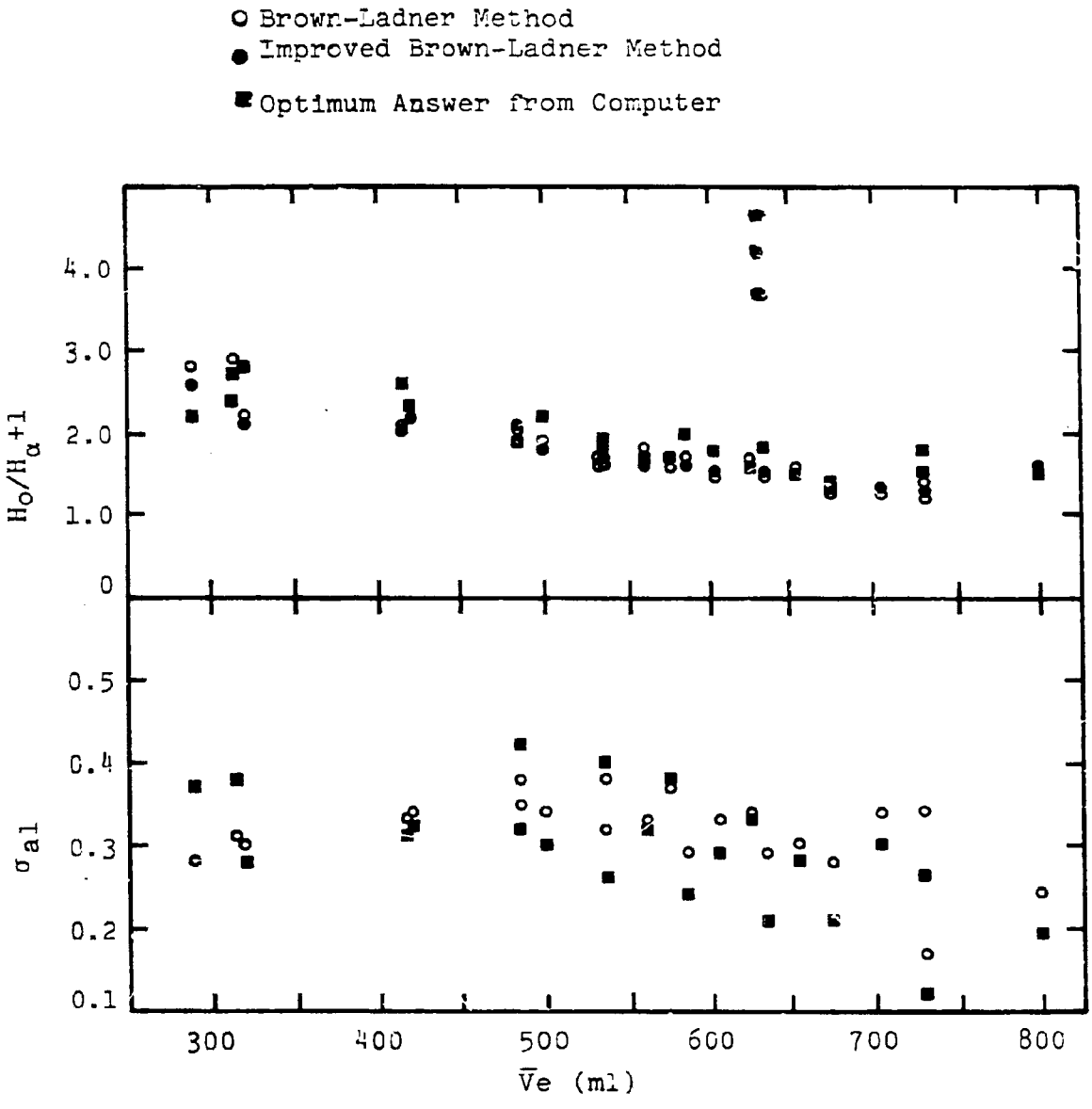

Figure 2. The Degree of the Alkyl Substitution of the Aromatic System (σ_{al}) and the Average Length of Aliphatic Carbon Chain ($H_o/H_\alpha+1$) vs. Elution Volume ($\bar{V}e$) for Asphaltenes.

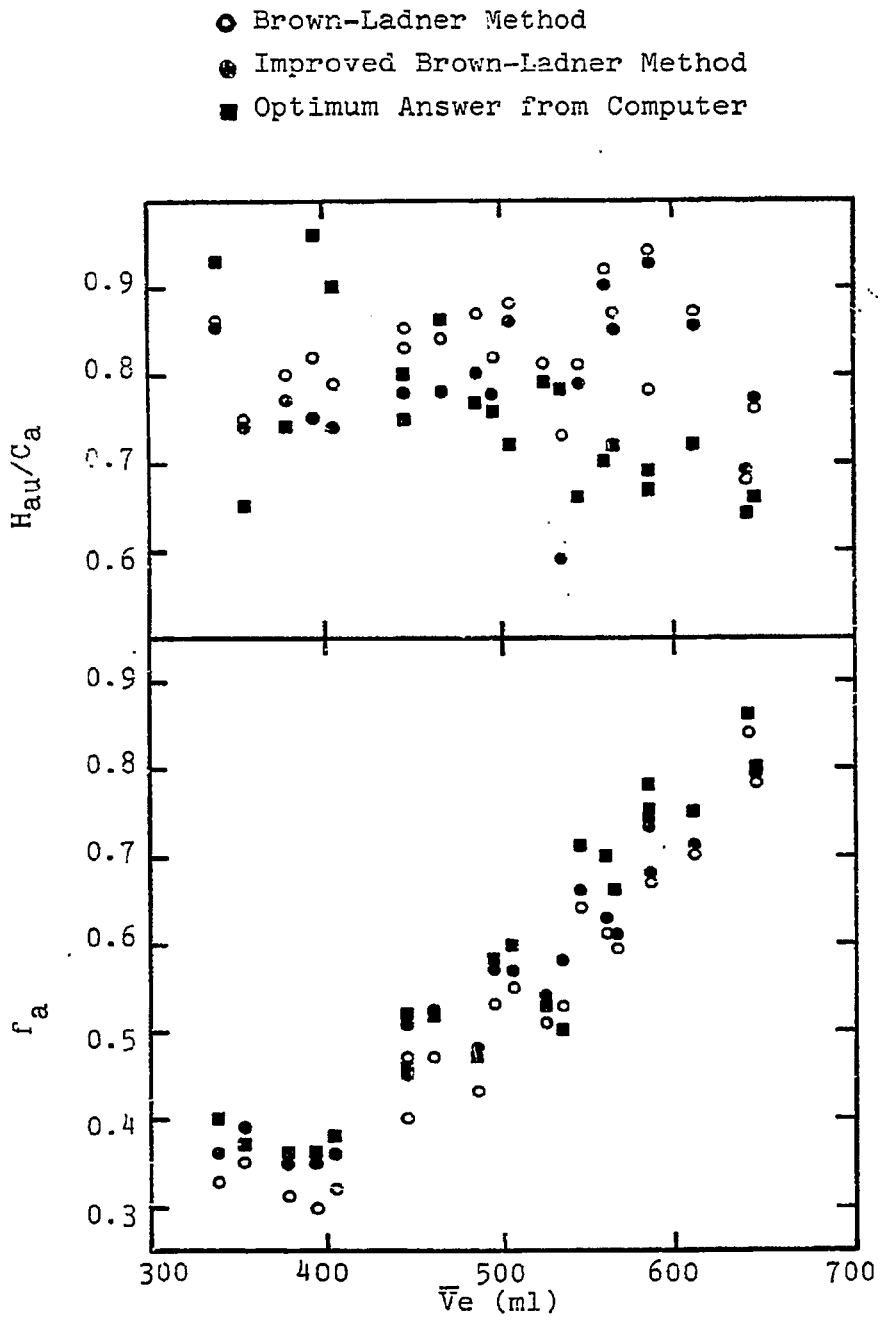

Figure 3. Carbon Aromaticity (f_a) and the Atomic Hydrogen to Carbon Ratio of the Hypothetical Unsubstituted Aromatic Material (H_{au}/C_a) vs. Elution Volume ($\overline{Ve}$) for Oils.

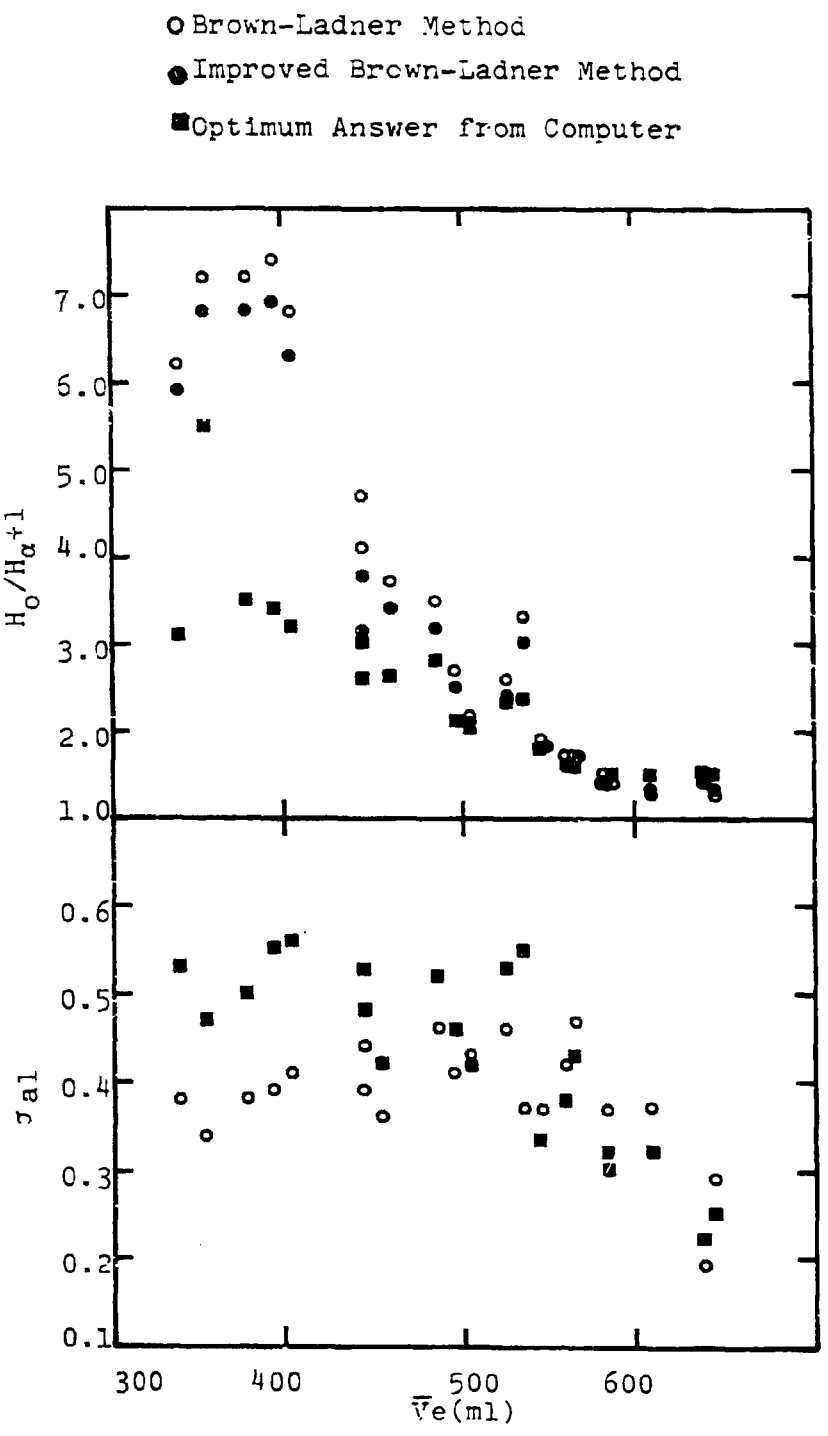

Figure 4. The Degree of the Alkyl Substitution of the Aromatic System (σ_{al}) and the Average Length of Aliphatic Carbon Chain ($H_o/H_\alpha+1$) vs. Elution Volume ($\bar{V}e$) for Oils.

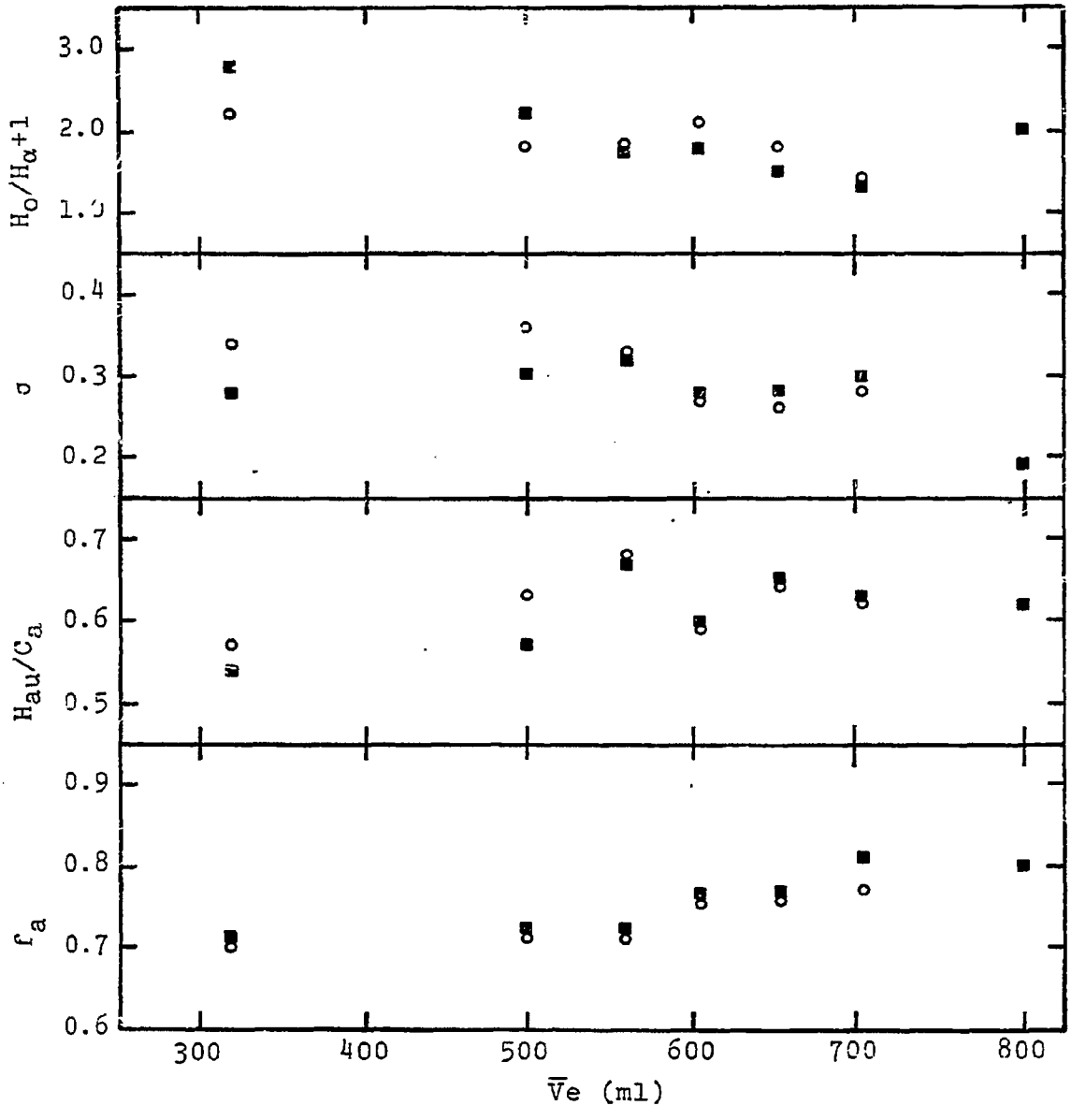

Figure 5. Comparison of the Structural Parameters of Asphaltenes Obtained by Computer Method I (■) and Method II (o).

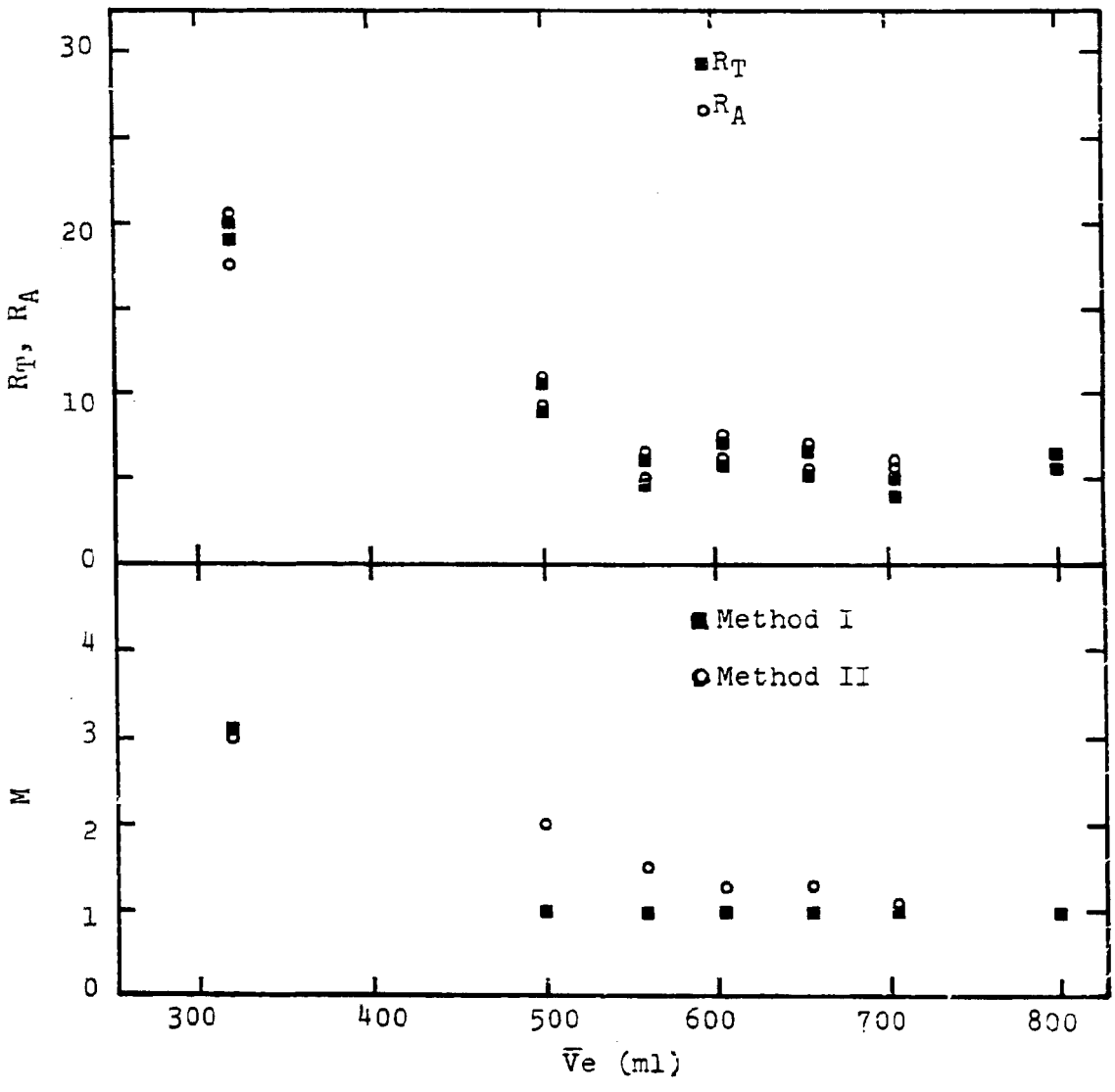

Figure 6. Comparison of the Polymerization Degree of Unit Structure (M), Total Ring Numbers (R_T) and Aromatic Ring Numbers (R_A) Within the Average Molecule of Asphaltenes Obtained by Computer I and II Methods.

Project B-4

Mechanism of Catalytic Hydrogenation by Metal Halide Catalysts

Faculty Advisor: R.E. Wood
Graduate Student: Doug Stuart

Introduction

The relatively new techniques of ESCA (Electron Spectroscopy for Chemical Analysis) and Auger Electron Spectroscopy are being used to investigate the catalytic hydrogenation of coal by metal halide catalysts. Data obtained from Auger Electron Spectroscopy studies are evidence that zinc chloride participates with coal-derived free radicals in the hydrogenation process. Attempts to find such interactions in a stannous chloride impregnated coal sample and a cuprous chloride impregnated coal sample were not successful. A possible explanation is the difference between the two ESCA units used. Work this quarter has been to evaluate these differences.

Project Status

The DuPont ESCA unit has been replaced by the Hewlett Packard (HP) ESCA unit. Selected samples similar to those analyzed with the DuPont unit are being prepared by the previously described method. However, there is a minor change after drying. The samples are now placed in a 65 millitorr vacuum overnight and sample mounting is accomplished in an inert atmosphere.

Table 1 is a brief comparison of the two ESCA units used. The X-ray source of the DuPont unit is closer to the sample for maximum X-ray flux. In the HP unit, the X-ray beam is about 100-fold less intense at the sample surface because of the monochromator. However, the monochromatic radiation improves the spectral resolution and eliminates interference from satellite peaks. Both instruments are calibrated to record intensity vs. binding energy of the photoelectron peaks. Because of this and the photoelectron peaks which are dependent on the energy of the incident X-rays and the Auger peaks which are independent of X-ray energy, the Auger electron peaks shift from one instrument to the other in binding energy by an amount equal to the difference in X-ray energies. Sample temperature also varies from one instrument to the other. The vacuum in the HP unit is at least two orders of magnitude better. In the

insulators in the HP unit, a stream of low energy electrons from the "flood gun" prevents the surface of the sample from becoming electrically charged. To compensate for the loss of X-ray flux, an electron lens and multiple channel detection system are used. All these differences between instruments may affect each sample and its spectrum.

The specta in Figure 1 were obtained from samples used in the original investigation. Curve A is for a 12 wt % zinc chloride (maf coal basis) impregnated Kaiparowitz, Utah coal sample prepared from a zinc chloride solution and dehydrated without the use of heat. Curves B and C are from similar samples dehydrated at 110°C overnight and heated to 450°C in a slow flow of hydrogen, respectively. These spectra were from the DuPont unit.

The spectra in Figure 2 were obtained during the past quarter using the HP unit. Curves A and B are from the same samples as Curves A and C in Figure 1, respectively. Curve C in Figure 2 is from a 12 wt % (maf coal basis) zinc chloride impregnated Kaiparowitz coal sample prepared similarly to the sample of Curve B in Figure 1. Curve D is obtained from the same sample as Curve C and has been heated in hydrogen to 450°C similarly to Curve C in Figure 1. Curve E is the same data as Curve D but has been mathematically smoothed using a device built into the HP unit.

In Figure 1 the spectra are drawn as recorded by the DuPont unit. The numbers are corrected binding energies since the entire spectrum is shifted by a constant correction factor. In Figure 2 the numbers are instrumental binding energies of the specific labled dot. The numbers in parenthesies are corrected binding energies.

Figure 1 illustrates the specified change originally observed. The peaks at 355 eV and 346 eV disappear and the peaks at 353 eV and 350 eV appear as a function of the temperature to which the sample has been heated. The two samples still available from the original study (Fig 1 Curves A and C) appear quite differently when analyzed with the HP unit (Fig 2 Curves A and B). Most noticeable is the 232 eV difference in binding energy as explained before. Also a peak corresponding to 349 eV in Figure 1A does not appear in Figure 2A. The impregnated coal sample heated to 450°C shows a distinct decrease in splitting between the two peaks (from 9 eV to 3.7 eV) in Figure 1C, but in Figure 2B the splitting is so nearly buried in the background that the data is questionable. Figure 2C is from a sample prepared similarly to the sample shown in Figure 1B. Again the sample spectra obtained from the DuPont unit showed some change with the 350 eV peak larger than the 348 eV peak. However, the HP unit showed no change in splitting from a

pure zinc chloride sample. When the sample of Figure 2C was heated to 450°C in hydrogen, Figure 2D resulted. The splitting is again buried in the background. Figure 2E is a smooth curve of the data in Figure 2D. A splitting of 4.5 eV between peaks can be seen, however, the data is quantitatively unreliable.

Because the change in splitting is still present, the [illegible]s need to be prepared more carefully so that the splitting can be measured precisely. The HP unit has improved spectral resolution over the DuPont unit but has decreased sensitivity. An alternate explanation for the low signal is that the improved vacuum causes a loss of zinc chloride.

Future Work

More work is needed to obtain optimum results with the zinc chloride impregnated coal sample before unknown samples can be trusted.

Table 1

Item	DuPont 650B Electron Spectrometer	Hewlett Packard 5950B
X-Ray source	1254 eV Mg K_a polychromatic	1486 eV Al K_a monochromatic
Sample temp	~50°C	<50°C cold probe: -50°C
Vacuum	10^{-6} to 10^{-7} torr	10^{-8} to 10^{-9} torr
Charging compensation	None	Electron flood gun
Method of data accumulation	Single scan at variable rate	Multiple scans at constant rate
Detector	Single energy	Multiple channel

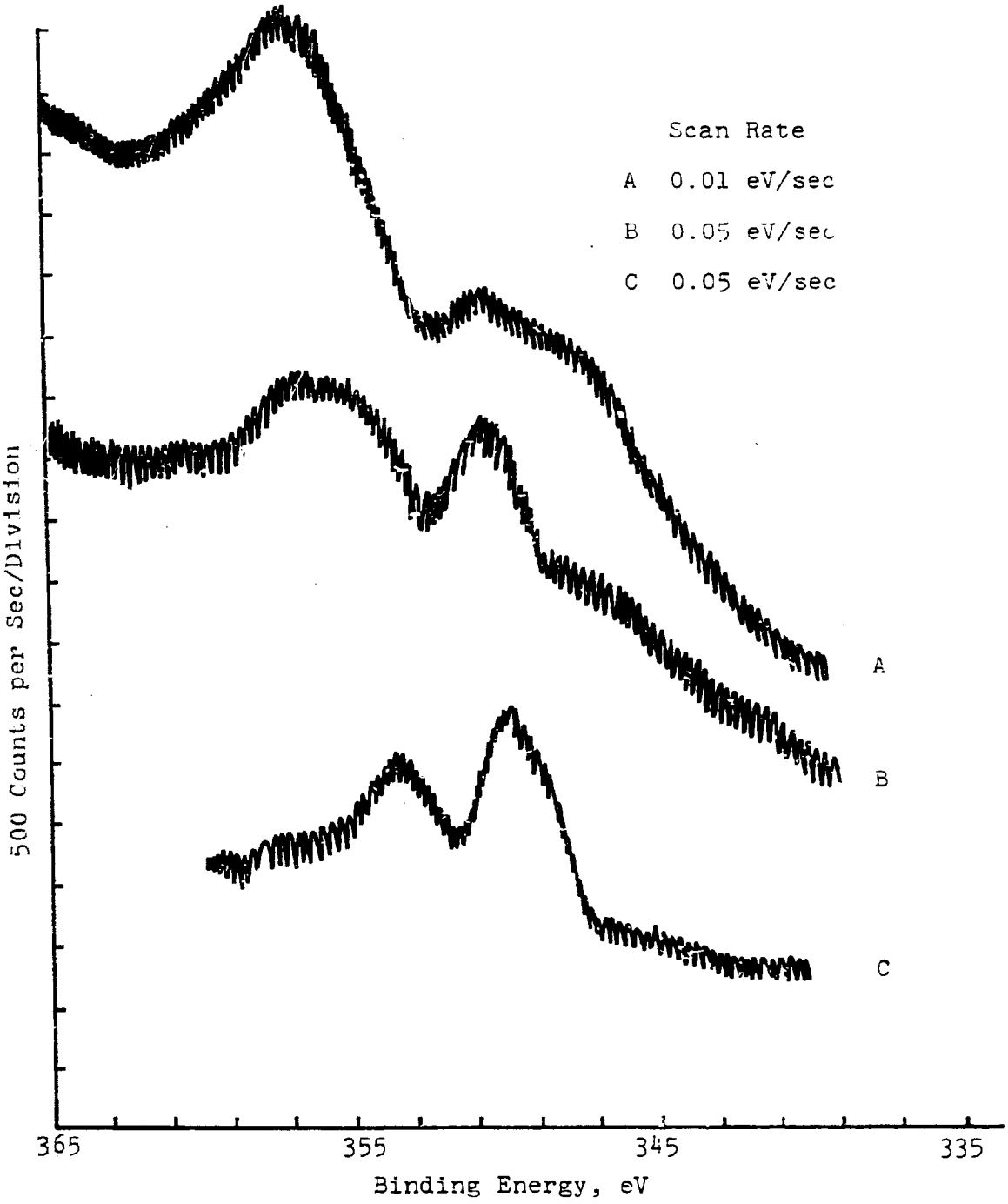

Figure 1. DuPont 650B Electron Spectrometer

Figure 2. Hewlett Packard 5950B ESCA Spectrometer

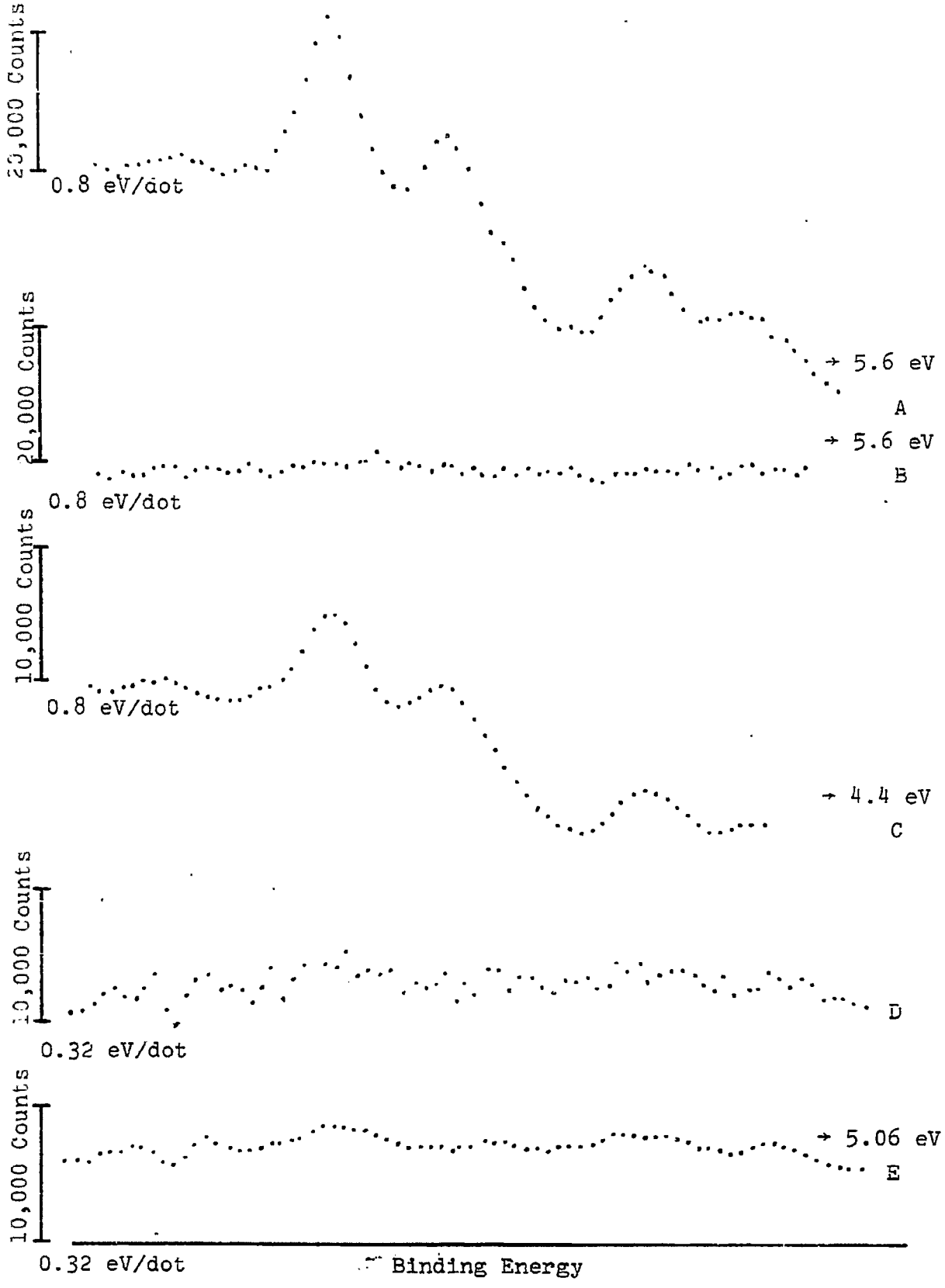

Project C-1

The Mechanism of Pyrolysis of Bituminous Coal

Faculty Advisor: W.H. Wiser
Graduate Student: R. Muthiah

Introduction

The mechanism of coal pyrolysis to yield liquid fuels has been of interest for a long time. Studies at this university have indicated that coal pyrolysis at constant temperature is second order with respect to the amount of unreacted coal. Lahiri has shown that hydroaromatic structures are essential for the production of tar during coal pyrolysis. Studies will be done to discern the actual role of hydroaromatic structures in bituminous coal in the production of volatile matter.

Project Status

The equipment components have been ordered. Efforts to find a supplier for the model compounds have been fruitless. These syntheses will be attempted in this laboratory; at the same time the search for a laboratory to synthesize the compounds will continue.

Future Work

Once the model compounds are obtained, they will be pyrolyzed and the volatile matter evolved examined to see if stabilization of thermally produced fragments from the model compound, such as benzene rings, has occurred involving transfer of the hydrogen from the hydroaromatic structure.

Project C-2

Heat Transfer to Gas-Solid Suspensions in Vertical Cocurrent Downflow

Faculty Advisor: J.D. Seader
Graduate Students: J.M. Kim
B. Scott Brewster

Introduction

The purpose of this study is to investigate the heat and momentum transport mechanisms for cocurrent downward, two-phase flow of gas and solids in a vertical tube. The application of such a flow mode to the University of Utah continuous hydrogenation reactor may be desirable. Coal particles and hydrogen would flow together through a heated tube such that the rate of heat transfer to the two-phase mixture could be the controlling factor in the reaction rate. Initial data on fluid mechanical phenomena, such as holdup and pressure drop, have been obtained for test glass beads at flow rates to 300 lb/hr carried by air at Reynolds numbers to 30,000. Apparatus is being constructed and assembled for subsequent experiments with coal particles.

Project Status

During the past quarter holdup and pressure drop data were obtained for various solids-to-gas loading ratios with the glass bead-air system at ambient conditions. A computer program was developed and used to process the raw data obtained. Two hundred pounds of newly obtained glass beads (Potters Industries, Inc, technical quality glass beads "P" series) were screened to obtain 100 lb of the -45/+50 mesh portion for the experiment. The average diameter and the sphere count percentage of the screened beads were determined to be 329 microns and 93.8 percent, respectively. New sets of regulators and a four-way pneumatic valve were added to the existing slide-valve actuating mechanisms to control each valve independently.

After about three months of test runs, several samples of the beads were examined under the microscope. Their breaking or attrition caused by pneumatic transport was not significant.

As a theoretical basis for the analysis of the data, the equation of particle motion (Eq 1) was solved together with the continuity equations for the gas and solids phase (Eq 2 and 3).

$$\frac{dU_p}{dt} = \left(\frac{\rho_p - \rho_g}{\rho_p}\right) g\rho + \frac{3\rho_g C_D}{4\rho_p d_p} V_s|V_s| \qquad (1)$$

$$U_g = \frac{U_{sg}}{1-E_p} \qquad (2)$$

$$U_p = \frac{U_{sp}}{E_p} \qquad (3)$$

where,

U_{sg}, U_{sp} = superficial velocities of gas and solids phase

U_g, U_p = actual velocities of gas and solids phase

C_D = drag coefficient, $f(N_{Re})$

V_s = slip velocity, $U_g - U_p$

E_p = solids holdup

It was assumed that no heat or mass transfer occurs and that the only body force acting on the mixture is gravity. Also particle interactions are not taken into account. Substituting Eq (2) and (3) into (1) and rearranging gives,

$$\frac{dE_p}{dZ} = \left\{\left(\frac{\rho_p - \rho_g}{\rho_p}\right) g + \frac{3\rho_g}{4\rho_p d_p} C_D V_s|V_s|\right\} \left(\frac{E_p^3}{U_{sp}}\right) \qquad (4)$$

where,

$$V_s = \frac{U_{sg}}{1-E_p} - \frac{U_{sp}}{E_p}$$

$$C_D = \frac{24}{N_{Re,p}} \quad (N_{Re,p} \leq 0.3)$$

$$C_D = \frac{18.5}{N_{Re,p}^{0.6}} \quad (0.3 < N_{Re,p} \leq 1000)$$

$$C_D = 0.44 \quad (1000 < N_{Re,p} \leq 20{,}000).$$

Solutions of Eq (4) for gas Reynolds numbers of 1500 (laminar flow) and 7930 (transition or turbulent flow) are shown as curves in Fig 1 and 2 together with experimental data. Results from Fig 1 indicate that experimental holdup values are always higher than predicted by Eq 4. The differences might come from a velocity gradient in the tube. In the transition or turbulent region, however, better agreement between experimental and calculated holdup values were obtained as are seen in Fig 2, especially in the low solids flow rate region where particle-to-particle interactions are thought to be insignificant. Increasing deviations at higher solids feed rates may be due to increasing particle interaction effects.

Figure 3 shows the effect of superficial gas velocity on pressure drop at various solids holdups (or solids concentration). A negative pressure drop occurs below gas velocities of 10 ft/sec. The presence of both negative and positive pressure drops is characteristic of the downflow system. More data are needed to fully explain the existence of a limiting gas velocity for the negative pressure drop.

During the past quarter the vibratory feeder arrived. Coal samples were obtained and screened, an appropriate phosphor was obtained for tagging the coal samples to be used in the velocity measurements, and preliminary experiments were conducted to determine whether the tagging technique would yield an accurate measurement of particle velocity.

The vibratory feeder (Syntral Model F-TOIA) has a two-inch diameter tubular trough and solid-state regulating control (Model RSAC-2B). The RSAC control has a feedback signal which is designed to keep the trough stroke constant regardless of a change or fluctuation in the line voltage. A stand for the control box was constructed and electrical wiring for the feeder was installed. The mechanism for feeding the coal particles from the hopper into the feeder is being fabricated.

A small sample of phosphorescent pigment Grade 100/A-F was obtained from United Mineral and Chemical Corporation for tagging the coal. The pigment which is ZnS:Cu is in the form of a powder with a particle size of about 25 microns. The powder can be excited by daylight, artificial white light or UV causing the emission of a strong green peak decaying over several hours. Coal particles with an approximate size of 400 microns have been tagged by the following method: The coal particles are washed with acetone to wet their surfaces and then rinsed in a solution of technical grade sodium silicate solution diluted with water. After removing the excess solution with paper toweling, the particles are mixed with the powder and stirred until dry to prevent agglomeration.

A light detector for detecting the injected coal samples is being fabricated. The detector which will be tested first is an RCA 931-A photomultiplier tube. It is inexpensive, rugged, has high gain and fast response, and is sensitive in the range of emission of the phosphor.

The system for injecting the tagged coal samples is shown in Figure 4. The injector utilizes a short pulse of compressed gas to blow the sample from the loading tee into the tube. The characteristics of the pulse can be varied by changing the injection pressure and volume of the compressed gas chamber. Two ball valves permit easy loading of the sample into the loading tee.

One ton of pulverized Sea Coal was obtained from Asbury Graphite Inc in Rodeo, California. The coal is a typical western grade bituminous coal and is used in the foundry industry for core and molding sand. No composition analysis has been performed. Several screenings are being done on a Tyler Ro-Tap sieve shaker to ensure minus 40/plus 80 mesh (US series) coal samples.

A study was conducted to determine the explosion hazards of using air as the transporting gas in the experiments. Because coal dust explosions occur when coal particles less than 1000 microns are transported by gas with an oxygen content greater than approximately 15 percent by volume, an inert gas is being considered.

Future Work

Future work with the glass bead-air system to assess the reliability and reproducibility of the obtained data will be performed. Theoretical study of the experimental data will be further developed to account for the more complex factors such as a two-dimensional velocity profile and particle interactions. The gas inlet section of the test tube will be slightly modified to insure smooth introduction of the air.

Plans for the coal-gas system include completing the screening of the coal samples, installation of the feeder and testing of the detector. The gas flow system will be planned and equipment ordered. If the phosphor tagging technique proves successful, larger quantities of the phosphor will be ordered and a second detector and a timing mechanism for the particle velocity measurement will be constructed.

Figure 1. Holdup Measurements at N_{Re} = 1500

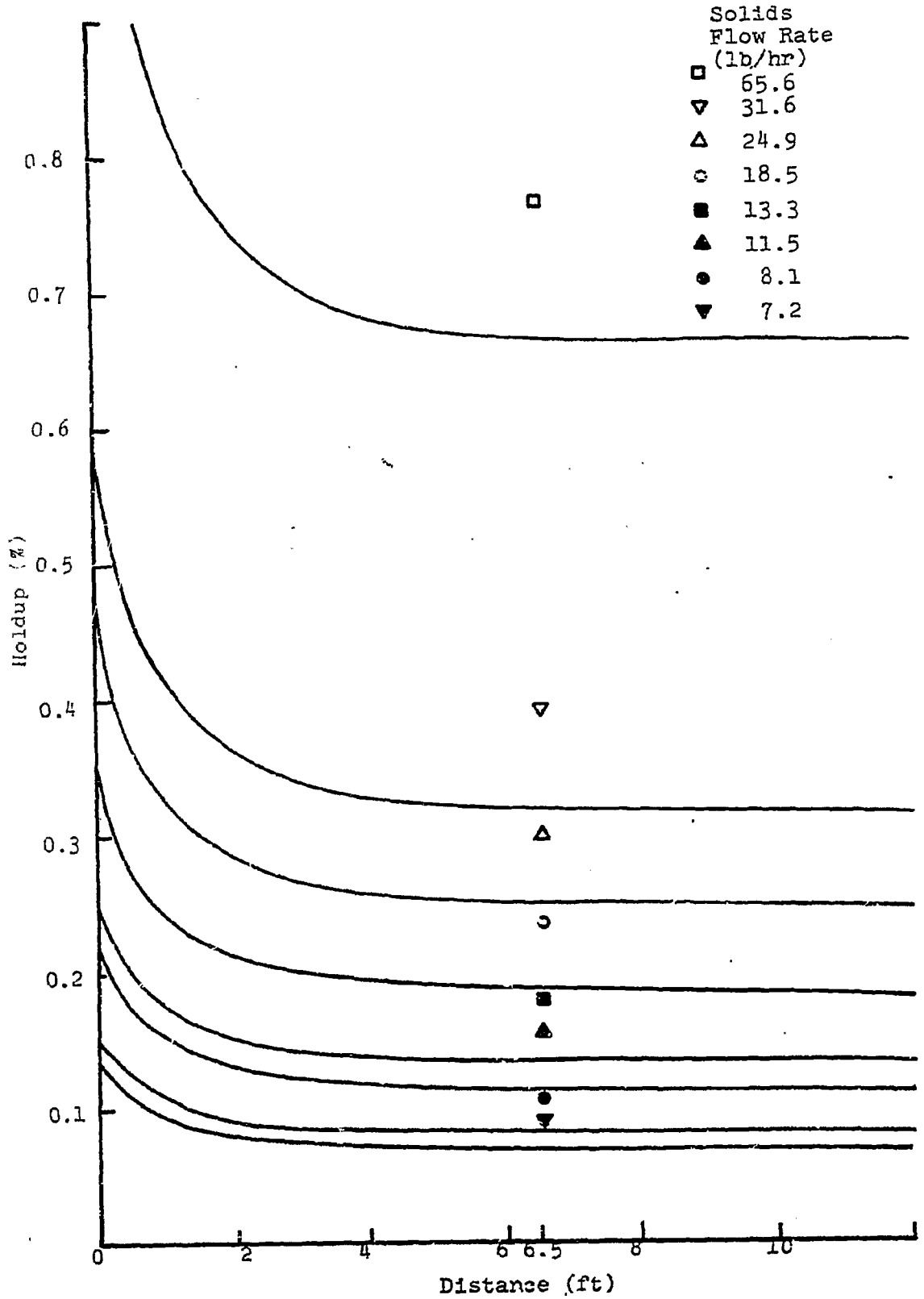

Figure 2. Holdup Measurements at N_{Re} = 7930

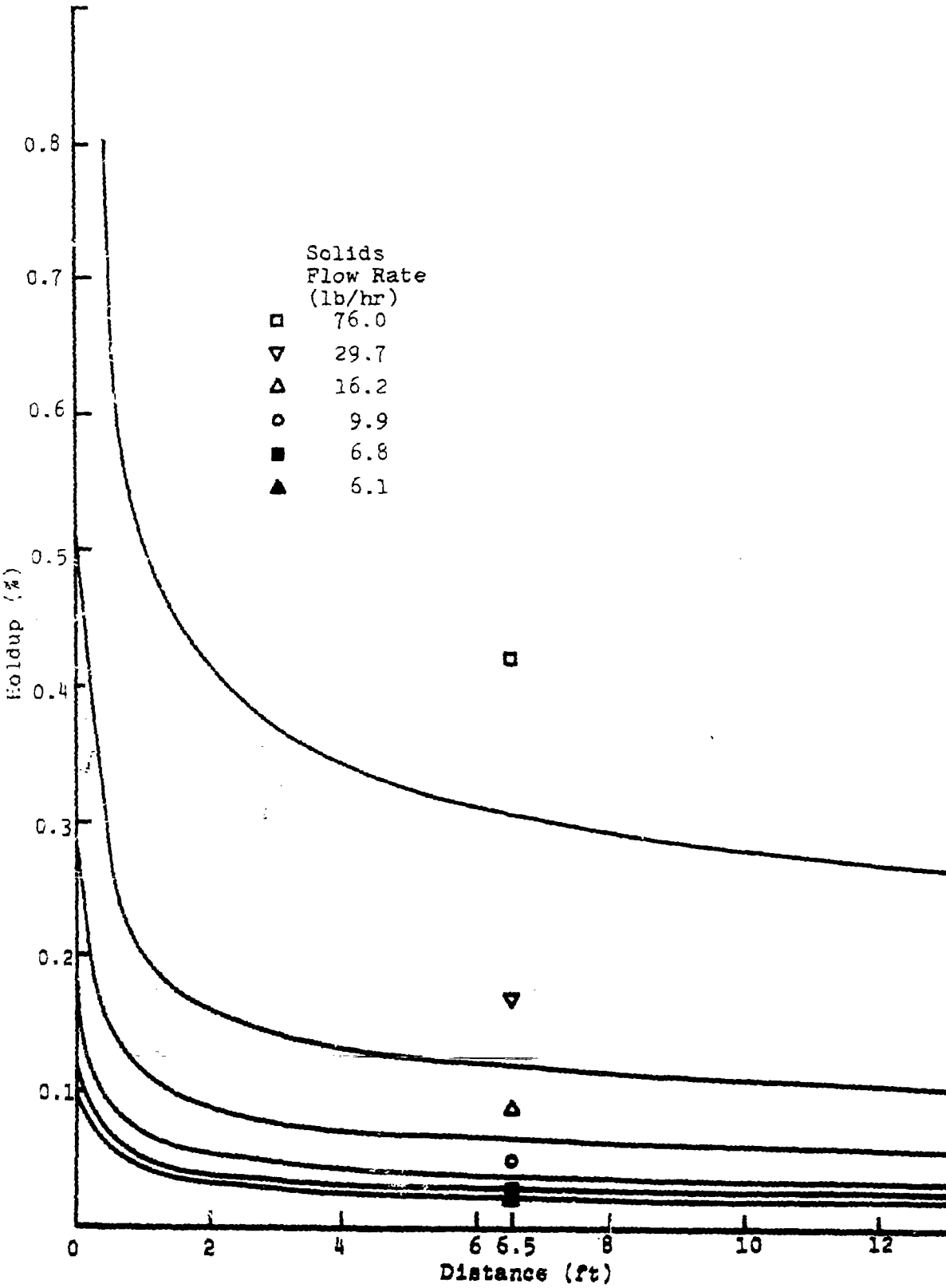

SC

Figure 3. Effect of Superficial Velocity on Pressure Drop

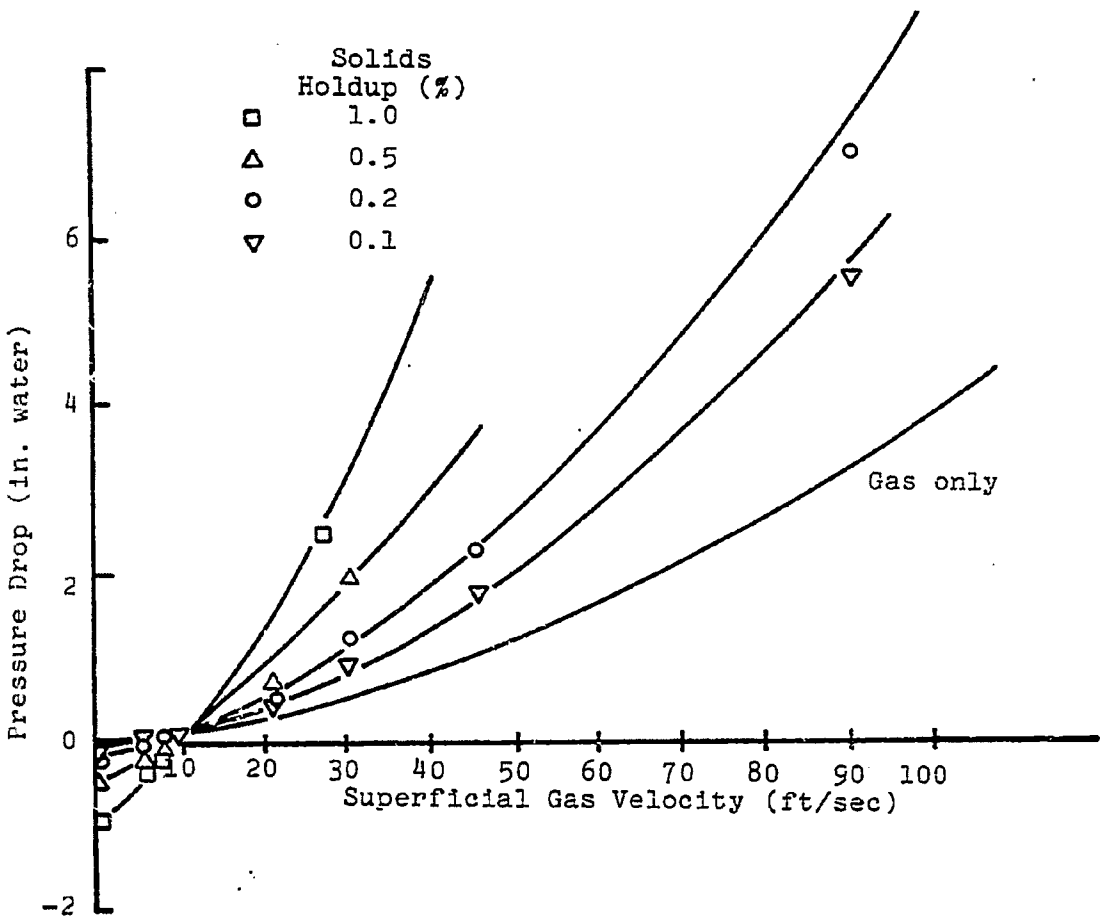

Figure 4. Air-Pulse Injector

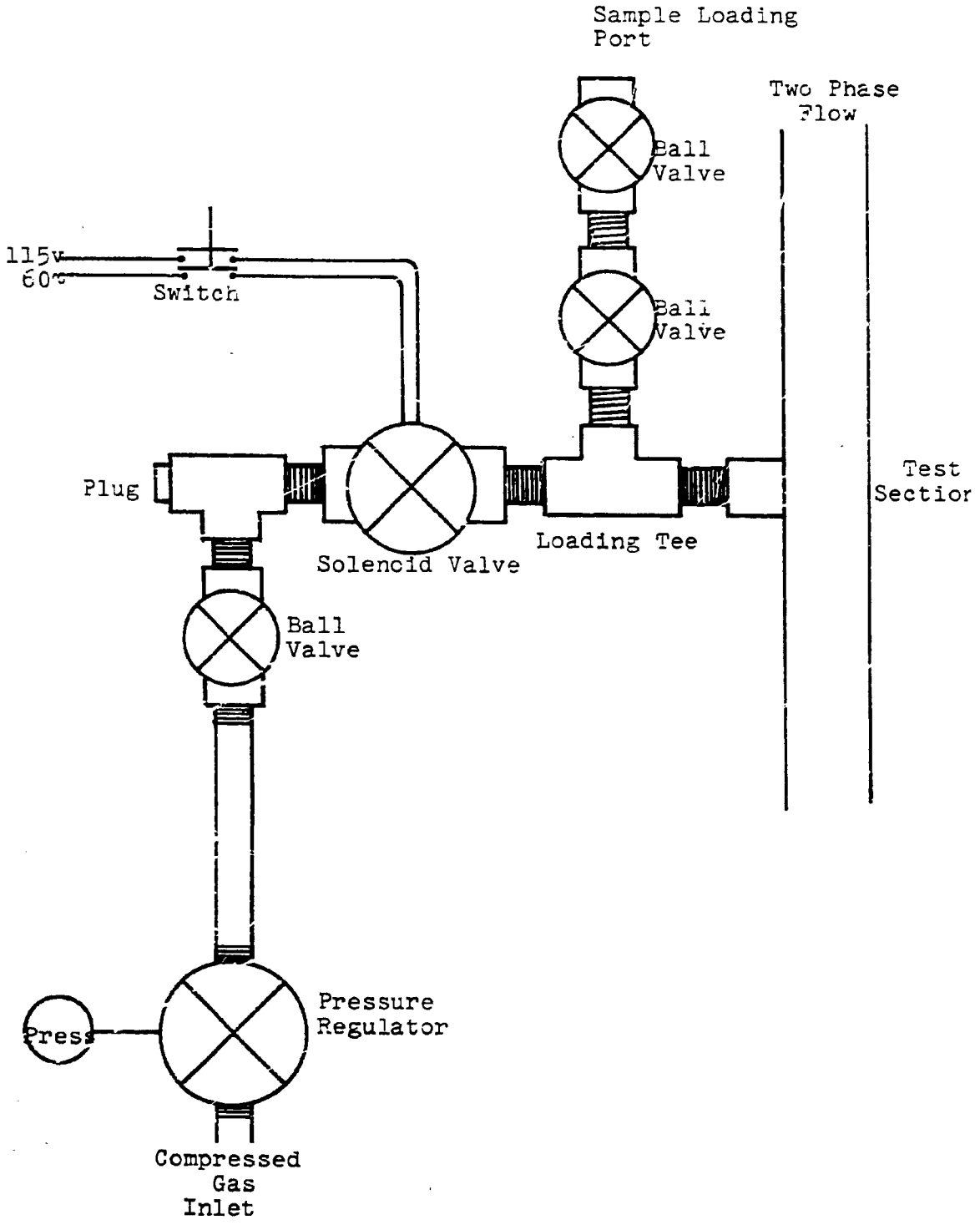

Project D-1

Coal Particle and Catalyst Characteristics for Hydrogenation Evaluation and Testing

Faculty Advisor: R.E. Wood
Graduate Student: J.M. Lytle

Introduction

This effort is related to the effects of coal particle size on coal hydrogenation. The existing hydrogenation equipment from ERDA Project FE(49-18) - 1200 is being used. The reaction vessel consists of a series of coiled tubes, each approximately 20 feet long. The reaction zone consists of a preheat and a reactor section. The preheat section contains two coiled tubes in series containing 44 feet of 3/16 inch ID tubing. The reactor section is in series with the preheat section and contains three tubes with a total length of 64 feet of 1/4 inch ID tubing.

The residence time of the coal in the reaction area is of major importance. For this reason a magnetic detection device has been developed. Using this device, iron powder may be detected by a coil of copper wire which is placed inside the reactor tubing. For residence time detection and measurement, one coil is placed at the beginning of the preheat section and a second at the end of the reactor section.

The residence time measurement will be used to help determine reactor stability or resistance to plugging with respect to the coal particle size, gas velocity, temperature and percent of catalyst applied.

With a continuous feed of coal the effect of residence time on coal conversion will be studied. This study will also include an examination of variables such as coal particle size, catalyst percentage, temperature and pressure.

Project Status

The pyrolysis of coal is only slightly endothermic or exothermic depending on the carbon content.[1] However, upon hydrogenation the reaction becomes highly exothermic. Fig 1 shows the relative heat of reaction of coal hydrogenation vs. conversion. Relative heat of reaction is evaluated by determining the amount of cooling necessary to keep the reactor temperature from rising above the set point. The scale from 0 to 10 refers to the amount of air blown onto the reactor for cooling. Very little heat is evolved below 60% conversion when using coal from Clear Creek, Utah.

However, the heat evolved increases rapidly at conversion levels above 60%. The proximate analysis of the coal used is shown in Table 1. The volatile matter is 45.63 percent.

Table 1

Clear Creek, Utah Coal
Proximate Analysis

		MAF[a]
H_2O %	6.73	
Ash %	8.19	
Volatile matter %	38.82	45.63
Fixed Carbon %	46.26	54.37

[a]MAF - moisture ash free basis.

Therefore, the pyrolysis reaction is probably predominant at conversion levels below 60% and only mildly exothermic. However, the highly exothermic hydrogenation reaction is predominant at higher conversion levels.

To minimize the consumption of hydrogen, an ideal conversion would be in the range of 60-70%. Figure 2 shows that the heat of reaction increases substantially at a residence time of 150 seconds. For hydrogen conservation the residence time should be less than 150 seconds.

The effects of particle size have been studied during this quarter. In Figure 3 the conversion is plotted against the residence time of the coal in the reactor at various particle sizes. The rate of conversion of coal to liquids and gases increases as the particle size decreases. The particle size effect diminishes as the conversion increases and disappears above 80%. This is probably because of the agglomeration or massing of particles. A viscous liquid made up of agglomerated coal particles results and is transferred through the reactor tube in the shape of an annular ring along the wall.

On the basis of increasing the reactor space rate utilization factor and decreasing hydrogen consumption the conversion should be 60-70%. The residence time should be less than 150 seconds and the particle size should be the smallest possible when considering grinding costs and feeding capability.

The reactor temperature has also been studied. Figure 4 shows an increase in residence time with an increase in

temperature. The residence time increases rapidly above 962°F indicating a plugged reactor at higher temperatures. The product distribution of these tests is shown in Figure 5. At a conversion level of 60-70% total hydrocarbon liquids would be in the range of 45-53% with gases at 5-6%. Increases in conversion at higher temperatures are primarily in the form of increased heavy liquids.

Future Work

In Figure 3 the present curves will be extended and other particle sizes will be included. More complete material balances will be made by the newly obtained C, H, N analyser. The hydrogen consumption will be monitored and more closely correlated with the relative heat of reaction and conversion. A material balance on zinc will be performed. The purchase of an X-ray fluorescence analyser which would permit a material balance on chlorine is being considered.

References

1. O.P Mahajan, A.Tomita and P.L. Walker Jr., Fuel (London), 55, 63 (1976).

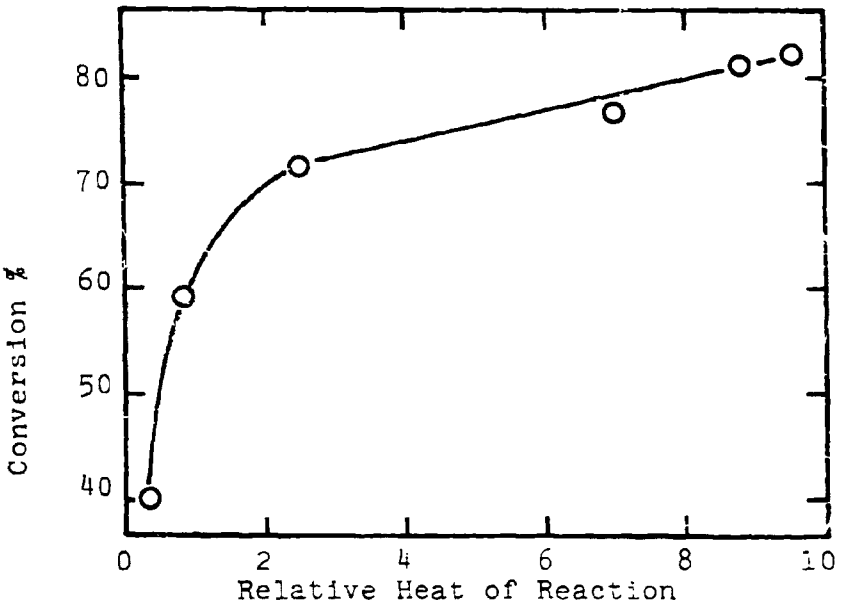

Figure 1. Increase in the heat evolved by the hydrogenation reaction vs. conversion of Clear Creek, Utah coal to liquids and gases.

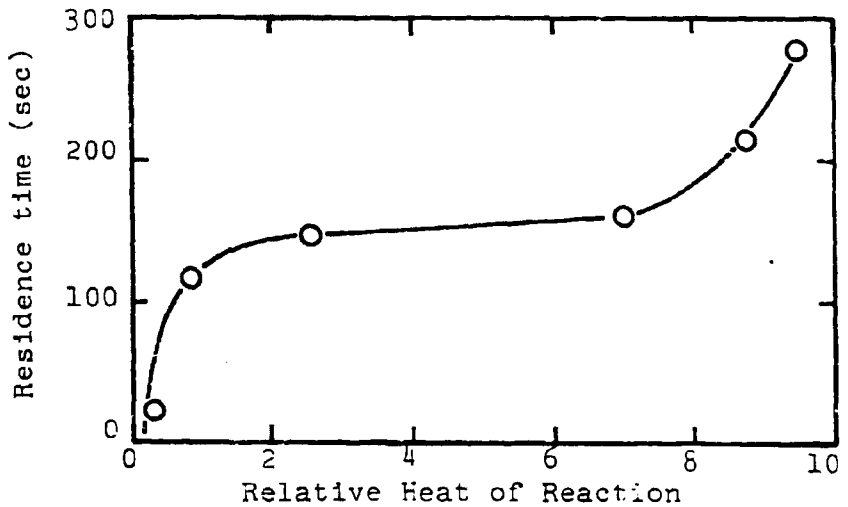

Figure 2. Increase in the heat evolved by the hydrogenation reaction vs. the residence time of Clear Creek, Utah coal in the coiled tube reactor.

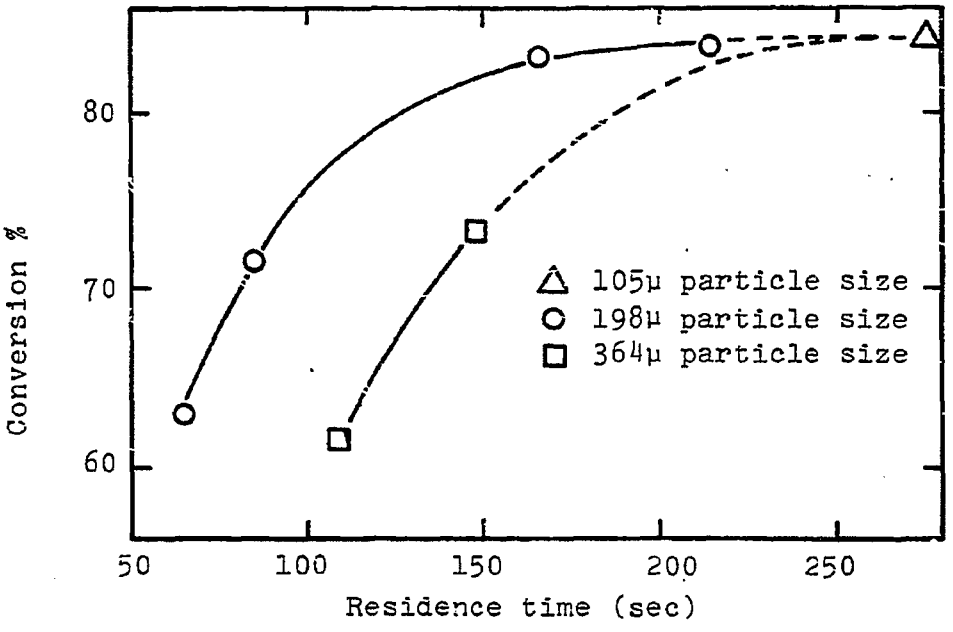

Figure 3. Residence time of Clear Creek, Utah coal in the coiled tube reactor vs. conversion to liquids and gases at various particle sizes (pressure 1800 psig, temperature 920°F).

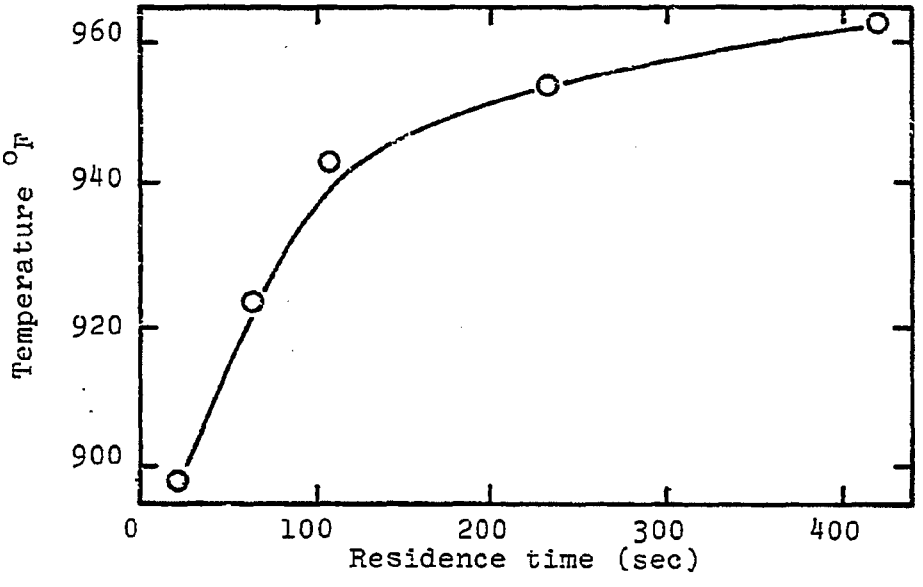

Figure 4. Residence time of Clear Creek, Utah coal in the coiled tube reactor vs. temperature (pressure 1800 psig).

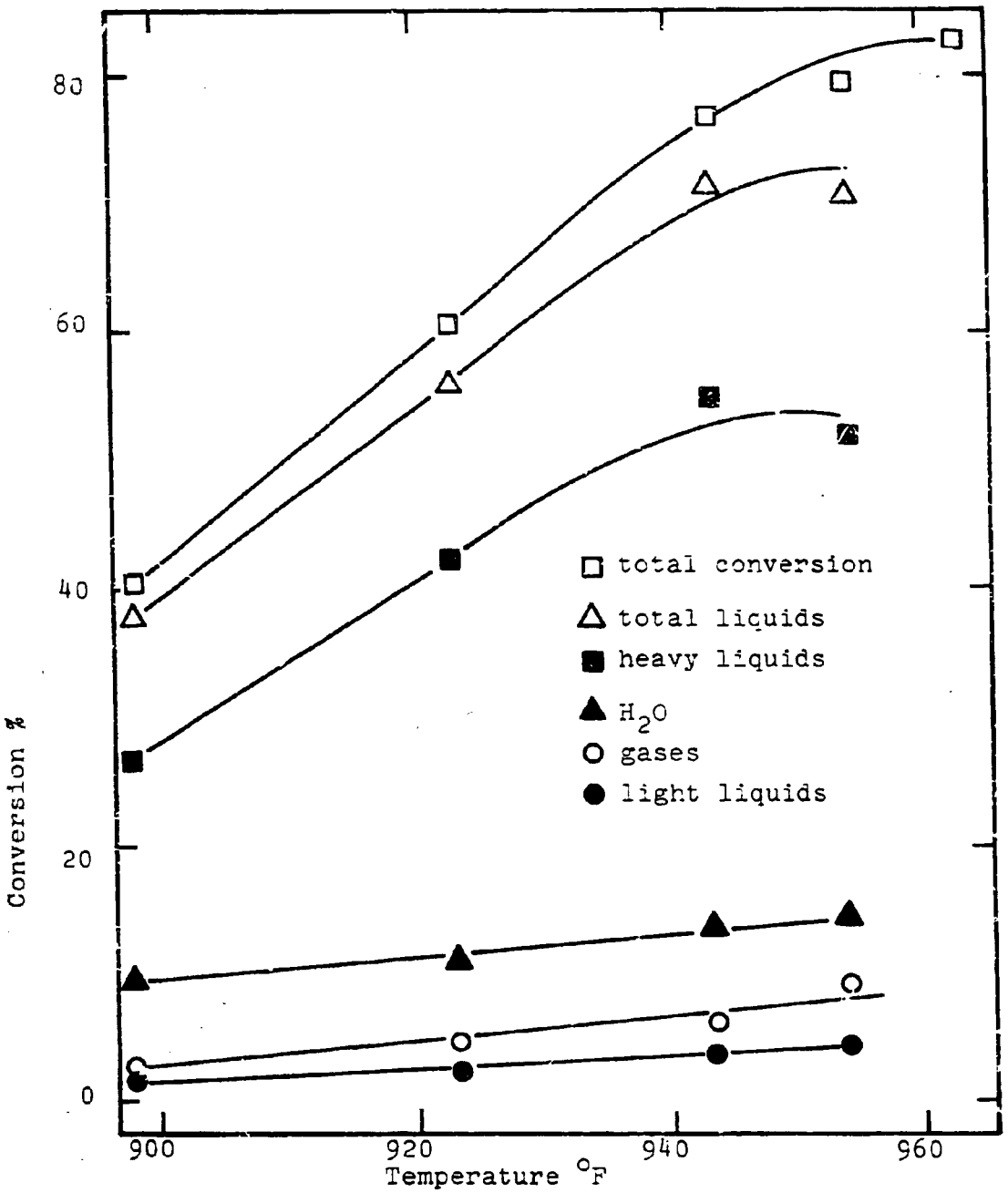

Figure 5. The product distribution of Clear Creek, Utah coal in the coiled tube reactor vs. temperature (pressure 1800 psig).

Project D-2

The Effect of Structure on Coal Reactivity

Structure of Coal Asphaltenes

Faculty Advisor: D.M. Bodily
Graduate Student: D. Roylance

Introduction

Asphaltenes have been thought by many investigators to be intermediates in the stepwise hydrogenation of coal to produce hexane-soluble oils. Recent reports have shown that coal can be liquified at very short reaction times and that asphaltenes and oils are produced by parallel reactions that can be interconverted by bond cleavage and polymerization reactions.[1,2] Work in this laboratory (Project B-4) has shown that asphaltenes and oils from catalytic hydrogenation of coal are similar in structure, the major difference being size. Hexane-soluble oils appear to be composed of structural units comprised of condensed aromatic ring systems with alkyl groups and hydroaromatic rings attached. Asphaltenes appear to be polymers of these basic structural units. The nature of the bonds which hold these units together is of interest in this research.

The asphaltenes will be separated from the heavy oil fraction obtained by coal hydrogenation and reacted in various ways to break specific bonds. Changes in the molecular weight will be determined by gel permeation. Structural analysis will be carried out on those samples which show extensive bond rupture to determine the types of bonding between structural units.

Project Status

Gel permeation columns were prepared using crosslinked polystyrene as a porous gel packing (Biobead SX-1 and SX-2, BioRad Laboratories). Benzene was used as a solvent and a pressure of 400 psi was applied during packing of the columns. Equipment for treating coal asphaltenes was prepared.

Future Work

Asphaltene samples will be treated and analyzed by gel permeation chromatography to determine structural changes.

References

1. R.C. Neavel, Fuel, 55, 237 (1976).

2. A.M. Squires, 1976, unpublished manuscript.

Project D-4

Pyrolytic Studies and Separation and Characterization of Coal-Derived Liquids

The Separation and Characterization of Coal-Derived Liquids

Faculty Advisor: R.R. Beishline

Introduction

This project deals with the investigation of promising methods for analyzing and identifying the lighter fractions of coal hydrogenation liquids. A spinning band (SB) distillation column is being used to determine whether fractionation can separate pure components directly from complex coal-derived liquids. Also SB distillation in combination with preparative gas chromatography (PGC) is being tested.

The long range objective is to formulate a reasonable analytical scheme for characterization of coal-derived liquids.

A procedure has been developed to remove tar bases and acids from crude coal hydrogenation liquids via distillation and extraction with aqueous acid and base, respectively. No organic solvents are used, thus avoiding contamination of the hydrogenation products.

The bromine numbers for five course neutral hydrocarbon cuts boiling from room temperature (atm) to 94°C (10 torr) have been determined.

SB fractionation of crude material boiling up to 100°C (atm) did not give distillates consisting of pure components, but did effectively cut the pot charges into smaller less complex fractions.

SB distillation in combination with PGC is an effective method for separating the light coal hydrogenation liquids boiling up to 100°C (atm) where identification by GC-MS is not available. (Identification by GC-MS is more time economical.) The information obtained in this research will be directly applicable to GC-MS identification and the column packings that give the best separations for PGC and GC-MS.

Using SB distillation plus PGC, the components in the 80-100°C (atm) coal fraction have been separated and isolated, and compounds representing about 70 volume % of the fraction have been spectroscopically identified (MS,IR, NMR).

Project Status

A general analytical scheme for light coal-derived hydrocarbon mixtures is being developed. A low boiling coal liquid was cut into standard fractions having sharply defined boiling ranges. This coal liquid was prepared in the University of Utah coal reactor by hydrogenation of Clear Creek, Utah coal. The light materials were steam distilled from the total coal hydrogenation liquid to 150°C. This distillate, which comprised 2-3 weight % of the original coal, was collected from several different runs in which the percent conversion ranged from 60-90%. Six weight % $ZnCl_2$ was used as a catalyst in all the runs. The crude distillate was extracted with 6N NaOH and 6N H_2SO_4 to remove tar acids and bases, respectively, and then washed with water and dried over anhydrous $MgSO_4$. The extractions reduced the volume of the coal liquid from 360 ml to 275 ml. The neutral sample was then rough cut (1 x 16 cm distillation column packed with 6 mm glass helicies) into three fractions (Table 1).

Table 1

Coarse Distillation of Light, Neutral Coal Hydrogenation Liquid

Rough Cut	Boiling Range (°C)	Pressure (torr)	Volume (ml)
1	65-103	atm	46
2	50-100	97	75
3	34-100	7	117

Rough Cut 1 (Table 1) was distilled through the SB column (200:1 reflux ratio) into the standard fractions shown in Table 2. SB distillation of Rough Cuts 2 and 3 (Table 1) has not been completed.

Table 2

SB Distillation of Rough Cut 1 , 200:1 Reflux Ratio, Atm Press.

Fraction	Boiling Range (°C)	Volume (ml)
1	30-40	1.5
2	40-50	1.0
3	50-60	3.2
4	60-70	10.2
5	70-80	5.8
6	80-90	12.5
7	90-100	10.2

Previous work has shown that coal-derived hydrocarbons boiling below 80°C are effectively separated (GC) on Carbopack C/0.19% picric acid, less well separated on SP2100 and poorly separated on Carbowax 20M, Apiezon L and TCEP columns. GC analysis of Fractions 1-5 (Table 2) shows the same trend. A combined fraction was made by mixing small quantities of Fractions 1-5 in amounts proportional to their volumes. The best GC separation of this combined fraction which has thus far been achieved (1/8" x 6' stainless steel column packed with Carbopack C/0.19% picric acid, 60ml/min He, initial temperature 55°C, programmed 1.5°/min to an upper limit of 120°C) is shown in Figure 1.

Future Work

Rough Cuts 2 and 3 will be distilled into 10° fractions through the SB column. GC examination of the 10° fractions will be continued to find the combinations of hydrocarbon boiling range and GC column packing that would give optimum separations.

Figure 1

Gas Chromatogram of Combined Fractions 1-5 (Table 2).

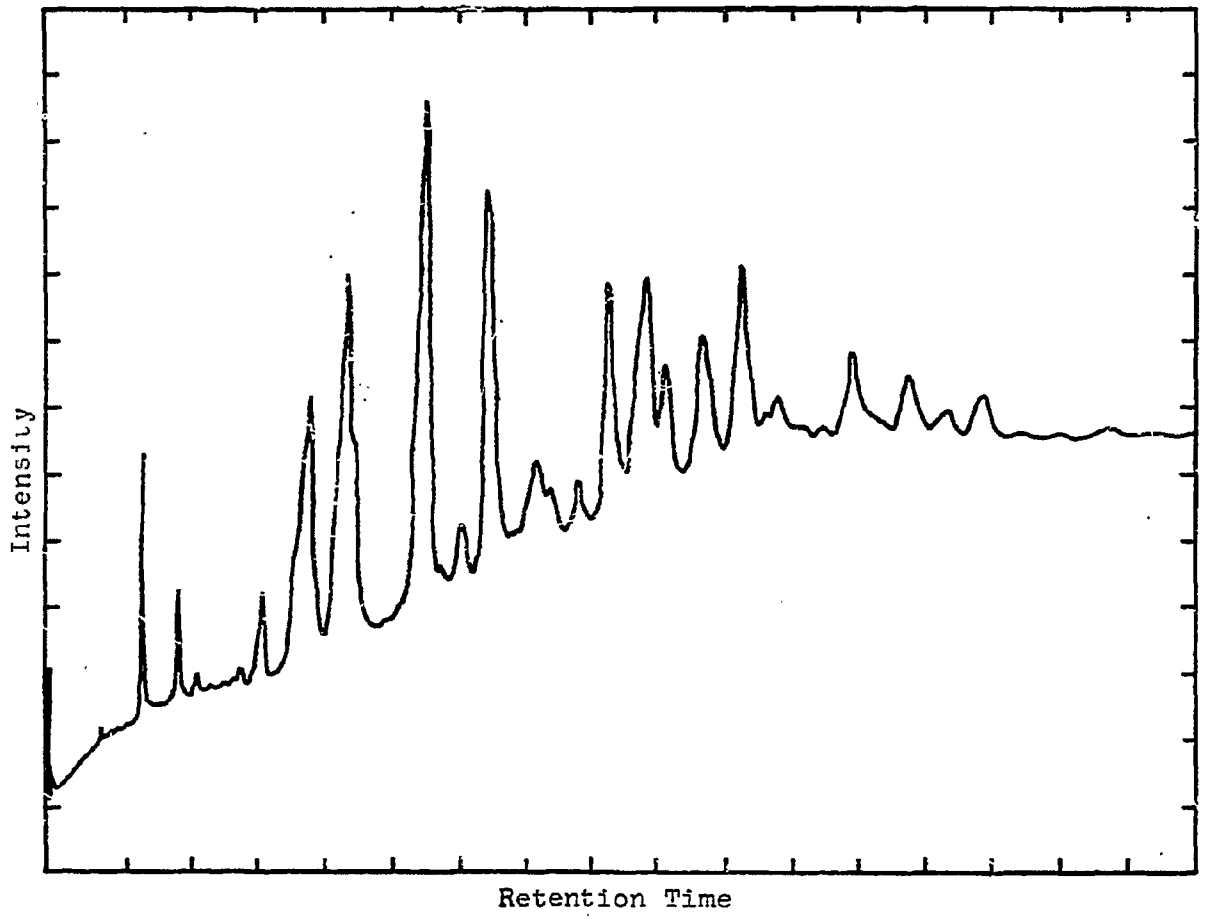

1/8' x 6' stainless steel column
Column packing: Carbopack C/0.19% picric acid
Flow rate: 60 ml/min He
Temp Prog: 55°C initial, programmed 1.5°/min to an upper limit of 120°C.

Project D-4

A Pyrolysis-Gas Chromatography Study of Coals and Related Model Compounds

Faculty Advisor: R.R Beishline

Introduction

The overall objective of this work is to study the pyrolysis and hydrogenation of coal and coal-related model compounds both in the presence and absence of catalysts. The model compound work is presently being pursued with the following objectives:

1. To study the catalytic effect of zinc chloride on the decomposition of model compounds at low temperatures, i.e., at temperatures below those required for thermal bond rupture. These studies will elucidate the zinc chloride-initiated carbonium ion reactions that take place in the absence of bond thermolysis.

2. To study the pyrolysis of model compounds in the absence of zinc chloride. These studies will elucidate the thermolysis reactions (free radical reactions) that take place in the absence of zinc chloride.

3. To study the pyrolysis of model compounds in the presence of zinc chloride. These studies should determine what happens when the catalyst-induced carbonium ion chemistry is superimposed on the thermally initiated free radical chemistry.

Reaction (1) has been shown to occur pyrolytically in the absence of zinc chloride and to occur at sub-thermolytic temperatures in the presence of zinc chloride.[1]

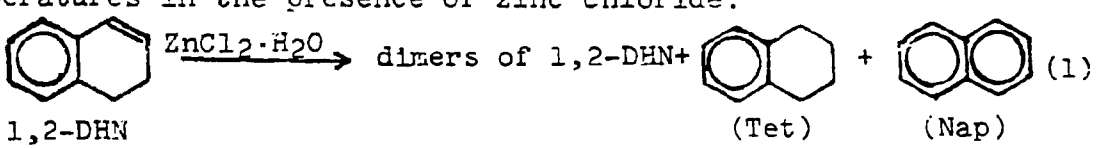

The following mechanism for reaction (1) at sub-thermolytic temperatures (165°C) is consistent with the structures of the products and with information obtained from $ZnCl_2$ hydration studies and deuterium tracer experiments:[2,3]

A $\quad H_2O + ZnCl_2 \longrightarrow H^+ + HOZnCl_2^-$

B $\quad$ 1,2-DHN + $H^+ \longrightarrow$  (defined as I)

C $\quad$ I + 1,2-DHN $\longrightarrow$ 3 different dimers of 1,2-DHN + H^+

D $\quad$ I + 1,2-DHN $\xrightarrow[\text{from 1,2-DHN}]{H^- \text{ trans}}$ Tet + Nap + H^+

Project Status

Additional quantities of the three dimer products of step C in the above mechanism have been isolated, and two have been tentatively identified.

Dimer 1, a yellow liquid, constitutes about 55 % of the total dimers produced in reaction (1) and is believed to have the structure shown at the right. The small letters represent hydrogens having different NMR chemical shifts (see description of NMR spectrum below).

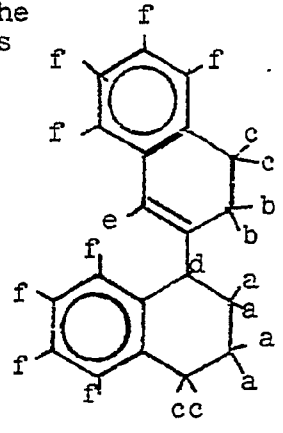

Spectral Data for Dimer 1

High Resolution Mass Spectrum

molecular weight 260.1580
formula $C_{20}H_{20}$

Infrared Spectrum

Absorption frequencies are in cm^{-1}
intensities: s = strong, m = medium, w = weak

Aromatic C-H stretch	3075m
Aromatic ring stretch	1606w, 1579w, 1493s, 1457s
Aromatic ring C-H wag for o-disub. benzene	749s
Double bond C-H stretch	3030s
C=C stretch	1648w
$=C<^{H}_{R}$ bend for trisub. double bond	808m

NMR Spectrum

δ= chemical shift (HZ), S = singlet, D = doublet, T = triplet, CM= complex multiplet

	δ		
a	1.69	CM	4H
b	1.92	CM	2H
c	2.59	T	4H
d	3.45	T	1H
e	6.04	S	1H
f	6.86	CM	8H

Eight different $C_{20}H_{20}$ isomers can be drawn by changing the points of attachment of the two ring systems and the

position of the double bond. The IR spectrum verifies the presence of an ortho disubstituted aromatic ring and a trisubstituted double bond. The resolution and integrations in the NMR spectrum are not as good as they should be due to small sample size. However, the observed NMR spectrum is consistent only with the particular structure proposed to be dimer 1, since it is the only one of the eight possible which would have one tertiary hydrogen (hydrogen d) appearing as a triplet at δ = 3.45 and one alkene hydrogen (hydrogen e) appearing as a singlet at δ = 6.04.

Dimer 2, a white crystalline solid, mp 88-89°C, constitutes about 30% of the total dimers produced in reaction (1) and is believed to have the structure shown at the right. The small letters represent hydrogens having different NMR chemical shifts (see description of NMR spectrum below).

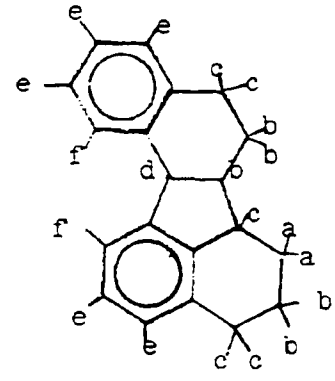

Spectral Data for Dimer 2

High Resolution Mass Spectrum

molecular weight 260.1559
formula $C_{20}H_{20}$

Infrared Spectrum

Absorption frequencies are in cm^{-1};
intensities: s = strong, m = medium,
w = weak

Aromatic C-H stretch	3070m
Aromatic ring stretch	1603m, 1573w, 1491s, 1453s
Aromatic ring C-H wag for o-disub benzene + ?	759s, 750s, 741s 732s

Note: There is no C=C stretch near 1650.

NMR Spectrum

δ = Chemical shift (HZ), S = singlet, D = doublet, T = triplet, CM= complex multiplet

	δ		
a	1.2	CM	2H
b	1.8	CM	5H
c	2.6	CM	5H
d	3.9	D	1H
e	6.9	CM	5H
f	7.15	CM	2H

There is no NMR evidence for a double bond.

The IR spectrum verifies the presence of an ortho disubstituted aromatic ring and shows no C=C stretch. As in the case of dimer 1, the NMR spectrum of dimer 2 shows poor resolution and integrations due to small sample size but still furnishes much evidence for the proposed structure. The coupling constant for the tertiary d hydrogen (J = 7.4HZ) indicates that the hydrogens at the b-d ring fusion are cis to one another.[4] The absence of alkene hydrogens together with the tertiary d hydrogen appearing as a doublet at $\delta = 3.9$ and the presence of two kinds of aromatic hydrogen (5 c hydrogens at $\delta = 6.9$ and 2 f hydrogens at $\delta = 7.15$) is compelling evidence in support of the proposed structure.

The structures of dimers 1 and 2 suggest that I (steps B, C and D in the mechanism of reaction (1)) attacks a molecule of 1,2-DHN to form carbonium ion II shown at the right. Part of II eliminates a proton to form dimer 1, and part forms dimer 2 by an electrophilic aromatic substitution (EAS) mechanism in which the positive charge attacks the bottom aromatic ring to form a new five membered ring. Models show that EAS cyclization of II can only give the particular structure proposed for dimer 2.

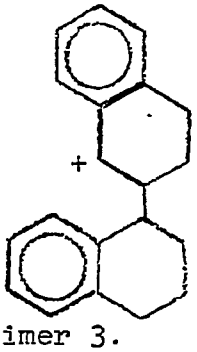

(II)

No attempt has yet been made to identify dimer 3.

Future Work

Larger quantities of the dimers will be isolated to confirm the identities of dimers 1 and 2 and hopefully allow identification of dimer 3. A kinetic study of reaction (1) will be initiated. Also the apparatus required for high temperature studies of reaction (1) will begin being constructed.

References

1. R.R. Beishline and W.H. Wiser, ERDA Contract No. E (49-18)-2006, Quarterly Progress Report, Salt Lake City, Utah, April-June 1976.

2. ibid., Oct-Dec 1976.

3. ibid., July-Sept 1976.

4. M.J. Karplus, J. Chem. Phys., 30, 11 (19590.

Hydrotreating of Heavy Coal-Derived Liquids

Faculty Advisor: A.G. Oblad
Graduate Student: L. Veluswamy

Introduction

Recent studies have indicated that high grade gasolines and jet fuels can be obtained in high yields by hydrotreating recycle stocks from catalytic cracking followed by catalytic cracking of the treated stock using zeolite catalysts. The effectiveness of this combination of processing steps depends on the degree to which hydrogen is added to the contained aromatics and the extent of removal of contained nitrogen and sulfur compounds.

The chemical composition of coal-derived oils is complex and these oils are known to contain condensed polyaromatic compounds, compounds of sulfur, nitrogen and metals which are detrimental to the catalytic cracking process (coke formation, poisoning of catalyst). Hydrogenation of this coal oil will convert the polyaromatics to saturated analogs which greatly improve the material as a catalytic cracking feedstock. Most of the S, N and metal impurities present in the oil will be removed thereby decreasing the coke formation and poisoning of the cracking catalyst.

The hydrogenation of relevant polyaromatic hydrocarbons (phenanthrene, pyrene, anthracene) and heterocyclics (7,8-benzoquinoline, 5,6-benzoquinoline and dibenzothiophene) were systematically investiaged as a function of different variables in a semi-batch reactor. The mechanism of the hydrogenation of these polyaromatics and heterocyclics will be suggested in the next report. The objective of the study of these model compounds is to contribute to the understanding of the behavior of these types of compounds present in the coal liquids.

Project Status

Hydrogenation of Phenanthrene over Sulfided Ni-W/Al_2O_3 Catalyst.

Temperature: Figures 1 and 2 show the change in product composition (g/100 g converted phenanthrene (P)) from the hydrogenation of P as a function of temperature (between 200-400°C) using a sulfided Ni-W/Al_2O_3 catalyst at 2900 psig and a reaction time of 2 hours. Extrapolation to temperatures below 200°C (Figure 1) clearly indicated that 1,2,3,4-tetrahydro P were the main product formed in the first hydrogenation step. The formation of 9,10-dihydro P , the other

primary product, reached a maximum at about 250°C and then decreased as the temperature increased. The gradual conversion of 1,2,3,4-tetrahydro P with an increase in temperature was accompanied by a corresponding increase in the yield of 1,2,3,4,5,6,7,8-octahydro P (56% at 299°C), the expected second step hydrogenation product. However, the gradual disappearance of 9,10-dihydro P with a temperature increase was not accompanied by any significant formation of the expected second step hydrogenation product indicating that 9,10-dihydro P was not an important intermediate in the overall hydrogenation process. The stepwise hydrogenation of the intermediate 1,2,3,4,5,6,7,8-octahydro P (via deca and dodecahydro P) into perhydro P is clearly indicated in Figure 2.

Pressure: Figures 3 and 4 show the change in product composition (g/100 g converted P) from the hydrogenation of P as a function of pressure (between 500 and 2900 psig) using the same sulfided Ni-W/Al_2O_3 catalyst at 341°C and a reaction time of 3 hours. The product composition again indicated that 1,2,3,4-tetrahydro P was the major primary product when compared with 9,10-dihydro P at 500 psig. With the increase in pressures, the 1,2,3,4-tetrahydro P and to some extent the 9,10-dihydro P were hydrogenated to the expected octahydro P derivatives (Figure 3). Beyond 1000 psig the intermediate 1,2,3,4,5,6,7,8-octahydro(P), 1,2,3,4, 5,6,7,8,9,10-decahydro P and 1,2,3,4,5,6,7,8,9,10,11,14-dodecahydro P were gradually converted into the final hydrogenation product, perhydro P . The yield of perhydro P converted P reached approximately 100% around 2600 psig (Figure 4).

Catalyst/Phenanthrene Ratio: Figures 5 and 6 show the change in product composition (g/100 g converted P) from the hydrogenation of P as a function of catalyst to hydrocarbon ratio using the same sulfided Ni-W/Al_2O_3 catalyst (pressure 1500 psig, temperature 341°C, reaction period 2 hours). At very low catalyst/phenanthrene ratios, e.g., 0.05 (Figure 5), the yield of 1,2,3,4-tetrahydro P was again markedly higher than that of 9,10-dyhydro P and the yield of 1,2,3,4,5,6,7,8-octahydro P was much higher than that of 1,2,3,4,9,10,11,12-octahydro P (Figure 5). As the catalyst/phenanthrene ratio increased, the yield of 1,2,3,4-tetrahydro P and 1,2,3,4,5, 6,7,8-octahydro P gradually decreased while the yield of the final hydrogenation product, perhydro P , gradually increased and reached approximately 70% at a catalyst/phenanthrene ratio of 0.04 (Figure 6).

Future Work

The results on the hydrogenation of pyrene, 5,6-benzoquinoline and 7,8-benzoquinoline will be reported in the next report.

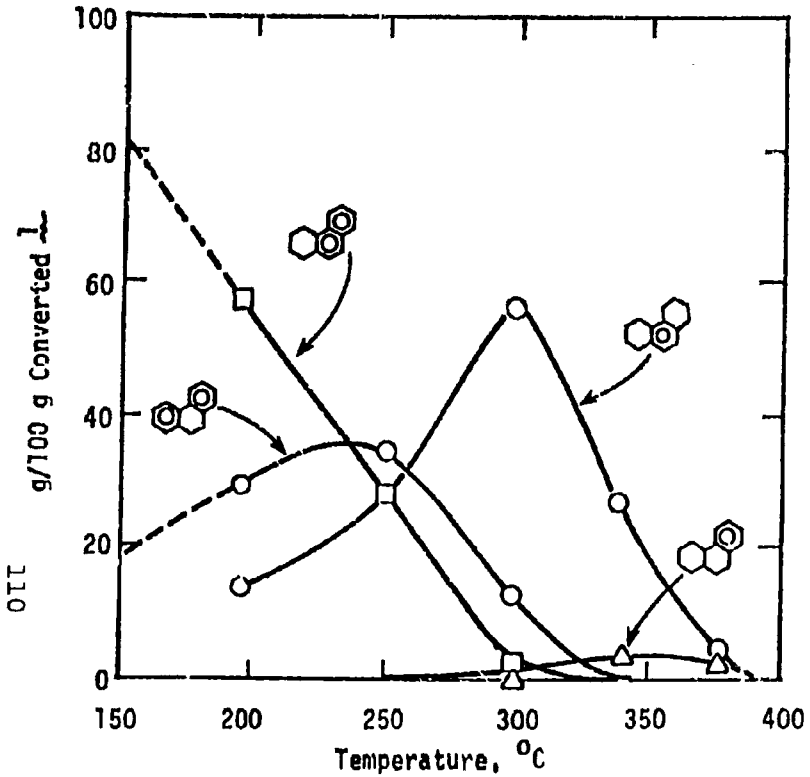

Fig. 1. Change in Product Composition from Hydrogenation of Phenanthrene (1) as a Function of Temperature (Step A)

Catalyst: Sulfided Ni-W on Alumina (Sphericat 550)

Pressure: 2900 PSIG

Reaction Time: 2 hr

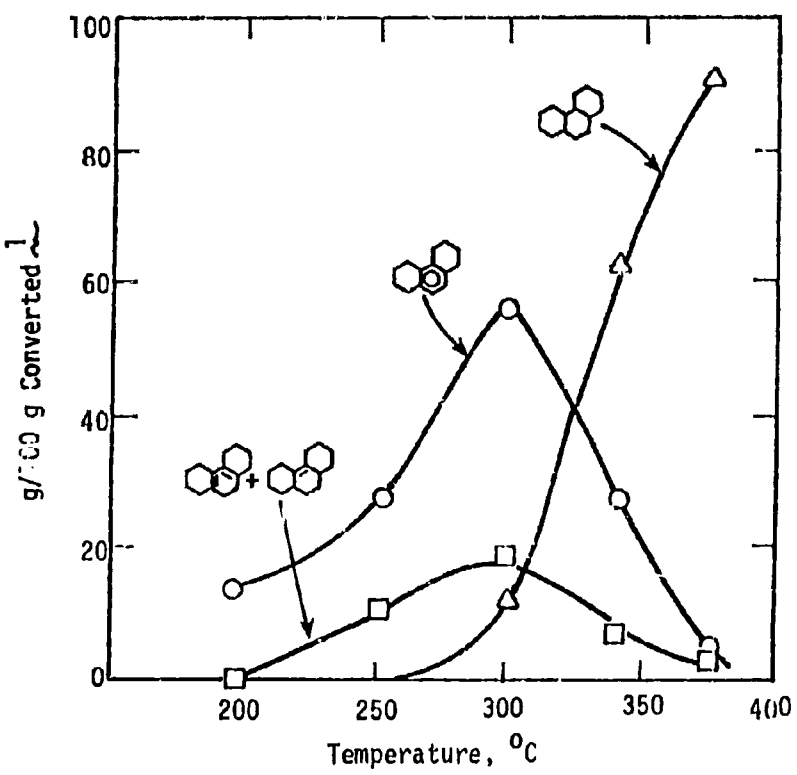

Fig. 2. Change in Product Composition from Hydrogenation of Phenanthrene (1) as a Function of Temperature (Step B)

Catalyst: Sulfided Ni-W on Alumina (Sphericat 550)

Pressure: 2900 PSIG

Reaction Time: 2 hr

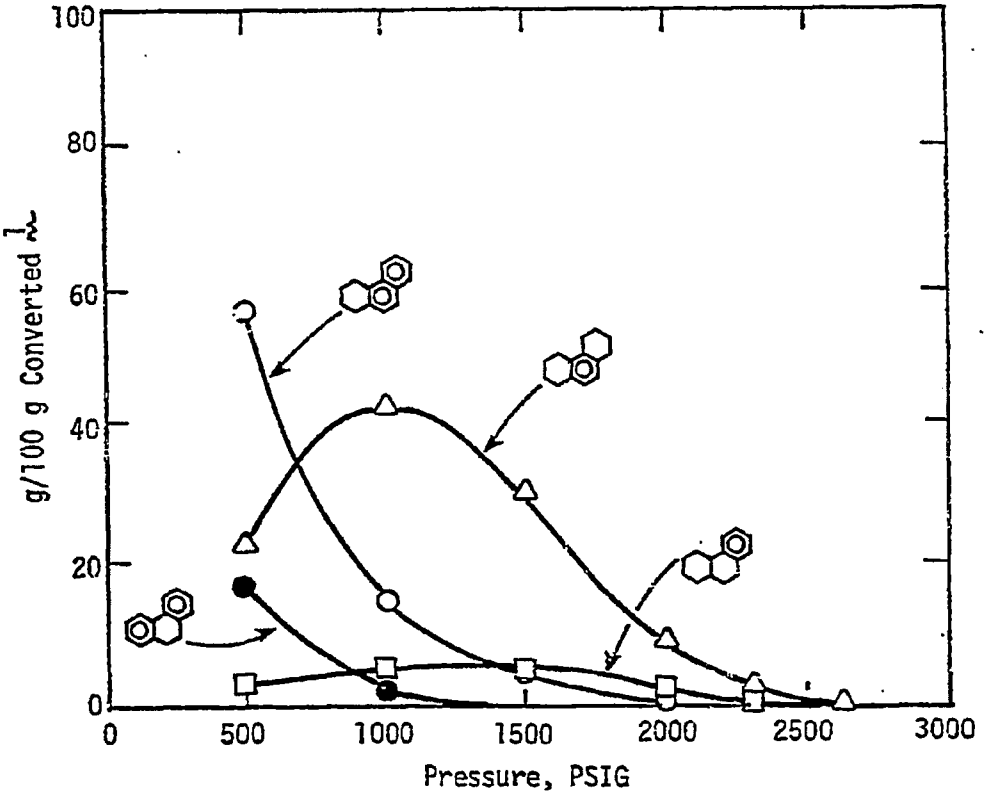

Fig. 3. Change in Product Composition from Hydrogenation of Phenanthrene (1) as a Function of Pressure (Step A)

Catalyst: Sulfided Ni-W on Alumina (Sphericat 550)

Reaction Temperature: 341°C

Reaction Time: 3 hr

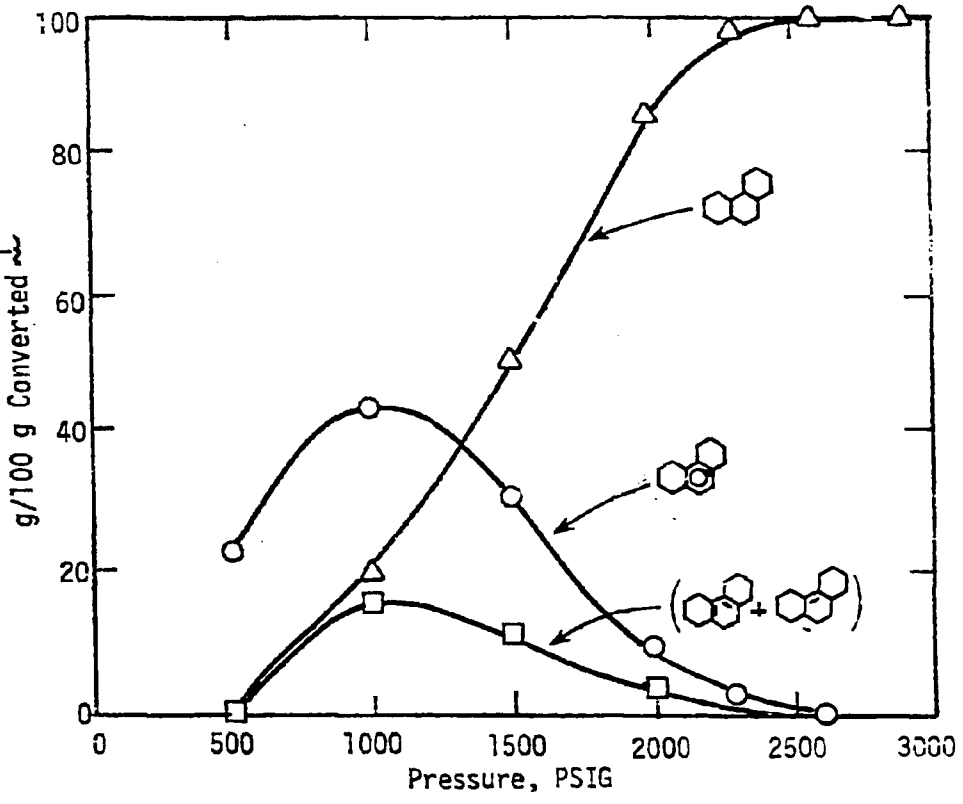

Fig. 4. Change in Product Composition from Hydrogenation of Phenanthrene (1) as a Function of Pressure (Step B)

Catalyst: Sulfided Ni-W on Alumina (Shericat 550)

Reaction Temperature: 341°C

Reaction Time: 3 hr

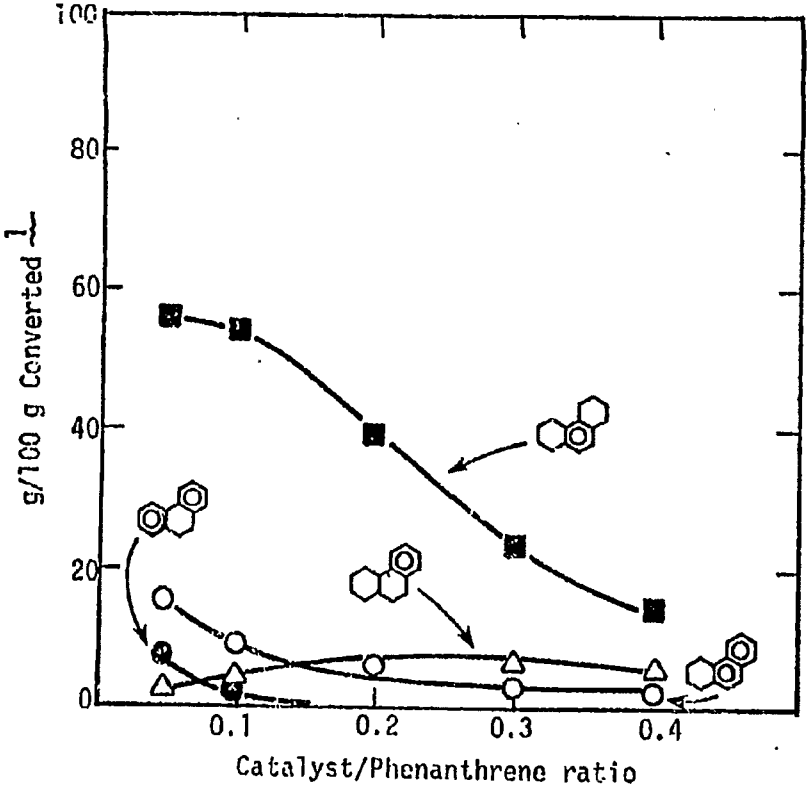

Fig. 5. Change in Product Composition from Hydrogenation of Phenanthrene (1) as a Function of Catalyst/ 1 ratio (Step A).

Catalyst: Sulfided Ni-W on Alumina (Sphericat 550)
Reaction Pressure: 1500 PSIG
Reaction Temperature: 341°C
Reaction Time: 2 hr

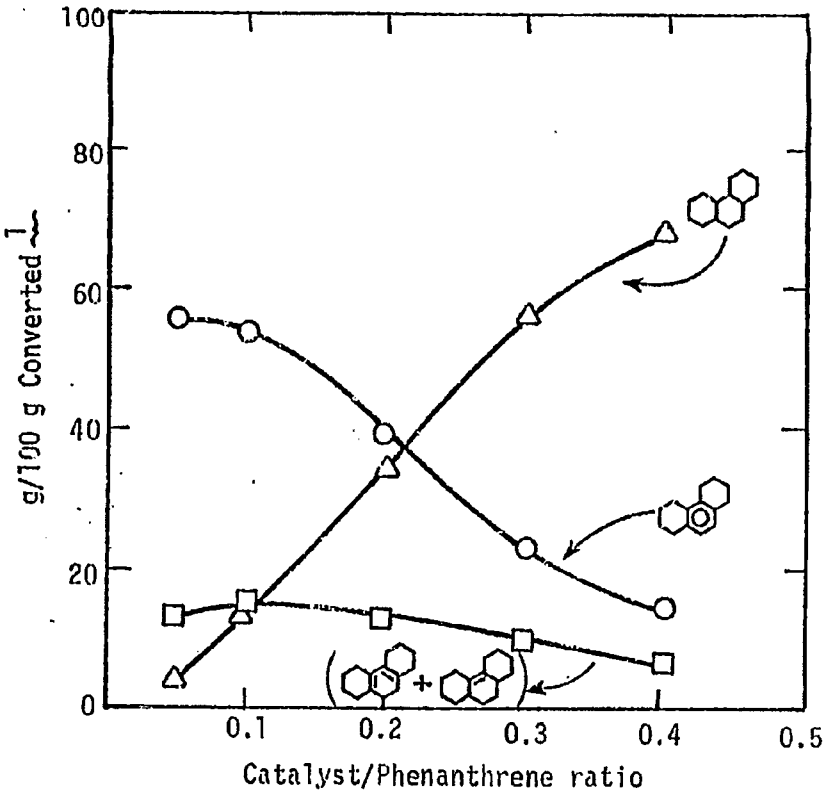

Fig. 6. Change in Product Composition from Hydrogenation of Phenanthrene (1) as a Function of Catalyst/ 1 ratio (Step B).

Catalyst: Sulfided Ni-W on Alumina (Sphericat 550)
Reaction Pressure: 1500 PSIG
Reaction Temperature: 341°C
Reaction Time: 2 hr

V. Conclusions

Fourteen projects and one continuation project are active. Work is progressing satisfactorily on each of these projects. Projects A-6 and A-9 are inactive at present.

U.S. DEPARTMENT OF COMMERCE
Technology Administration
National Technical Information Service
Springfield, VA 22161 (703) 605-6000